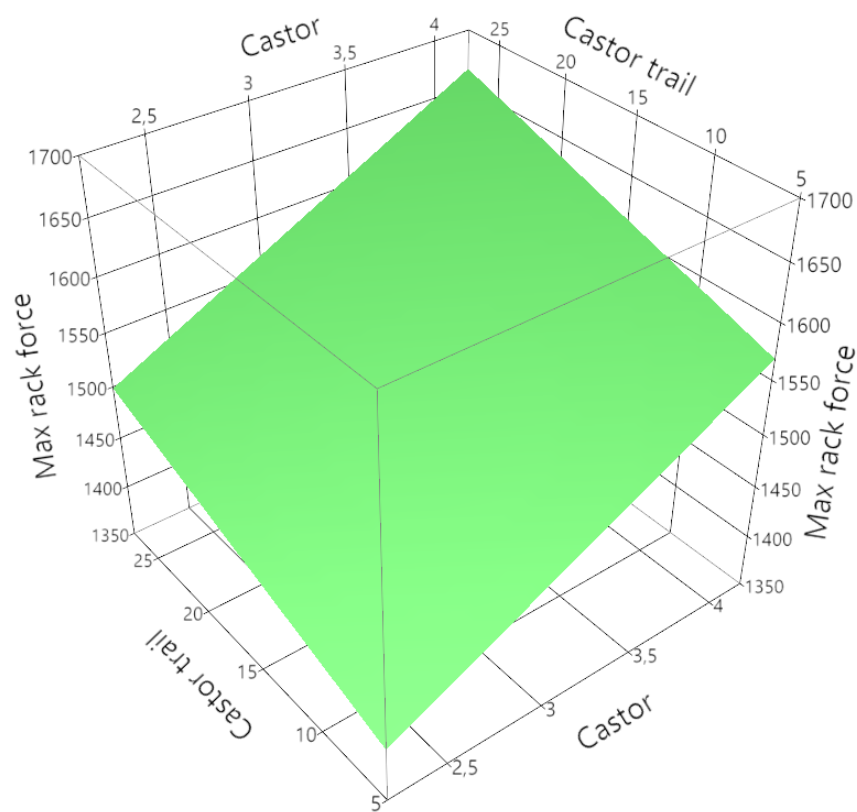




CHALMERS



STEERING PERFORMANCE DEPENDENCE ON FRONT SUSPENSION DESIGN

Master's thesis in Automotive Engineering

JOACIM GILLBERG
DIEGO ZAPARDIEL

Department of Applied Mechanics
CHALMERS UNIVERSITY OF TECHNOLOGY
Göteborg, Sweden 2015

MASTER'S THESIS IN AUTOMOTIVE ENGINEERING

STEERING PERFORMANCE DEPENDENCE ON FRONT SUSPENSION
DESIGN

JOACIM GILLBERG
DIEGO ZAPARDIEL

Department of Applied Mechanics
Division of Vehicle Engineering and Autonomous Systems
Vehicle Dynamics Group
CHALMERS UNIVERSITY OF TECHNOLOGY
Göteborg, Sweden 2015

STEERING PERFORMANCE DEPENDENCE ON FRONT SUSPENSION DESIGN
JOACIM GILLBERG
DIEGO ZAPARDIEL

© JOACIM GILLBERG, DIEGO ZAPARDIEL, 2015

Master's thesis 2015:64
ISSN 1652-8557
Department of Applied Mechanics
Division of Vehicle Engineering and Autonomous Systems
Vehicle Dynamics Group
Chalmers University of Technology
SE-412 96 Göteborg
Sweden
Telephone: +46 (0)31-772 1000

Cover:
Regression surface for maximum force in the rack.

Chalmers Reproservice
Göteborg, Sweden 2015

STEERING PERFORMANCE DEPENDENCE ON FRONT SUSPENSION DESIGN

Master's thesis in Automotive Engineering

JOACIM GILLBERG

DIEGO ZAPARDIEL

Department of Applied Mechanics

Division of Vehicle Engineering and Autonomous Systems

Vehicle Dynamics Group

Chalmers University of Technology

ABSTRACT

'Steering performance parameters' are the measures defined in this thesis to quantify the steering behavior of vehicles. The parameters are important for the earlier stages of the design process and therefore a good understanding on how these parameters may change when designing the suspension is vital. The objective of this work is to establish a general frame that describes the relation between the steering performance parameters and the suspension design factors regardless of the suspension type.

The work was done by studying one steering performance parameter, namely forces in the steering rack under a simulated driving condition. A population of different suspension configurations with different design factors was studied. A model of a McPherson suspension, including both kinematics and steering forces, was developed in Matlab to simulate these scenarios and gather all the necessary data for the study. Different suspension configurations with different design factors were simulated in this environment and the output forces and other steering parameters were statistically post processed to find trends and confidence intervals to find the relations.

The objective of the statistical analysis was to find a model that isolated the effect of each suspension design factor on the different steering performance parameters. Linear regression models were used to fit the data and variability of the estimators was specially studied.

The result of the study evidenced the difficulty of this problem. There is only statistically significant relation between castor trail and castor angle with all the steering performance parameters studied. The statistical study also reveals a close relation of the suspension design factors between themselves and the same for the steering performance parameters.

Keywords: Steering, Suspension, McPherson, Steering performance, Suspension design factors, On-centre steer, Simulation.

PREFACE

This thesis is done as a part of the Master of Science in Automotive Engineering programme at Chalmers University of Technology, Gothenburg. The project topic is proposed by LeanNova Engineering A.B., Trollhättan. The thesis work was performed between January 2015 and June 2015 at LeanNova and Chalmers.

ACKNOWLEDGEMENTS

First of all, we would like to express our gratitude to LeanNova and especially Gunnar Olsson for initiating the project. Also, we would like to thank our supervisors Oskar Eklund and Erik Hartelius, at LeanNova, for valuable inputs and guidance during the thesis work.

Moreover we would like to extend our appreciation to Anders Boström at Chalmers for the guidance of rigid body dynamics and Sergei Zuyev at Chalmers for the support around the statistical study part of the work.

Last but not least we would like to thank Bengt Jacobson at Chalmers for his help and guidance throughout the work.

NOMENCLATURE

Symbols

a_y	- Lateral acceleration [m/s ²]
B	- Euler-Rodrigues rotation matrix
f	- Constraints vector
F_{ly}	- Lateral force from Pacejka (Y-direction) left wheel[N]
F_{lz}	- Vertical normal force (Z-direction) left wheel[N]
F_{ry}	- Lateral force from Pacejka (Y-direction) right wheel [N]
F_{rz}	- Vertical normal force (Z-direction) right wheel [N]
$F_{steering}$	- Force in track rod [N]
F_y	- Lateral force (y-direction) [N]
g	- Gravity constant [m/s ²]
$h1...h8$	- Hardpoint coordinates in global reference system
\vec{h}'	- New position of the strut upper mount point when body roll
h_{CoG}	- Centre of gravity height [m]
J_f	- Jacobian of f
k	- Longitudinal slip [%]
L'	- New strut length after roll [mm]
Lst	- Strut length [mm]
m	- Mass of the whole car [kg]
M_Z	- Self-aligning torque [Nm]
\vec{M}_δ	- Moment around the steering axis [Nm]
O'	- Origin of local reference system after roll
p_x	- Roll gradient [deg/g]
$\vec{q}1...q8$	- Position vector for the hard points in the local reference system
$R2$	- Coefficient of determination
R	- Rotation matrix for body roll
$R_{chassis}$	- Reaction force upper strut mounting point [N]
R_e	- Loaded wheel radius
R_{lca}	- Reaction force lower control arm outer ball joint [N]
\vec{rOm}	- Position vector for the origin of the local reference system
Rw	- Characteristic length of the lower control arm
tol	- Tolerance value for Newton-Raphson
v	- Velocity [km/h]
w	- Track width [m]
X	- Solution vector for Newton-Raphson
α	- Slip angle [deg]
δ	- Steering axis
$\vec{\lambda}$	- Steering axis direction unit vector
ϕ	- Roll angle [deg]

Abbreviations

CAD	-	Computer Aided Design
CoG	-	Centre of Gravity
EHPS	-	Electro-Hydraulic Power Steer
EPS	-	Electric Power Steer
GND	-	Ground
HP	-	Hard Points (suspension/steering)
HPS	-	Hydraulic Power Steer
KPIA	-	Kingpin Inclination Angle
KPO	-	Kingpin Offset
PSO	-	Particle Swarm Optimization
RC	-	Roll Centre
SDF	-	Suspension Design Factors
SPP	-	Steering Performance Parameter
SUV	-	Sport Utility Vehicle
VIF	-	Variability Inflation Factor
WC	-	Wheel Centre

CONTENTS

Abstract	i
Preface	iii
Acknowledgements	iii
Nomenclature	v
Contents	vii
1 Introduction	1
1.1 Background	1
1.2 Problem Definition	1
1.3 Objective	2
1.4 Deliverables	2
1.5 Delimitations	2
1.6 Method	2
2 Theory	5
2.1 Coordinate Systems	5
2.2 Suspension Design Factors	6
2.3 Suspension Layout	8
2.4 Steering Performance Parameters	9
2.5 Mathematical Problem	9
2.5.1 Numerical Methods For Equations Solving	10
2.6 Pacejka Tire Model	11
3 Kinematic Model	13
3.1 Kinematic Study Purpose	13
3.2 Geometrical Relations	13
3.3 SDF Calculation	15
3.4 Matlab Implementation for the Kinematic Model	17
3.5 Validation of the Kinematic Model	18
4 Front Axle Model	19
4.1 Quarter Car Model	19
4.2 Front Axle Study	20
4.3 Tire Model Calculation	21
4.4 Matlab Implementation for the Force Model	22
4.5 Total Calculation Setup	23
5 Analyzing the Gathered Data	27
5.1 Data Analysis and parameters selection	27
5.2 Statistical Study	28
6 Results	31
6.1 Suspension Model	31
6.2 Statistic Result	31
7 Conclusions and Future Work	35
7.1 Conclusions	35
7.2 Future Work	36
Bibliography	37

A	Vehicle data	3
B	Matlab Program Manual	5
C	Matlab Model Code	7
C.1	Matlab main program	7
C.2	Initial condition	15
C.3	SDF	16
C.4	Roll to travel	17
C.5	myfunsysms	17
C.6	Newton-Raphson	18
C.7	Transformation	19
C.8	Lateral load transfer	19
C.9	Magic formula	20
C.10	Force in the rack	21
C.11	interpo	22
D	Statistical Data	23
D.1	Lateral acceleration at maximum force	23
D.2	Drop rate (acceleration)	27
D.3	Drop rate (slip angel)	30
D.4	Maximum force in the steering rack	33
D.5	On-centre slip angle	37
D.6	On-centre rate (acceleration)	40
D.7	Slip angle for maximum force	43

Chapter 1

Introduction

1.1 Background

Steering performance is an important field of study among automotive engineers since it is a key factor in vehicle handling and driver feel. Steering performance can be divided into vehicle steering response and steering feel. Steering performance is measured in Steering performance parameters (SPP). The industry provides steering assistance solutions such as Hydraulic power steering (HPS), electric power steering (EPS) and electro-hydraulic power steering (EHPS) which reduces driver effort, thereby increasing driver comfort. The interest on sustainable transportation in cities is making car manufacturers invest in small, light-weight and cheap vehicles where HPS, EPS and EHPS are desirably avoidable to reduce costs. This makes it interesting to study how to influence the steering performance characteristics just by changing suspension hardpoints and thus suspension design factors (SDF). Exampels of SDFs are given in 2.2.

These SDF can be seen as an universal communication vehicle between automotive engineers. This is very useful when sharing information regardless of the platform or suspension type you are working with as it is possible to define these factors for all of them through their different geometries.

Literature on this topic is not abundant, and even less so for the approach presented in this work. Rohit Vaidya et al. [1] studied the on-centre handling behavior of vehicles depending on six different vehicle characteristics although not suspensions design factors. Ragnar Ledesma and Shan Shih [2] studied the effect of steering axis inclination angle and wheel offset on medium-duty truck handling and found clear relations between these two factors and the steering responses that they studied. R. P. Rajvardhan et al. [3] studied the effect of wheel geometry parameters on vehicle steering using a model of a SUV type vehicle in ADAMS/CAR, a multibody dynamics software used in the automotive industry. Skip Essma [4] wrote about the steering effort evaluation and modification for a Champ Car type of vehicle. He studied the change in steering effort while modifying camber, castor and castor trail. Yung-Hsiang Judy Hsu and J. Christian Gerdes [5] studied the peak lateral performance and handling limit estimation through steering torque. The lack of information on SDFs impact on SPPs motivates this study. It is important to highlight that this work tries to find a general frame to describe the relation between SDFs and SPPs for any kind of vehicle, independent of suspension type.

1.2 Problem Definition

All car manufacturers have their own ideas and philosophies when setting the targets for the suspension design factors. For achieving these target numbers based on the suspension design different computer software is available. However, these computer software do not give a clear general correlation between the SDFs and the SPPs. Therefore this master thesis project is proposed to provide this correlation of suspension design factors and steering performance parameters of a vehicle. This is useful for the engineers designing suspension systems and will help them to set these design targets in the future. With this knowledge the engineers can, independent of the suspension type, find what to change in the suspension to achieve a desired value for a steering performance parameter. Also the communication between engineers will be improved due to the fact that SDFs says more of a suspension than just hardpoints positions and configurations in space. A benefit of SDF as opposed to hardpoints is that suspensions of different suspension types can be compared, e.g. a certain McPherson can be compered with a certain Double Wishbone.

In Figure 1.1 a basic scheme shows how the suspension and steering hardpoints (HP) gives the SDFs which then gives a specific steering performance. Some examples of SDFs are toe angle, camber angle and the kinematic variations of these, like ride camber, ride toe, track width change, etc..



Figure 1.1: *Vehicle Steering Performance Parameters, SPPs.*

1.3 Objective

The main purpose of this master thesis is to create an understanding of how the suspension design factors, given by the front suspension geometry, affect the steering performance of the vehicle. This understanding is provided by studying trends in steering performance when changing suspension hardpoints for a fixed suspension type in a statistical environment.

1.4 Deliverables

The deliverables of this thesis are:

- Computer program to simulate/calculate SDF from HP
- Computer program to sweep HP and analyze correlation between SDF and SPP
- Computer program to simulate/calculate SPP from SDF
- A report summarizing the study and the results
- A manual for the computer programs

1.5 Delimitations

Although the study is intended for all suspension types in this project a McPherson suspension of a front wheel driven car is used as a base. The study only focuses on front steering cars without power steering systems and the effects produced in the intermediate shaft and steering column. The focus of the study lies on the front axle, thus the theoretical model in this thesis will be a half-car model.

In this thesis only steering force related SPPs were studied and at a significant velocity ($v > 25\text{km/h}$) [6], so no parking forces or low speed manoeuvrability is taken into account. The scenarios studied and model used applied to passenger vehicles.

To get a real in-depth understanding of the suspension and steering system functionality the suspension model will be developed in Matlab instead of using a commercial multi-body (black box) software.

1.6 Method

A complete model was done in Matlab. Starting from a set of hardpoints (of an already existing suspension) the first step was to create a kinematic model. the next step was to calculate the SDFs for the entire movement of the suspension. This included bump, rebound and steering motions, both individual and combinations of them. Multi body simulation data was provided by LeanNova Engineering AB to verify the results.

By implementing the tire and input forces (in this case a high speed turning driving scenario) the car

experiences a lateral acceleration and roll motion. The correct suspension travel left/right shall be calculated for this roll and then the net force in the rack can be calculated using the resulting suspension geometry.

By varying the hardpoints of the suspension model, resulting in changed SDFs, it was possible to study the net rack force versus lateral acceleration and thereby find the relation between SPPs and SDFs. A database with all the different suspension configurations was created. Each entry contained information about the hardpoints, the SDFs and the SPPs for a certain configuration. This database was statistically post processed to find a model that directly relates SPPs and SDFs.

An alternative method that could have been used is to use a conventional multi body program to create the database that then could be evaluated using statistical methods. This was never an option because it was set as a delimitation. This was because it would not give a good enough understanding of the relation between suspension hardpoints and suspension characteristics (SDFs) and their correlation [7]. Real vehicle testing methods could have also been thought of for this work but since the intention was to obtain a general frame valid for any type of suspension and configuration it would take a huge amount of time and money to test a sufficient population of vehicles to draw conclusions.

Chapter 2

Theory

2.1 Coordinate Systems

The coordinate systems used in this thesis follow the ISO 8855-standard [8] as defined below.

Intermediate axis system

The X and Y axis are parallel to the ground plane and the Z axis is orthogonal to this one. The X-axis is pointing forward in the car's direction and the Y-axis is pointing left of the car's direction. The Z-axis is pointing upwards. This is illustrated in Figure 2.1.

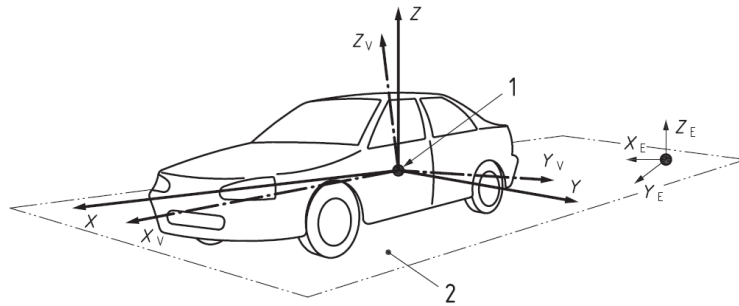


Figure 2.1: *ISO 8855 vehicle and intermediate axis systems.*

Tire and wheel axis system

The tire and wheel axis system in this thesis is according to ISO 8855 and is illustrated in Figure 2.2. The subscript T stands for the tire and the subscript W stands for wheel.

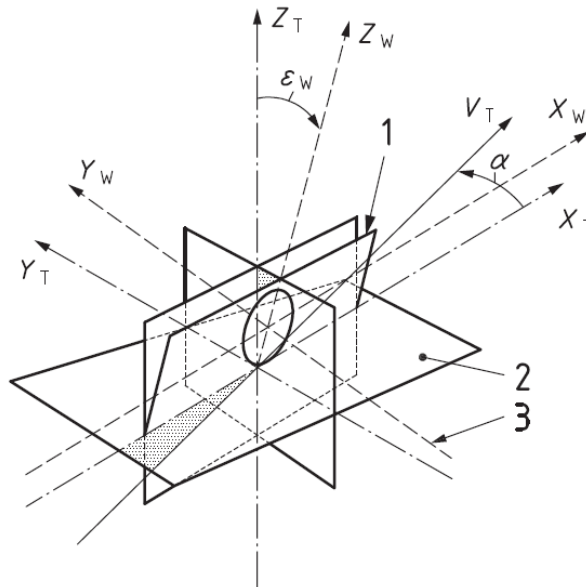


Figure 2.2: *ISO 8855 tire and wheel axis system.*

2.2 Suspension Design Factors

The suspension design factors are defined by the suspension hardpoints. The relevant SDFs for this thesis are defined in this section. These SDFs are chosen mostly for their direct relation with the steering axis. Camber and toe are included for validation purposes and future implementation in a tire model.

Camber angle at design load

The camber angle is the angle between the Z-axis and the centreline through the wheel in the car's Y-Z plane. If the wheel is leaning inwards to the car this angle is defined negative and if it is leaning outwards it is positive. This is illustrated in Figure 2.3.

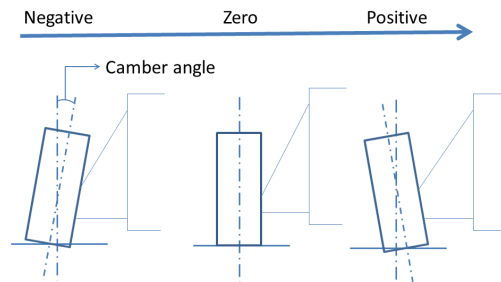


Figure 2.3: Wheel seen in the Y-Z plane to illustrate camber.

Steering axis

The steering axis is defined as the axis around which the steering takes places. For example in a McPherson suspension the upper mounting point is the top strut and the lower outer hardpoint is the lower control arm outer ball joint.

Castor

Castor angle is the angle between the steering axis (seen in the X-Z plane) and the Z-axis. This is illustrated in Figure 2.4.

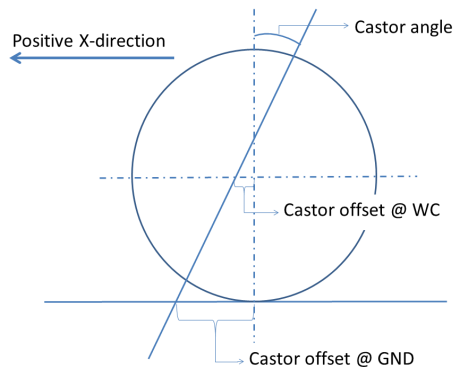


Figure 2.4: Wheel seen in the X-Z plane to illustrate castor.

Castor offset at wheel centre

Spindle trail

The castor offset is the distance given by the centre line of the wheel (Z-axis) and the steering axis seen in the X-Z plane (castor axis). Therefore the castor offset at wheel centre is the distance orthogonal to the wheel centre line in Z-direction to the castor axis in the wheel centre point. This is illustrated in Figure 2.4.

Castor offset at ground

Castor trail, kinematic trail

The castor offset at ground is the orthogonal distance to the centre line of the wheel in Z-direction to the castor axis at ground level. This is illustrated in Figure 2.4.

Steering axis inclination angle

Kingpin inclination angle, KPIA

The steering axis inclination angle is the angle given by steering axis seen in the Y-Z plane and the centre line through the wheel. This is illustrated in Figure 2.5.

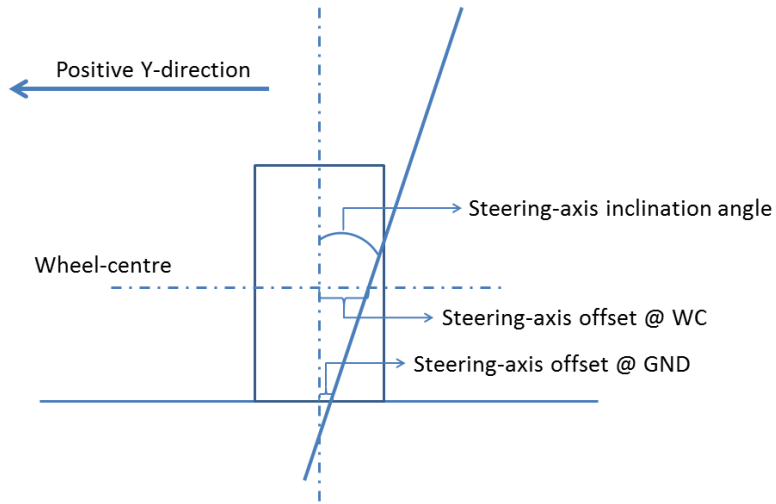


Figure 2.5: Wheel seen in the Y-Z plane to illustrate steering axis inclination angle and its offsets.

Steering axis offset at wheel centre

Kingpin offset at wheel centre

The kingpin offset is the distance given by the centre line of the wheel (Z-axis) and steering axis seen in the Y-Z plane. Therefore the kingpin offset at wheel centre is the distance orthogonal to the wheel centre line in Z-direction to the kingpin axis in the wheel centre point. This is illustrated in Figure 2.5.

Steering axis offset at ground

Kingpin offset at ground

The kingpin offset at ground is the distance orthogonal to the centre line of the wheel in Z-direction to the kingpin axis at ground level. This is illustrated in Figure 2.5.

Static toe angle

The Static toe angle is the angle generated by the offset of the wheel centerline (X-direction) and the X-axis of the vehicle, see Figure 2.6. It is considered positive when the wheel centreline leans towards the vehicle and negative when it leans outwards. Total static toe angle is defined for steering rack in the centre position, meaning that is a design measure for the axle, not the wheel.

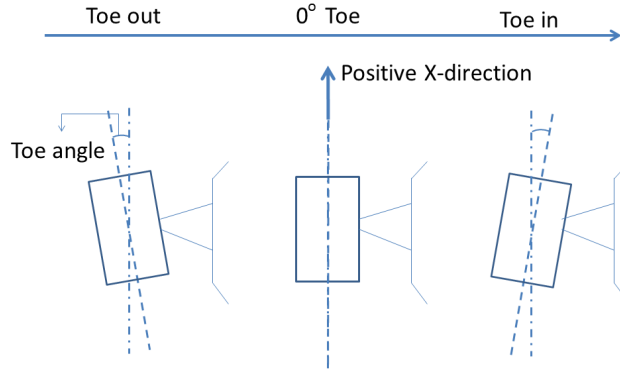


Figure 2.6: Wheel seen in the X-Y plane to illustrate toe, sign definition valid for both view from above (left wheel) and from under (right wheel).

2.3 Suspension Layout

The suspension used as base in this thesis is a front suspension of McPherson type. The base hardpoints are from a front wheel drive car. There are eight different hardpoints that are of significant interest for the study of this thesis. With these hardpoints it is possible to reproduce the whole suspension movement and calculate all the SDFs described in chapter 1. They are specified in Table 2.1 and illustrated in Figure 2.7.

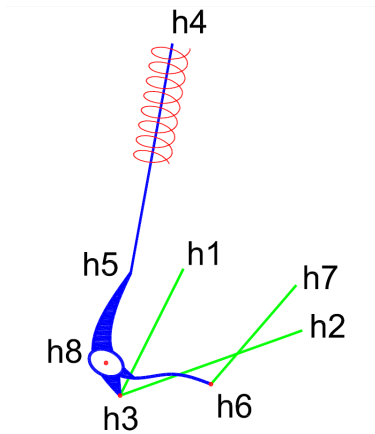


Figure 2.7: Figure of suspension with hardpoints.

Table 2.1: Table showing the hardpoints

h1	Lower wishbone front pivot
h2	Lower wishbone rear pivot
h3	Lower wishbone outer ball joint
h4	Strut upper mount point
h5	Strut slider upper axis point
h6	Outer track rod ball joint
h7	Inner track rod ball joint
h8	Wheel centre point

It is possible to divide the hardpoints in two different groups depending on whether they are part of the sprung or unsprung mass. This is of importance further in the thesis to calculate the position of the suspension when the car rolls. h1, h2, h4 and h7 are the hardpoints fixed to the body (sprung mass). The rest of the hardpoints, h3, h5, h6 and h8, form part of the unsprung mass and will remain in their position with body roll (since ride toe effect is not considered).

2.4 Steering Performance Parameters

The steering performance parameters to be studied in this thesis are all related to steering force in the rack, Figure 2.8. This means that the study is more driver-focused than vehicle-focused. Maximum force in the rack is an interesting parameter to study because it can be useful for design engineers to dimension the steering system. Force increment rate is also studied at low slip angles. This rate works as a parameter to measure the on centre steering feel and it is representative for most of the time driving a passenger vehicle at high speed. The rate at which force goes down when the vehicle loses grip is another parameter studied. This rate is useful to provide a measure of how the driver feels that the steering torque decreases, and although this is not such a common situation as straight driving, it occurs when driving in icy conditions or during evasive maneuvers. The last parameter studied is the maximum acceleration before losing grip. This last one is more performance orientated and tells how much grip is possible to gain through the suspension geometry. Depending on the intention of the vehicle, race car or passenger vehicle, the objective for these parameters may vary. This thesis is focused on passenger vehicles.

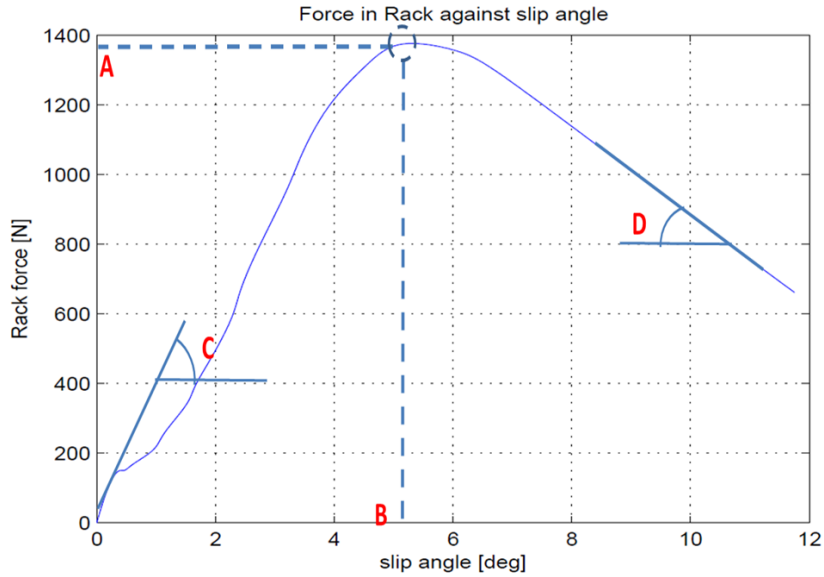


Figure 2.8: *SPPs in Rack force VS slip angle.*

2.5 Mathematical Problem

In a McPherson suspension all the links are joined to the knuckle. The real system is constrained so that every position of the knuckle corresponds to a unique position of the whole suspension system. By knowing the position and orientation of the knuckle the coordinates of all hardpoints can then be found.

The knuckle has six degrees of freedom, three translational motions in X, Y, Z and three rotational motions around X, Y, Z. The local system defined in chapter 3 has the same degrees of freedom since it is fixed to the knuckle. To know the position and orientation of this local system a system of six equations is needed. Since rotation is also involved there will be trigonometrical equations between these six so the mathematical problem to solve is a system of six non-linear equations. To make the formulation in Matlab easier the parametric variant of the Euler-Rodrigues rotation matrix is used instead of the angular one. This matrix uses the classic Rodrigues' rotation formula but including Euler notation, and is used to calculate rotation of bodies in three dimensional space. This parametrical formulation gives both an extra variable and an extra equation so the final problem is a system of seven non-linear equations. Further study of this kinematic problem is presented in Chapter 3.

2.5.1 Numerical Methods For Equations Solving

In numerical analysis there are different types of algorithms to solve mathematical problems, from simple linear equations to complex large systems of non-linear equations. The simplex method is the most used for linear problems but it is of no interest for this thesis since the problem to solve here is non-linear. It is possible to separate the non-linear algorithms in two groups: gradient-free algorithms and gradient-based algorithms. The first kind is used when the constraints cannot be differentiated well from the objective and are generally approximation models that start with a random input and look for trends that improve the initial input iteratively until a satisfactory solution is found. Some examples of gradient-free algorithms are the Pattern search algorithm, Particle swarm optimization (PSO) and genetic or evolutionary algorithms [9]. Since the mechanical problem studied in this thesis is well constrained, and the equations are differentiable, a gradient-based algorithm is employed since it is way faster and accurate. The most used method in this group, and the one chosen for this project, is the Newton-Raphson method. This algorithm requires an initial point close to the solution to assure convergence and that the solution found is the one looked for (see Figure 2.9).

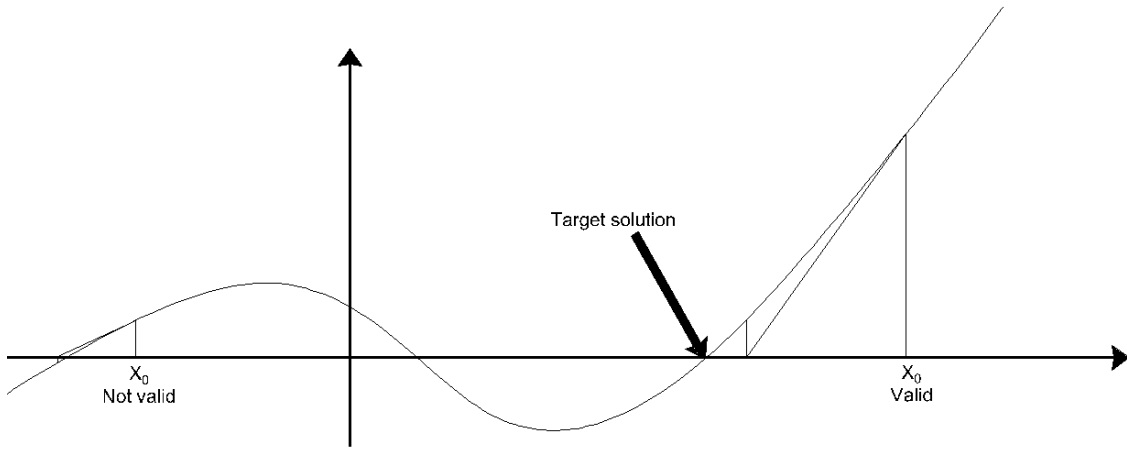


Figure 2.9: *Importance of initial conditions for non-linear functions*

Since the initial design layout of our problem is given, and the movement starts from this position in a continuous way, the initial point is not an issue. An iteration example is shown in Figure 2.10. The mathematical formulation for this algorithm is shown in Equations 2.1-2.2.

$$\mathbf{X}_{n+1} = \mathbf{X}_n - [\mathbf{J}_f(\mathbf{X}_n)]^{-1} \cdot \mathbf{f}(\mathbf{X}_n) \quad (2.1)$$

$$\|[\mathbf{J}_f(\mathbf{X}_n)]^{-1} \cdot \mathbf{f}(\mathbf{X}_n)\| < tol \quad (2.2)$$

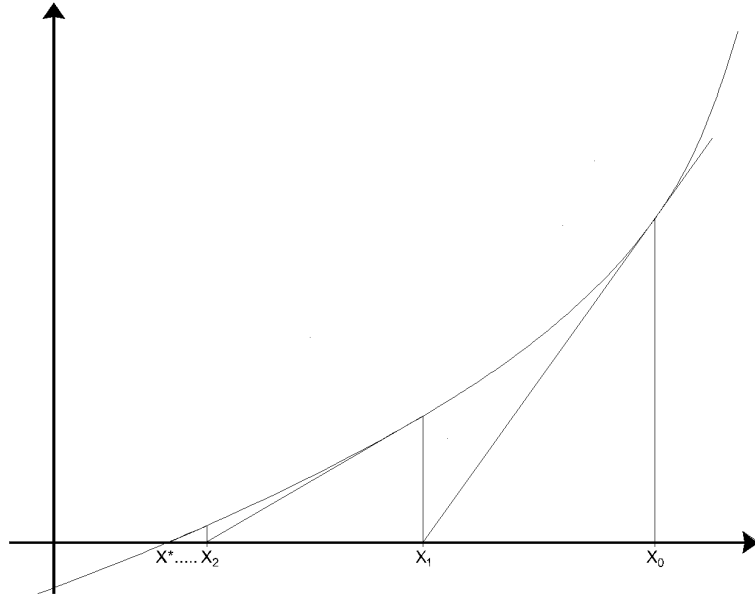


Figure 2.10: *Algorithm approximation to solution*

Where \mathbf{X} is the vector of solutions (or initial conditions in the first iteration), \mathbf{f} is the vector containing the constraint functions and \mathbf{J} is the jacobian matrix of \mathbf{f} . *tol* is the value of the maximum tolerance desired.

2.6 Pacejka Tire Model

It is necessary for this study to adopt a tire model capable to give lateral force and self-aligning torque for a certain vertical load and slip angle. This force and torque is used to calculate the SPPs. Other authors have studied tire behavior and have developed different tire models like Dugoff et al. [10] and Bernard et al. [11]. Existing models vary from empirical to purely physical and the purpose of the study determines which method is best. In this thesis the objective is not to study the tire itself so the in depth physical study of the tire is not of interest. The tire model adopted is the Magic Formula [12], of the semi-empirical type. This model is conceived to present the tire as a component for a simulation environment, thus is computationally fast and intended for the steady-state calculations carried away in this work. Since only high speed maneuvers are aimed for (chapter 1) it is not necessary to include the spin torque and the Magic Formula is sufficient to cover the thesis needs.

Pacejka's model is solely based in empirical data from tire tests. The data is statistically treated so that finally a regression model that adjusts to the reality is created. The coefficients of the regression model have a physical meaning making the magic formula a very used model as it provides physical information about tire characteristics as well as it faithfully reproduces the tire behavior. Expression 2.3 shows the simplest variant of the magic formula. This expression can be equalled to longitudinal force, lateral force or self-aligning torque depending on the coefficients used.

$$D \sin(C \arctan(B \alpha + E (\arctan(B \alpha) - B \alpha))) \quad (2.3)$$

with stiffness factor B, peak factor D, cornering stiffness factor C and curvature factor E. Depending on the values used for the different coefficients the magic formula yields longitudinal force, lateral force or self-aligning torque. Equations 2.4 to 2.8 show how these factors are calculated for lateral force and self-aligning torque [13].

$$D = a_1 \cdot F_Z^2 + a_2 \cdot F_Z \quad (2.4)$$

$$C = \begin{cases} 1.3 & \text{Numerical value for Lateral force} \\ 2.4 & \text{Numerical value for Self-aligning torque} \end{cases} \quad (2.5)$$

$$B \cdot C \cdot D = \begin{cases} a_3 \sin(a_4 \tan(a_5 \cdot F_Z)) & \text{Lateral force} \\ \frac{a_3 \cdot F_Z^2 + a_4 \cdot F_Z}{e^{a_5 \cdot F_Z}} & \text{Self-aligning torque} \end{cases} \quad (2.6)$$

$$B = \frac{B \cdot C \cdot D}{C \cdot D} \quad (2.7)$$

$$E = a_6 \cdot F_Z^2 + a_7 \cdot F_Z + a_8 \quad (2.8)$$

Where $a_1 \dots a_8$ are the coefficients that give the dependency with normal load (see Table 2.2) [13].

Table 2.2: Normal load coefficients.

	a_1	a_2	a_3	a_4	a_5	a_6	a_7	a_8
F_y	-22.1	1011	1078	1.82	0.208	0	-0.354	0.707
M_z	-2.72	-2.28	-1.86	-2.73	0.110	-0.07	0.643	-4.04

Chapter 3

Kinematic Model

3.1 Kinematic Study Purpose

Given a set of hardpoints for the front suspension, the kinematics of all these hardpoints has to be calculated in order to know the position of the suspension throughout the wheel travel and steering maneuver. The hardpoints positions (X-, Y- and Z-positions) were taken from a CAD software and the programs made in the thesis were made with these hardpoints as the main input.

3.2 Geometrical Relations

The knuckle is the solid body in which the interest is focused since this is the part that carries the wheel and will define its movement. To study the movement of this part (that will immediately give the movement of the whole suspension system) a typical approach in rigid body dynamics was used [14]. A local reference system was defined so it was possible to work with both global and local coordinates. To ease the calculations this local reference system was defined as fixed to the knuckle. The Z' direction was chosen to be the one of the strut, the X' was obtained as the cross product of the directional vector of the track rod and the Z' and finally, the Y' was defined as the cross product of Z' and X' to make the reference system orthogonal and right handed. This is illustrated in Figure 3.1.

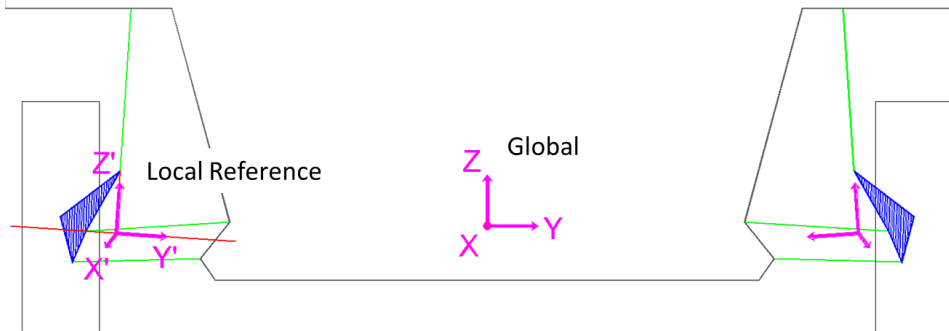


Figure 3.1: *Illustration of the local reference system in the knuckle, front view.*

It is possible to determine the movement of the knuckle by knowing, for each instant, the position and orientation of the local reference system, given a series of constraints. The local reference system has six degrees of freedom so a set of six constraint equations must be found. Using the Euler-Rodrigues rotation matrix \mathbf{B} in its parametric form (eq. 3.1) introduced another variable in the system. The new equation needed is the trigonometry relation between this new variable and the other three Euler parameters (eq. 3.2).

$$\mathbf{B} = \begin{pmatrix} 2e_0^2 + 2e_1^2 - 1 & 2e_1e_2 - 2e_0e_3 & 2e_0e_2 + 2e_1e_3 \\ 2e_0e_3 + 2e_1e_2 & 2e_0^2 + 2e_2^2 - 1 & 2e_2e_3 - 2e_0e_1 \\ 2e_1e_3 - 2e_0e_2 & 2e_0e_1 + 2e_2e_3 & 2e_0^2 + 2e_3^2 - 1 \end{pmatrix} \quad (3.1)$$

$$e_0^2 + e_1^2 + e_2^2 + e_3^2 = 1 \quad (3.2)$$

where e_0 is the cosine of half the rotated angle and $[e_1 e_2 e_3]$ is the unit vector of the rotation axis times the sine of half of the rotated angle.

These movement constraints were mathematically treated using vectors. The length constraints were specified by the magnitude of certain vectors and the fixed movements were set by means of scalar product as is shown in the following equations. “q” vectors were referred to the local system and “r” vectors to the global system. Figure 3.2 shows the points used in the calculations

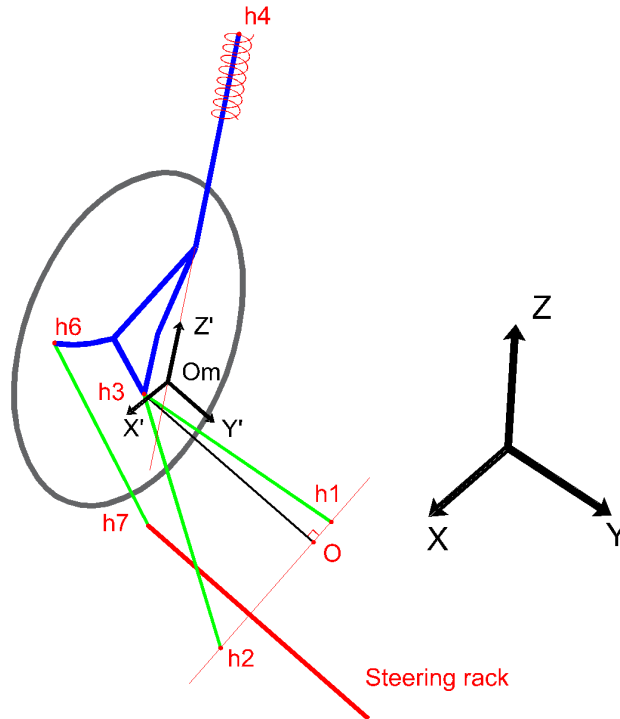


Figure 3.2: *Points used in the movement and SDFs calculations.*

For the lower control arm there are two constraints (equations 3.3 and 3.4): the fixed length of the arm and the plane of the movement respectively. This plane is the one whose normal is the axis defined by the control arm front and rear pivots in the chassis and passes through h3.

$$\left\| \vec{rOm} - \vec{rO} + \mathbf{B} \cdot \vec{q3} \right\| - R_w = 0 \quad (3.3)$$

$$\frac{(\vec{h1} - \vec{h2}) \cdot (\vec{rOm} - \vec{rO} + \mathbf{B} \cdot \vec{q3})}{\left\| \vec{h1} - \vec{h2} \right\|} = 0 \quad (3.4)$$

For the track rod the length is set as a fixed value (equation 3.5).

$$\left\| \overrightarrow{rOm} - h\vec{7} + \mathbf{B} \cdot q\vec{6} \right\| - R_s = 0 \quad (3.5)$$

The remaining three constraints come from the strut (equations 3.6 - 3.8). The length of the strut, even though it was the parameter that varied during the simulation itself, it was a fixed value in each simulation step. The last two constraints came from the orientation of the strut in the local reference system. The strut has to be perpendicular in every step to the Y' and X' axis so this gave the two remaining constraints.

$$\left\| h\vec{4} - \overrightarrow{rOm} \right\| - L_{st}^2 = 0 \quad (3.6)$$

$$\mathbf{B} \cdot (1, 0, 0)' \cdot (h\vec{4} - \overrightarrow{rOm}) = 0 \quad (3.7)$$

$$\mathbf{B} \cdot (0, 1, 0)' \cdot (h\vec{4} - \overrightarrow{rOm}) = 0 \quad (3.8)$$

The variable parameter selected as input for the mathematical model was the length from the strut top point to the origin of the local reference system. By changing this parameter, which can be viewed as a change in the spring length (compression caused by a change in road elevation for instance), the different positions of the suspension system were calculated.

3.3 SDF Calculation

According to the objective of the thesis (Chapter 1) it was necessary to calculate the suspension design factors to investigate how the SPPs are related to them and draw conclusions regarding this relation. The main SDFs of interest for this study were the ones directly related to the steering axis. Change in steering axis produces the most significant change in steering performance of the vehicle. Steering axis inclination angle as well as its ground offset and wheel centre offset were studied. Separating front view and side view it was possible to differentiate six different SDFs. Seen in the X-Z plane (side view) these were the castor angle, castor offset at ground and castor offset at wheel centre. For the front view the SDFs were the steering axis inclination angle, steering axis offset at ground and steering axis offset at wheel centre [8].

Apart from the mentioned parameters and for validation purposes the toe and camber angles were also calculated to compare them with the data from the multi body software. The results of the calculations of these SDFs are the ones illustrated in Figure 3.3.

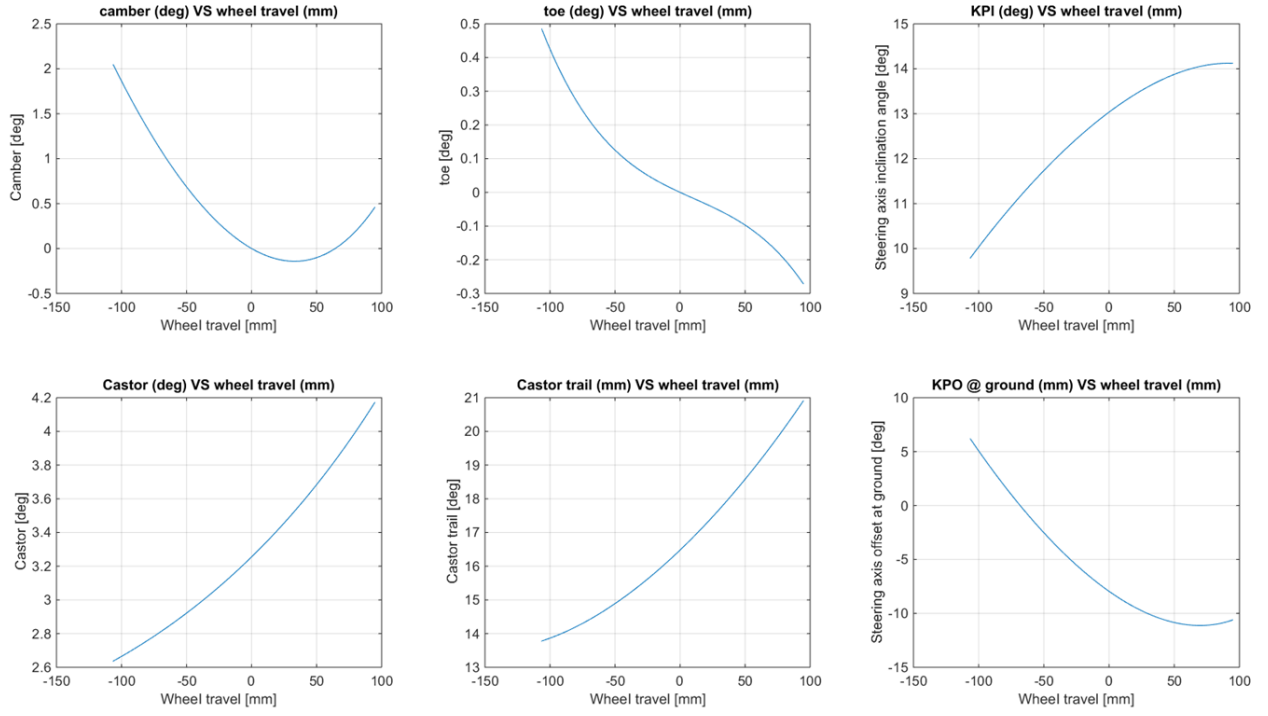


Figure 3.3: How the SDFs change due to positive (> 0) and negative (< 0) wheel travel

The steering axis offsets at wheel centre were calculated using the normal vector to the axis that passes through the wheel centre ($r_{steerWC}$). This vector was calculated by finding the intersection point between the steering axis and a plane containing the wheel centre, with the steering axis unit vector ($\vec{\lambda}$) as its normal vector. Equations 3.9 to 3.11 shows how this point was calculated.

$$\vec{\lambda} = \frac{\vec{h4} - \vec{h3}}{\|\vec{h4} - \vec{h3}\|} \quad (3.9)$$

$$\mathbf{A} = \begin{pmatrix} 1 & 0 & 0 & -\lambda(1) \\ 0 & 1 & 0 & -\lambda(2) \\ 0 & 0 & 1 & -\lambda(3) \\ \lambda(1) & \lambda(2) & \lambda(3) & 0 \end{pmatrix} \quad (3.10)$$

$$\mathbf{b} = \begin{pmatrix} h3X \\ h3Y \\ h3Z \\ \vec{\lambda} \cdot \vec{h8} \end{pmatrix} \quad (3.11)$$

The first three rows of \mathbf{A} and \mathbf{b} correspond to the parametric equations of the steering axis in 3-D and the fourth row to the equation of the plane. By solving the system of equations in equation 3.12 it was possible to obtain the wheel center point, O_{WC} , by taking the first three components of x .

$$\mathbf{A} \cdot x = \mathbf{b} \quad (3.12)$$

The vector used to calculate the SDFs later on was calculated in equation 3.13

$$r_{steerWC} = (O_{WC} - h8) \quad (3.13)$$

All of these SDFs were calculated as follows (equations 3.14 - 3.19):

$$\text{Steering axis inclination angle (KPIA)} = \arctan\left(\frac{h4_Y - h3_Y}{h4_Z - h3_Z}\right) \quad (3.14)$$

$$\text{Steering axis offset at WC} = \sqrt{r_{steerWC}(3)^2 + r_{steerWC}(2)^2} \quad (3.15)$$

$$\text{Steering axis offset at GND} = \tan(KPIA) \cdot \left(R_e - h8_Z - h3_Z + \left(\frac{h3_Y - h8_Y}{\tan(KPI)}\right)\right) \quad (3.16)$$

$$\text{Caster angle} = -\arctan\left(\frac{h3_X - h4_X}{h4_Z - h3_Z}\right) \quad (3.17)$$

$$\text{Caster offset at WC} = \sqrt{r_{steerWC}(3)^2 + r_{steerWC}(1)^2} \quad (3.18)$$

$$\text{Caster offset at GND} = \tan\left(\text{Casterangle} \cdot \left(R_e + \left(\frac{h3_X - h8_X}{\tan(\text{caster})}\right) + h8_Z - h3_Z\right)\right) \quad (3.19)$$

3.4 Matlab Implementation for the Kinematic Model

Figure 3.4 shows the process followed with the Matlab script to calculate the coordinates of the suspension throughout the wheel travel. This flowchart with the loop is meant to calculate the hardpoints for a wheel travel of $\pm 100\text{mm}$ from the design positions just for plotting and validation purposes. Further on in the project when a certain position was needed to make calculations the loop was no longer needed since it was only used for calculating a whole range. If the length parameter L_0 was known beforehand for a certain position it could be directly used as an input without starting from the beginning and doing all the loops. This length parameter was the distance between the strut top mount point and the origin of the local reference system, as defined on chapter 2

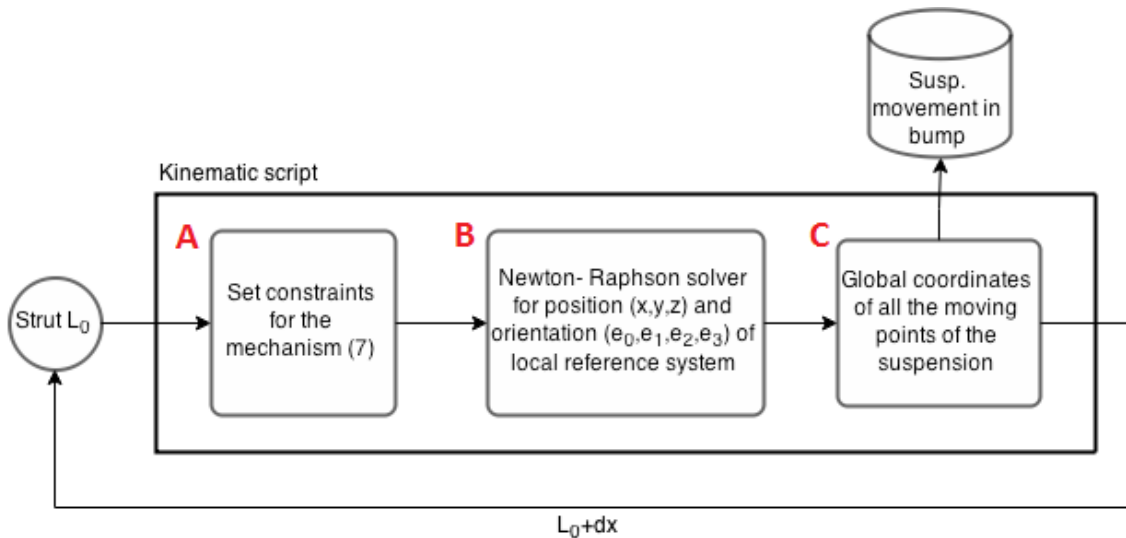


Figure 3.4: Flowchart for the Kinematic Model

The first function (block A) calculates the seven constraints for the mechanism given a series of hardpoints and lengths. The points fixed to the chassis were expressed in global coordinates and the ones in the unsprung mass were expressed in the local reference system. The lengths defined were the track rod, the lower control arm characteristic length and the strut input length parameter L_0 . The output of this function was a vector of seven equations and seven unknowns that made a system to be solved in the next step.

The Newton-Raphson function (block B) calculates the solution for the constraints system of equations using the iterative Newton-Raphson calculation process explained in the theory chapter 2. A vector X_0 was used as initial position and from this point the algorithm iterated until the error became smaller than the tolerance value and at that point the solution was given. For each step in the simulation of the suspension movement, the initial position vector X_0 used was the position calculated in the previous step. By doing this the number of iterations the solver requires was reduced and computation time was saved. It was also a way to ensure the convergence of the algorithm.

The output of the Newton-Raphson function was a seven components vector containing the global position of the local system of reference and the coefficients in the rotation matrix for the local reference system for a certain amount of wheel travel.

Finally this vector was used as an input for the last function (block C). This transformation function calculates the moving hardpoint coordinates first in the local system and then transforms the coordinates to the global system. The final output was a matrix with the global coordinates of all eight hardpoints used.

3.5 Validation of the Kinematic Model

The validation process was necessary to be able to rely on the created model and use the data extracted from it with confidence. The validation process chosen involved both visual and numerical procedures. For the visual part an animation of the suspension moving in bump and steer was performed to confirm/verify the model. This first verification permitted to check in a quick glimpse if there were major errors and it was not compared directly with any real animation from multi body software. The comparisons with the multi body software were done through the SDF plots gotten from our Matlab model and the ones from the multi body software shown in figure 3.5.

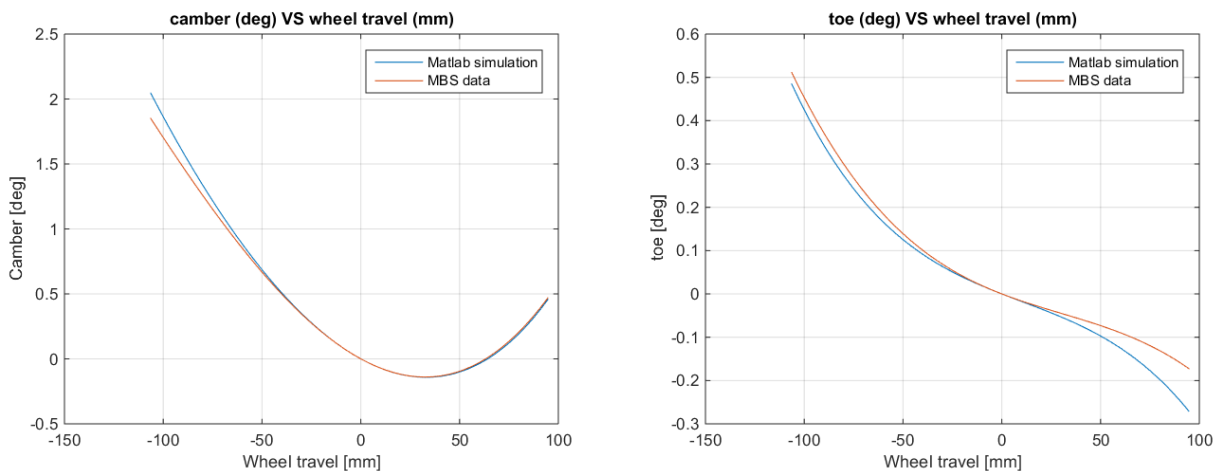


Figure 3.5: Kinematic SDF for developed Matlab model (blue) and multi body simulation (red).

By inspecting that the kinematic model worked correctly it was possible to proceed with the study and start looking into the forces in the rack. With the maximum lateral acceleration the roll of the body produced a bump/rebound of 38mm in the suspension. In this range of wheel travel (± 38 mm) the maximum relative error for camber was 1.7% and for toe 2%. This deviation far from zero travel might be explained by the fact that the multibody simulation includes bushing deflections while the Matlab model did not include them. The rest of the SDFs were in the same range of relative error.

Chapter 4

Front Axle Model

4.1 Quarter Car Model

To ease the calculations, and since the origin of the tire forces is not a main part of this thesis, an ideal scenario was used to calculate the forces into the system. The front axle was modeled as fixed to a fictitious test rig, Figure 4.2. This rig sits on a directional rolling band which gives the wheel both slip angle and angular speed. The steering was locked so there was no translation of the rack when the forces were calculated.

If the wheel and spindle were considered as a continuous solid system (this is neglecting the stiffness of the tire) it was possible to define its two degrees of freedom: wheel travel and rotation around steering axis. Since longitudinal forces and torques in the hub or brake discs were not studied the rotation of the wheel was not considered.

The system had an applied force and three reaction forces applied in four points: tire patch, lower control arm ball joint, track rod outer ball joint and strut top point. To get the steering rack force, the force at the track rod was the one that needed to be calculated. Tire patch forces and self-aligning torque were known but the rest were not. This problem was solved by doing the momentum equilibrium study around the steering axis (Equation 4.1).

$$\sum \vec{M}_\delta = (\vec{M}_Z \cdot \vec{\lambda})\vec{\lambda} + \vec{F} \times \vec{r} + \vec{F}_{steering} \times \vec{r}_2 = 0 \quad (4.1)$$

Since the forces from the strut and the lower control arm to the spindle were applied in points of the steering axis (momentum equals zero) this left the force in the track rod as the only unknown. With the force in the track rod calculated, the force in the rack was obtained just by projecting the former on the rack axis (Y-axis).

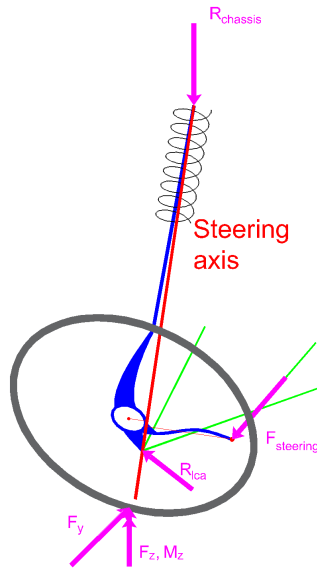


Figure 4.1: *Free body diagram of one side of the suspension*

4.2 Front Axle Study

To compute the net force in the rack it was necessary to take into account both right and left wheels. With lateral force and lateral acceleration comes body roll and load transfer which broke the symmetry and caused a net force to appear in the rack that was felt in the steering wheel. Due to body roll the geometry of the inner and outer suspension was different (bump and rebound) and due to load transfer the inner and outer lateral force and self-aligning torque were also different. Figure 4.2 shows the fictitious rig that provides this load case.

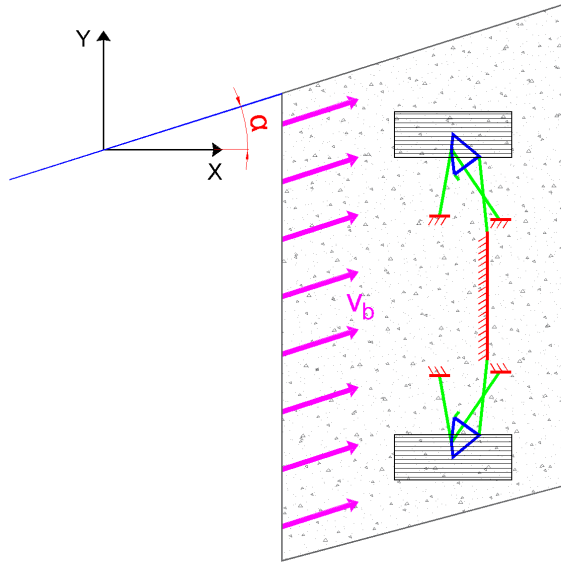


Figure 4.2: *Illustration of the half-car rig*

For the body roll study, and since the objective of this thesis was not getting exact values but trends, a roll gradient (p_x) of 4 deg/g was used in the calculations [7]. The roll centre changed from one set of hardpoints to another. On the other hand roll centre was assumed to be constant with body roll. This assumption was made due to time limitations [7] and taking into account that the conditions of the simulations did not involve body rolls greater than 3°. Roll angle (ϕ) was calculated as in Equation 4.2:

$$\text{Roll angle, } \phi = p_x \cdot \frac{a_y}{g} \quad (4.2)$$

With the roll angle it was possible to geometrically know the position of the strut upper point, $h4'$, since this point was fixed to the chassis. The origin of the local reference system (Om) did not move with the roll so with these two points' coordinates it was possible to obtain the length parameter to use in the kinematic model and obtain the rest of the points' coordinates (Equations 4.3 – 4.5).

$$R = \begin{pmatrix} \cos(\phi) & -\sin(\phi) \\ \sin(\phi) & \cos(\phi) \end{pmatrix} \quad (4.3)$$

$$\vec{h4'} = R \cdot \vec{h4} + R\vec{C} \quad (4.4)$$

$$L' = \|\vec{h4'} - \vec{O'}\| \quad (4.5)$$

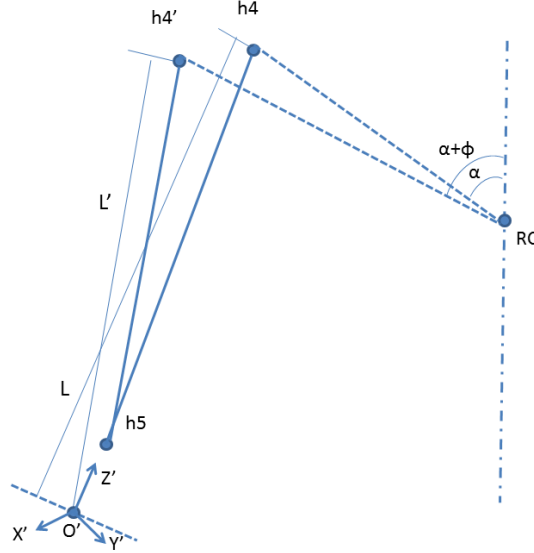


Figure 4.3: *Illustration of the change of the suspension due to roll*

R is the rotation matrix for the rolling chassis and RC is the position vector of the roll centre in the global system.

For a given lateral acceleration (a_y) the lateral load transfer was calculated as in Equation 4.6 and Equation 4.7 [15]:

$$F_{lz} = m \cdot \left(\frac{g}{2} - a_y \cdot \left(\frac{h_{CoG}}{w} \right) \right) \quad (4.6)$$

$$F_{rz} = m \cdot \left(\frac{g}{2} + a_y \cdot \left(\frac{h_{CoG}}{w} \right) \right) \quad (4.7)$$

4.3 Tire Model Calculation

There are a lot of different variants of the basic magic formula which allows studying different tire situations. One example of this is the conicity and ply-steer effects of the tire that may introduce offsets near the origin of coordinates into the formula. These effects were not taken into account for the purpose of this thesis and since the work was done at zero camber the most basic version of the magic formula with no horizontal or vertical shifts was used. The lateral force F_y was then calculated from the magic formula in Equation 4.8.

$$F_y = D_F \sin(C_F \arctan(B_F \alpha + E_F (\arctan(B_F \alpha) - B_F \alpha))) \quad (4.8)$$

For the self-aligning torque M_Z the same formula was used but with different coefficients, equation 4.9

$$M_Z = D_M \sin(C_M \arctan(B_M \alpha + E_M (\arctan(B_M \alpha) - B_M \alpha))) \quad (4.9)$$

To calculate the input forces in the model this formula was used with the vertical load previously calculated taking the load transfer into account and for a sweep of slip angles. Figures 4.4 and 4.5 show the characteristic lateral force and self-aligning torque for pure slip condition (longitudinal slip (k) = 0, no combined slip).

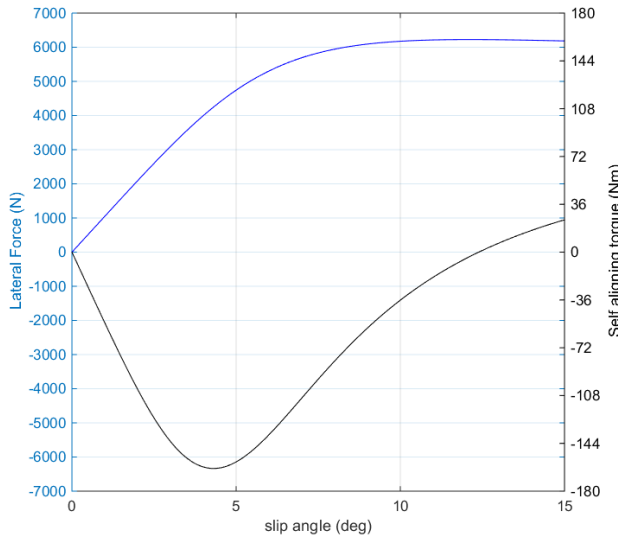


Figure 4.4: F_y and M_Z for the outer tire.

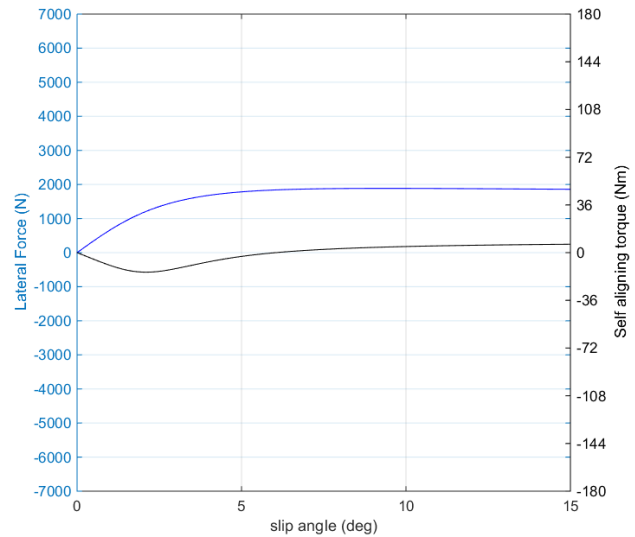


Figure 4.5: F_y and M_Z for the inner tire.

4.4 Matlab Implementation for the Force Model

The dynamic part of the Matlab program is meant to calculate the force in the rack. Figure 4.6 shows a flowchart of this Matlab model.

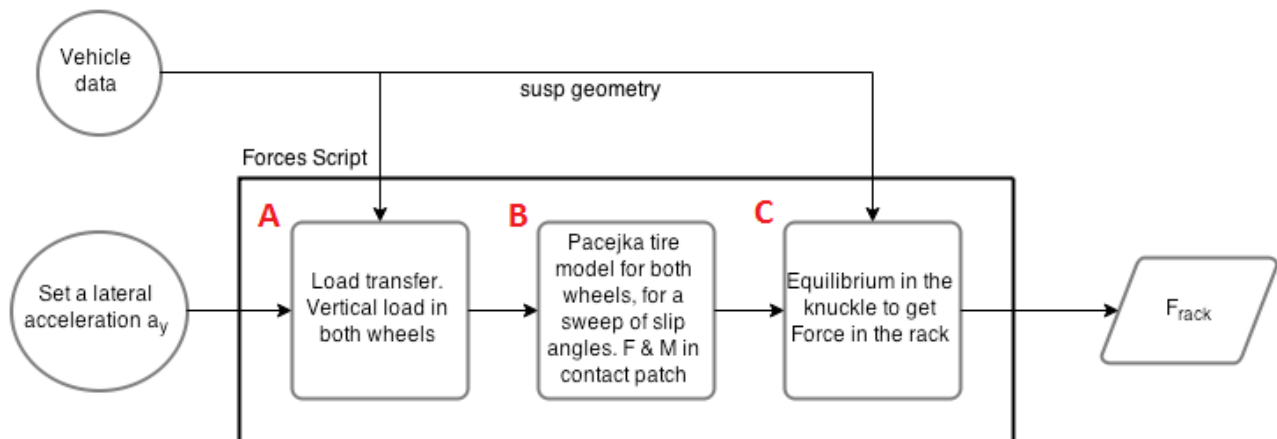


Figure 4.6: Flowchart for Force Model

The first function (block A) calculates the load transfer and the total vertical load in the two wheels given the lateral acceleration and vehicle data (centre of gravity height, track width, mass, et cetera.) given as inputs.

With the vertical load for both wheels in the front axle the second function (block B) implements the magic formula to calculate the lateral force and self-aligning torque that the wheel produced for that amount

of vertical load for a sweep of slip angles. According to the driving situation described both inner and outer wheels have the same slip angle since the road was the surface that changed direction. The lateral force in each tire was calculated so that the sum of both tires at the same slip angles gave the total amount of lateral force needed to cope with the inertia of the vehicle (Equation 4.10).

$$F_{ly} + F_{ry} = m \cdot a_y \quad (4.10)$$

The calculated force and self-aligning torque for the slip angle were used as input forces in the suspension system and the third function (block C), using again the geometry from the vehicle data, calculates the net force in the rack as shown in section 4.1.

4.5 Total Calculation Setup

The Matlab program as a whole works as described in the flowchart shown in Figure 4.7. The objective of the program is to gather data to see how forces in the rack change when changing hardpoints (and in consequence the SDFs). To gather a database with a variation of SDFs and load cases, hardpoints in the base suspension system were changed. There are three hardpoints that directly affect the chosen SDFs for this study: h3, h4 and h8. The position of these three hardpoints was changed in each iteration of the script. H3 and h4 move in all X,Y and Z directions while h8 only moves in X and Y, as a movement in Z direction could be interpreted as a change in wheel size rather than in suspension geometry.

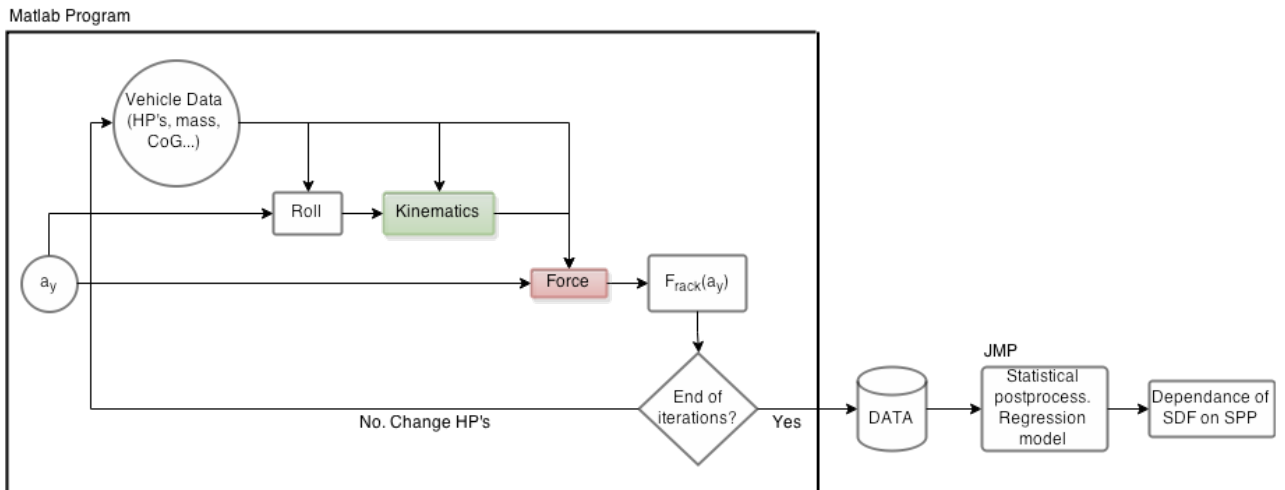


Figure 4.7: Flowchart for the general simulation

There are different design of experiments approaches to study a statistical phenomena. The most used are the factorial experiments (full or fractional) and the randomized blocks.

For these movements a fractional factorial design was discarded since there was no clear variable or correlation that could be discarded at first hand. Besides, the low calculation time of the full factorial design made the latter the chosen one.

Randomized blocks experiments such as the ones performed with latin hypercube generated data were also discarded due to the low calculation time of the full factorial and the easiness of data analysis since all the factors had a clearly stated variation values rather than random possibilities in a range. This type of experiment could reduce the simulation runs to the half but as stated before, the time was not a problem. Furthermore, to use a Latin hypercube model the level two and three interactions had to be zero and it was not possible to affirm it in this stage of the analysis.

The simulations were then carried out with a full factorial methodology in two phases. First the hardpoints were changed 10mm in positive directions and then 10mm in negative directions, h3 and h4 were moved in X-, Y- and Z-direction but h8 was only changed in the X-Y plane (see Figure 4.8). The changing hardpoints moved along the corners of the cubes and planes.

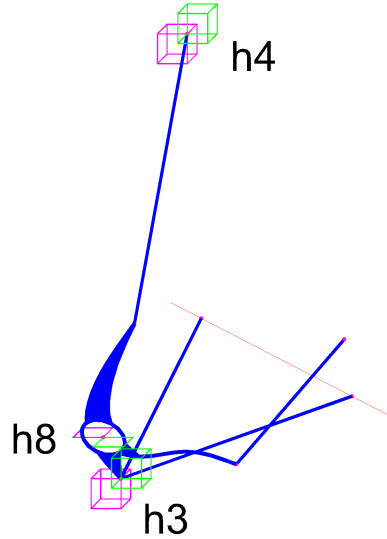


Figure 4.8: *Illustration of how the hardpoints changes*

This specific movement was chosen to remain in the design space of a vehicle. The changes could not be too big but big enough to appreciate variation in the output. This gave 512 configurations of the suspension which was more than sufficient for the study [16].

Figure 4.9 shows an example of how the force in the rack changed when moving h3 +10mm in Z-direction. The peak force increased by $\approx 100\text{N}$ and both initial and final slope were steeper.

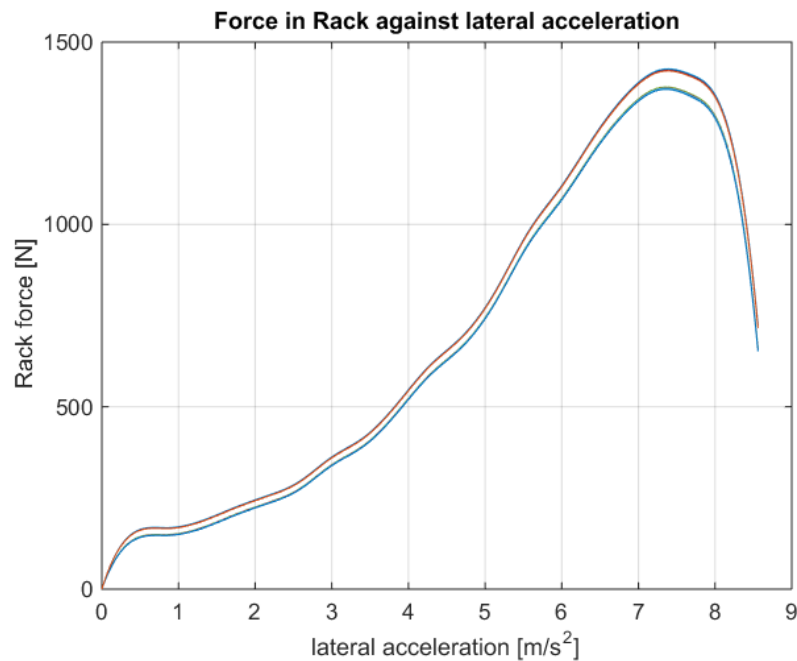


Figure 4.9: *Different force in the rack when changing h3 in Z-direction*

All this data was tabulated and for each hardpoints configuration it gave a certain value for the studied SDFs as well as the SPPs. The tabulated data was afterwards processed using JMP, a statistics software package, to see the relation between the SPPs and the SDFs and to study how good a regression model could describe these phenomena.

Chapter 5

Analyzing the Gathered Data

5.1 Data Analysis and parameters selection

To evaluate the steering performance parameters it was necessary to define them. Figure 4.9 shows the net force in the rack plotted against lateral acceleration for two hardpoints' configurations. The shape of the curves does not change from one set of hardpoints to the other. It was possible then to compare steering performance between different configurations by calculating the maximum values and rates. These parameters of study are shown in Figures 5.1 and 5.2. The first three values to study have to do with the maximum net force in the rack. These are the maximum value of the force (A in Figure 5.1 and 5.2) as well as the slip angle and lateral acceleration at which this maximum force occurs (B in Figure 5.2 and E in Figure 5.1 respectively). Observing the slopes it was possible to get information for the initial and final rates. Studying the region with small slip angles it was possible to define another parameter (C in Figure 5.2). This is the ascending force/slip rate and describes the on-centre feel. Studying the region with high slip angles the fifth and last parameter was defined, the drop rate (D in Figure 5.2). This last parameter is a way to identify the feeling in the steering wheel when the grip in the tires is lost.

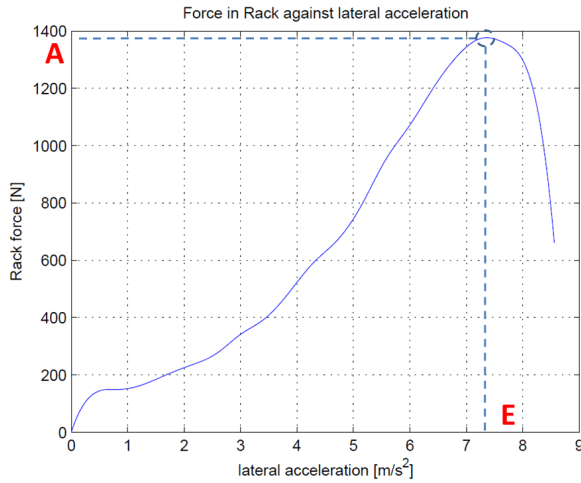


Figure 5.1: *SPPs in Rack force VS lateral acceleration.*

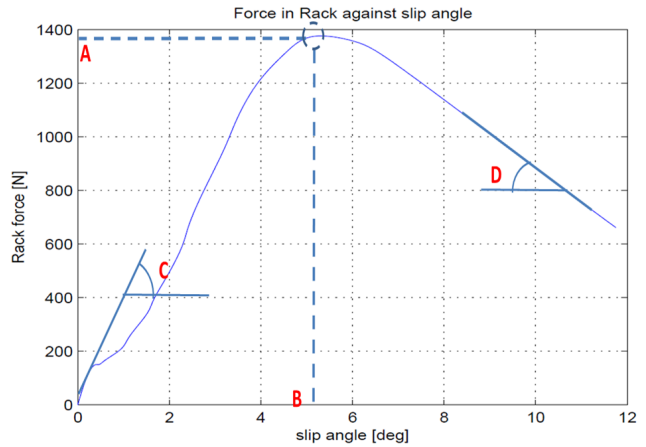


Figure 5.2: *SPPs in Rack force VS slip angle.*

Table 5.1: Table describing the SPPs

A	Maximum force in the rack
B	Slip angle at which this maximum force is obtained
C	Ascending force/slip angle rate
D	Drop rate
E	Lateral acceleration at which this maximum force is obtained

5.2 Statistical Study

The mechanical complexity of the problem made it really hard to isolate the effect of a particular SDF on the SPPs (which is the main objective of the thesis). Taking this into account, the best way to approach the problem and draw results was to statistically treat the obtained database and, through regression models, draw conclusions on the relation between SDFs and SPPs.

After running the simulations a database of 512 different suspension configurations was created with information about the value of SPPs and SDFs for each and all of them.

The objective of the statistical study was to find a model that fitted the results obtained in the 512 Matlab simulations and explained the correlation between each SDF and each SPP individually. Different models were made for each SPP. The response variable of each regression model was the SPP studied and the regressors or estimators were the SDFs.

A regression model with all SDFs and significant interactions up to fourth grade is created for all the SPPs. The first thing to study was the coefficient of determination R^2 , which measures how well the data fitted the model. As a general guideline it is possible to classify regression models oriented to prediction as shown in Table 5.2 [16].

Table 5.2: R square values classification.

< 0,3	0,3 – 0,4	0,4 – 0,5	0,5 – 0,85	> 0,85
Very bad	Bad	Regular	Good	Suspicious

Figure 5.3 shows the graphical representation of these regression models for maximum force. After eliminating all estimators with t-statistic value under 2 (p-value > 0.05) it presented an R^2 of 0.46 and adjusted R^2 of 0.44. This model was able to predict half of the variability of actual cases, and the prediction formula could be useful but not a hundred percent reliable. In any case the aim of this thesis was not that much the prediction potential of the model because it is obvious that a general formula capable of giving the SPP for any vehicle does not exist. The focus was more in the structural behavior and the impact that the estimators have on the response. Studying the p-value column in Table 5.3 it was possible to observe that all the SDFs have a significant influence in the model except for the interactions Castor * Castor offset at WC and Castor trail * Castor offset at WC. These two were not removed from the model because the adjusted R^2 decreases by doing so.

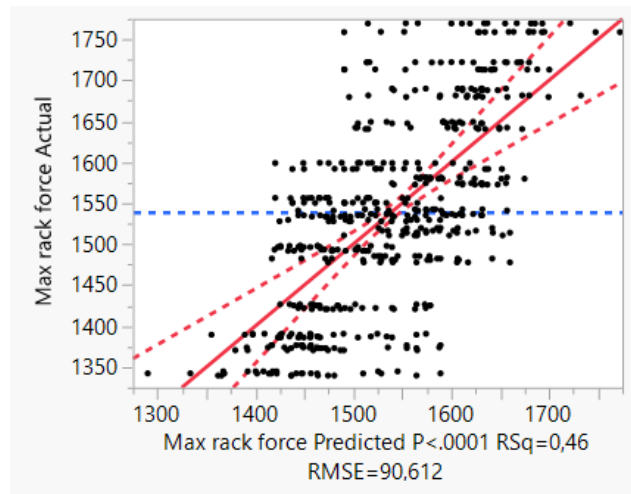


Figure 5.3: Regression model for maximal force with all SDFs.

Table 5.3: Parameter estimates table.

	Estimate	Std Error	t-Ratio	p-value	VIF
Intercept	-302,69	199,13	-1,52	0,1291	
Castor	111,29	10,34	10,76	<,0001	2,60
Castor trail	52,40	8,43	6,22	<,0001	173,99
KPO at WC	10,67	2,29	4,66	<,0001	14,49
(Castor-3,25)*(Castor offset at WC-14,45)	6,87	5,48	1,25	0,2103	2,18
(Castor trail-16,51)*(Castor offset at WC-14,45)	1,01	0,71	1,43	0,1529	5,43
(Castor-3,25)*(Castor-3,25)*(Castor trail-16,51)	-51,61	7,95	-6,49	<,0001	31,12
(Castor trail-16,51)*(Castor trail-16,51)*(Castor trail-16,51)	-0,47	0,09	-5,52	<,0001	125,78
(KPI-13,03)*(KPI-13,03)*(KPI-13,03)	-160,40	30,08	-5,33	<,0001	13,38
(KPI-13,03)*(KPI-13,03)*(KPO at GND+7,76)	-40,43	8,42	-4,8	<,0001	122,52
(KPO at WC-57,64)*(KPO at GND+7,75)*(KPO at GND+7,75)	-0,14	0,02	-6,63	<,0001	25,69
(KPI-13,03)*(KPO at GND+7,75)*(KPO at GND+7,75)	-2,70	0,51	-5,33	<,0001	94,87
(Castor-3,25)*(KPI-13,03)*(Castor offset at WC-14,45)	-55,66	18,71	-2,97	0,0031	7,79
(Castor-3,25)*(KPO at GND+7,75)*(Castor offset at WC-14,45)	-5,86	1,86	-3,16	0,0017	22,00
(Castor-3,25)*(Castor offset at WC-14,45)*(Castor offset at WC-14,45)	21,67	6,53	3,32	0,001	22,78

The Correlation or Pearson matrix (Figure 5.4) was studied to find the relation and dependence of the design factors and performance parameters in the raw data. A high correlation between the different SDFs was found. Taking only the submatrix for the SDFs it was possible to check for linear dependence between them by looking at the value of the determinant of the matrix. For this case the value is in the order of magnitude of 10^{-5} which clearly means that some of the estimators are strongly dependent [17]. This dependency was even emphasized when observing the SPPs submatrix where the determinant value is approximately 10^{-10} .

Table 5.4: Person matrix for raw data.

	Suspension Design Factors						Steering Performance parameters				
	KPI	Castor	KPO at GND	KPO at WC	Castor trail	Castor offset at WC	Max rack force	Drop rate	On centre rate	Slip at max force	Acc at max force
KPI	1,000	0,013	-0,661	-0,367	0,002	0,021	-0,061	0,008	-0,048	-0,038	-0,038
Castor	0,013	1,000	-0,008	-0,005	0,136	-0,005	0,463	0,454	0,438	0,454	0,454
KPO at GND	-0,661	-0,008	1,000	0,941	0,008	0,468	-0,122	-0,136	-0,128	-0,124	-0,124
KPO at WC	-0,367	-0,005	0,941	1,000	0,011	0,590	-0,179	-0,165	-0,180	-0,170	-0,170
Castor trail	0,002	0,136	0,008	0,011	1,000	0,013	0,283	0,277	0,266	0,277	0,276
Castor offset at WC	0,021	-0,005	0,468	0,590	0,013	1,000	-0,139	-0,110	-0,134	-0,128	-0,128
Max rack force	-0,061	0,463	-0,122	-0,179	0,283	-0,139	1,000	0,991	0,973	0,983	0,982
Drop rate (slip)	0,008	0,454	-0,136	-0,165	0,277	-0,110	0,991	1,000	0,970	0,976	0,975
On centre rate (slip)	-0,048	0,438	-0,128	-0,180	0,266	-0,134	0,973	0,970	1,000	0,916	0,914
slip for max force	-0,038	0,454	-0,124	-0,170	0,277	-0,128	0,983	0,976	0,916	1,000	1,000
Acc at max force	-0,038	0,454	-0,124	-0,170	0,276	-0,128	0,982	0,975	0,914	1,000	1,000

The Pearson matrix gives a hint of possible multicollinearity in the model. This is precisely what was not desired in the results. Multicollinearity does not affect the predictability potential of the model but makes it harder to interpret the results and separate the role that the different estimators have in it. The model tries to separate the effect of the estimators when in reality they are bound and redundant [17]. To go deeper into this analysis and tell whether multicollinearity was present or not it was possible to look into diagnosis tools like the VIF (variability inflation factor) for each estimator. This factor tells how much the standard error of an estimator increases due to the effect of collinearity. Values above 10 for this factor are worrisome and indicate presence of collinearity [18]. Figure 5.3 shows the VIF value for the different estimators in the model and it exceeded by far the value of 10 in practically all the cases. Leaving only the estimators with VIF value below 10 in the model and eliminating the rest the coefficient of determination goes drastically down to 0.25 which was a very poor value (Table 5.2). The estimators left out were castor and castor trail which are the only two SDF moderately correlated with the SPPs according to the Pearson correlation matrix for the raw data.

The space for the data is a seven dimension space (six estimators and one response for each model). Reducing the dimension of the study space could be useful for the comprehension of the problem and to get rid of some of the dependence of the variables. The scatter plots for different SDFs were studied to find patterns or ranges of values to divide the first big model into several models of smaller dimension. Scatter plots for castor (Figure

5.4) clearly presented three different ranges so new regression models were made for each different level.

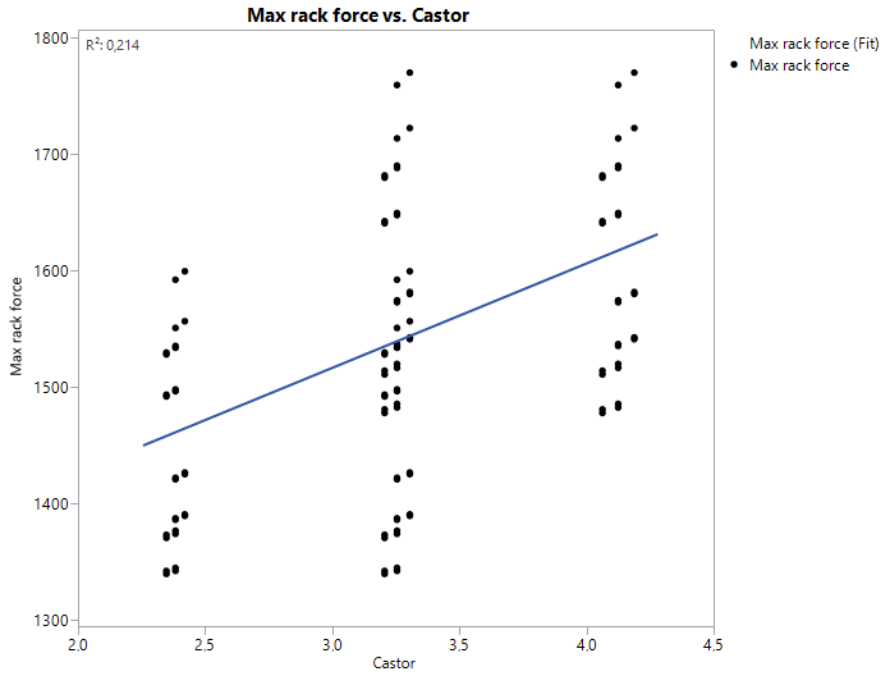


Figure 5.4: Scatter plot for castor angle VS max net force in the rack.

These models seemed to give a better fit (between 0.65 and 0.85) but looking carefully into the estimators it was found that they have high VIF values and unusually high coefficients values in the prediction formula. This is because the variance of the estimators depends on the inverse value of the determinant of the Pearson matrix for the estimators which for this new model is around 10^{-13} . This makes the variance approach infinity and makes the estimators very sensitive to the sample and thus not accurate or precise. At this point, estimators do not give any relevant information. This can basically mean that the response variable has really no relation with the estimators (which is not true because there is a physical relation) or it can also mean that the estimators used were redundant and highly correlated. Removing these estimators with high VIF from the model made the trust curves tend asymptotically to the average as shown in Figure 5.5, which indicates that the model is not significant.

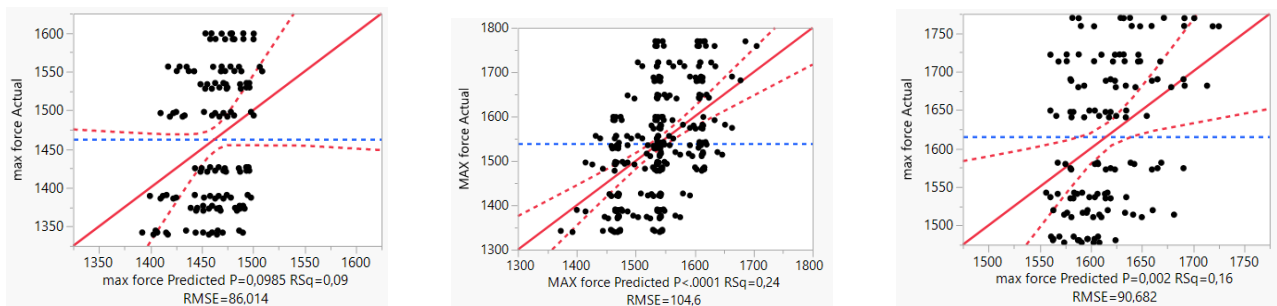


Figure 5.5: Regression for 2°, 3° and 4° castor angle

The 3° castor level is not that sensitive to removal of castor because the correlation between force and this SDF at the 3° castor angle range is not significant.

Chapter 6

Results

6.1 Suspension Model

A working kinematic model has been made from scratch including the correct movement of the unsprung mass as well as the calculation of the forces in steering rack when applying a load case for a simulated lateral acceleration. As this thesis focuses on the study of trends and not exact values the model presented in this thesis should be good enough to give an insight on what forces the steering rack feels under the simulated scenarios.

6.2 Statistic Result

The scatter plots shown in Figure 6.1 confirm that there is only relation of the SPPs with castor and castor trail.

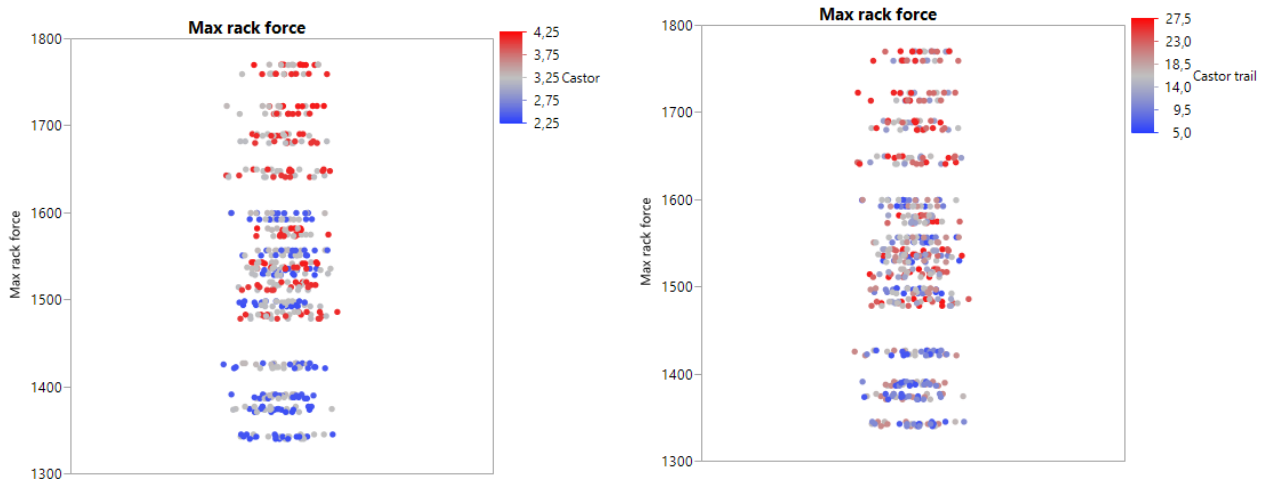


Figure 6.1: Scatter plots for Castor angle and Castor trail VS maximum force in rack.

Observing the correlation matrix for the raw data with all the SPPs and the SDFs, it was possible to see that the SPPs depend only with a correlation of 0.45 and 0.3 with the castor and castor trail. With the rest of SDFs the correlation is less than 0.15 in most cases. These correlation values support the results given by the models studied when cutting by planes of constant castor and castor trail. The relation left between the SDFs and the SPPs is so small, when taking out of the equation castor and castor trail, that the model loses its significance as shown in Figure 5.4. Another interesting result that could be obtained from the Pearson matrix is that all the studied SPPs are highly correlated with a value for the correlation coefficient above 0.9 for all cases, so the study of the trends and the structural behavior of the problem could be done studying only one of the different SPPs. The individual study of all of them would only make sense if the objective was obtaining the different coefficients for the prediction formulas but since the models explain only the 25% of the variability this formulas were better not used.

Figure 6.2 shows the regression model for max force with only castor and castor trail as regressors. Both regressors are significant in this model and there is no trace of collinearity. The numerical values of the coefficients for the estimators lack of interest because of the low R^2 .

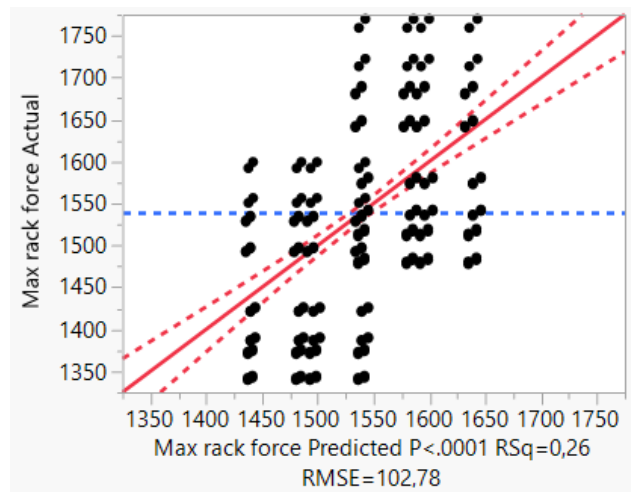


Figure 6.2: Regression model for max force with castor and castor trail as regressors.

The response surface of this model (Figure 6.3) tells that the relation of the maximum force in the rack, and by extension of all the SPPs, is positive with castor angle and castor trail. This means that increasing these two SDFs will result in an increased value of maximum force in the rack.

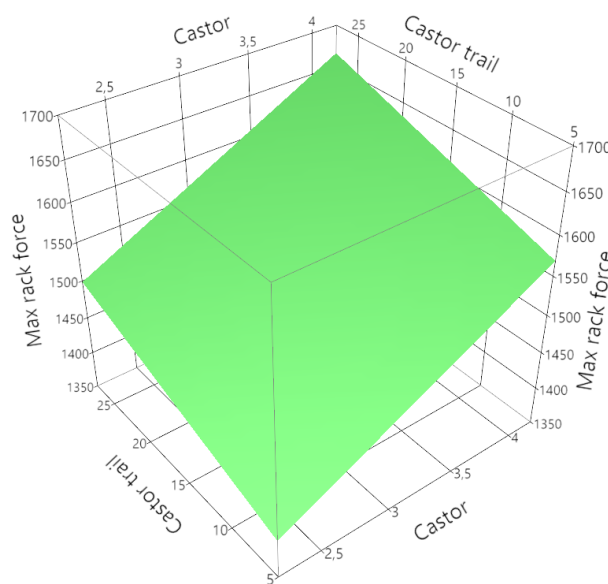


Figure 6.3: Regression surface for maximum force in the rack.

Another result derived from the statistical study is the evidence of correlation existence between SDFs. Figure 6.4 shows both the relation between KPO at ground and KPO at wheel centre and the absence of relation between these two SDFs and the SPPs.

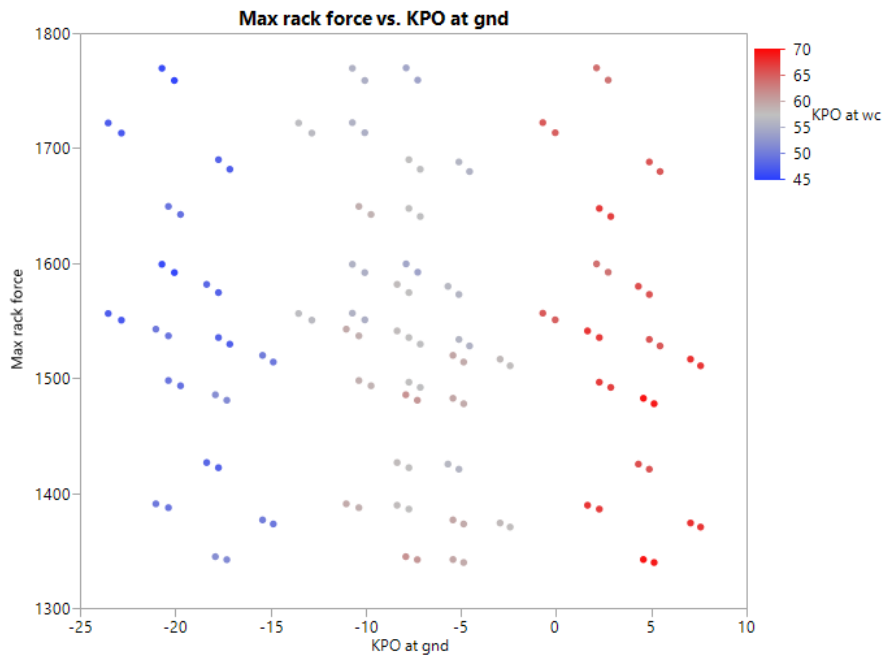


Figure 6.4: Correlation between KPO at WC and KPO at GND.

Chapter 7

Conclusions and Future Work

7.1 Conclusions

The results shown in Chapter 6 may suggest that different SDFs should have been chosen when preparing the study or that there is no general correlation between the SDFs and SPPs studied. It is logical that the estimators are highly correlated because they are all geometric parameters of the wheel steering axis. It is then obvious that changing angles will have an effect in offsets and the other way around. Thus it is difficult to isolate the effect of only one parameter.

The study of the correlation of the SDFs leaves only two variables (castor and castor trail) to study a phenomenon that depends on a lot of different things, and the model shows that two variables is not sufficient to explain most of the variability of the SPPs (only 25%). It will be necessary to introduce new SDFs to use as estimators to create a better model capable of explaining the relation between SPPs and SDFs. This argument supports the idea that the poor results obtained, in terms of explaining the correlation, are more likely caused by the lack of studied SDFs than the evidence of a non existing relation.

It is important to not forget that this master thesis tries to explain how SPPs vary in a very general framework. That is regardless of the type of suspension and other parameters. It is clear that, within a vehicle, conclusions can be drawn about each and every one of the SDFs leaving the rest fixed. For example an increase in suspension arm's length will mean higher forces, et cetera. But in a general case you cannot establish a direct relation based on a database that does not take into account all the parameters that affect the system. In this work for example the steering arm length, which is a key parameter, is not being taken into account so therefore is not possible to say with confidence what the dependence is between the different SPPs with the SDFs as we cannot know the relation between these SDFs and the steering arm (or the rest of the non-considered parameters). There are two different ways of acting on this problem: keeping all the non studied SDFs constant or monitoring their changes and include them in the statistical study.

It is possible to discuss whether the method chosen for the realization of the thesis has been adequate. A lot of time has been invested preparing the Matlab model capable of generating all the data required for the study. This has made the time available to prepare simulations very limited. Having started from scratch using a multi body program would have been beneficial to obtain the necessary database for the study and the time and effort could have been focused more on results than on preparing the Matlab model. On the other hand following this methodology would imply losing the learning advantages in using Matlab. Making a simulation environment of a suspension helps to understand how it works and this learning is very beneficial facing the design of these systems.

The results obtained are not quite the ones expected at the beginning of the work. The lack of literature regarding this topic makes it necessary to dig into an unknown field and the expectations change quickly. Rather than conclude that the results are bad it is possible to say that this thesis is only the tip of the iceberg of a way bigger problem and with this previous study done, and the computer models already developed it stands like a good starting point to keep working on the project.

7.2 Future Work

It is possible to improve the method in all its stages and keep going on obtaining more valuable results out of the topic of this master thesis. The primary points where it is necessary to take action are:

- Introduce more SDFs in the study and analyze their effect, the steering arm being the most relevant
- Verify the force calculations to be sure of its outcome
- Rethink the way of obtaining the statistical population. Aim for a random distribution to avoid repeated and ranged output.
- Minor implementations to the calculation such as including camber, ride toe, rear axle, roll centre movement, etc.

There are more design factors that affect the steering performance parameters than the ones studied in this thesis. By implementing these design factors the result will be more accurate and will show relations that are hidden when only studying the six SDFs chosen for this work. The main new design factor to take into account is the steering arm length. Adding this new design factor will add the most effective information that will have a positive impact on the results. A validation of the force model similar to the one made with the kinematic model is needed to get more trustworthy results.

A new way of getting the statistical population to analyze is needed to further improve the results. The recommendation here is to forget the full factorial design and go for a bigger population of random configurations in a wider range of movement for each hardpoint ($\pm 20\text{mm}$ instead of $\pm 10\text{mm}$ for example). This way repeated output is avoided and the complete database will have more useful information.

There are several other things that can be implemented into the model. The change of camber that is created by the wheel travel is one thing that can be implemented by expanding the tire model. The kinematics of this change is already in the model but was not considered due to time limitations. To be able to investigate more SDFs and SPPs a whole car should be implemented into the model, this meaning implementing a rear axle. It will be possible then to add the effect of ride toe to the steering of the wheels. Ride toe already exists in the kinematic model but without a rear axle it cannot be implemented. Roll centre movement with roll is another improvement to implement into the model.

Bibliography

- [1] R. Vaidya, P. Seshu, G. Arora, Study of on-center handling behaviour of a vehicle.
- [2] R. Ledesma, S. Shih, The effect of kingpin inclination angle and wheel offset on medium-duty truck handling, Tech. Rep. 2001-01-2732, SAE technical paper series (2001).
- [3] R. Rajvardhan, Effect of wheel geometry parameters on vehicle steering, Master's thesis, Ramaiah School of Advanced Studies, Bangalore (09 2010).
- [4] S. Essma, Steering effort analysis of an oval racing track setup champ car (2000).
- [5] Y.-H. J. Hsu, J. C. Gerdes, The predictive nature of pneumatic trail: tire slip angle and peak force estimation using steering torque, Tech. rep., Stanford University (2008).
- [6] B. Jacobson, Professor in Vehicle Dynamics, Chalmers University of Technology, 2015.
- [7] G. Olsson, Senior Integration Engineer, Adjunct Professor of Vehicle Dynamics, LeanNova Engineering AB, Chalmers University of Technology, 2015.
- [8] J. Y. Wong, Road vehicles – Vehicle dynamics and road-holding ability – Vocabulary (ISO 8855:2011, IDT), 2nd Edition, Swedish Standards Institute, 2012.
- [9] P. Y. Papalambros, D. J. Wise, Principles of Optimal Design : Modeling and Computation, Cambridge : Cambridge University Press, 2000.
- [10] D. et al., Tire performance characteristics affecting vehicle response to steering and braking control inputs, final report, Tech. rep., Highway Safety Research Institute, Ann Arbor, Michigan (1969).
- [11] B. et al., Tire shear force generation during combined steering and braking maneuvers, Tech. Rep. 770852, SAE technical paper (1977).
- [12] H. B. Pacejka, Tyre and vehicle dynamics, Elsevier Butterworth-Heinemann, 2004.
- [13] J. G. de Jalon, Formula magica de pacejka, Lecture notes for the course Metodos Matematicos de Especialidad (2007).
- [14] A. B. et al, Rigid body dynamics, Chalmers University of Technology, 2013.
- [15] B. J. et al, Vehicle Dynamics, Compendium for Course MMF062, Chalmers University of Technology, 2012.
- [16] J. M. R. Abuin, Regresion lineal multiple, Tech. rep., Instituto de Economia y Geografia, Madrid, Spain (2007).
- [17] R. Stine, Colinearity and multiple regression (2001).
- [18] S. O'Halloran, Lecutre 5: Model checking.

Appendices

Appendix A

Vehicle data

Table A.1: Table showing Vehicle data

mass (front)	945 kg
roll gradient	4 deg/g
wheel radius loaded	289 mm
track width	1.5 m
COG height	0.5 m

Table A.2: Table showing the hard points original position (NOT ACCORDING TO ISO)

Hard point	X-coordinate [mm]	Y-coordinate [mm]	Z-coordinate [mm]
h1	1660.748	-393.961	151.0192
h2	1959	-378	160.5
h3	1721.542	-724.545	142.444
h4	1758.84	-572.697	798.379
h5	1735.09	-600.87	377.53
h6	1862.58	-693.74	239.33
h7	1898.0	-317.5	245.0
h8	1728.1	-756.71	259.1

Appendix B

Matlab Program Manual

This appendix is a manual for the usage of the matlab code for further development. In chapters three and four we explained the flow of the matlab script with the help of several flowcharts. This manual is useful to let the user know where to change parameters and which parts to keep untouched. The code is commented so most of the information can be directly extracted from the program. The script starts with the definition of the constants that will take part in the program. Here it is possible to change vehicle characteristics such as mass, CoG height, etc. Base hard points should also be changed here. H3, h4 and h8 can be directly modified in the main script. To modify the rest of the hard points step in function 'initcondition'.

The preallocation of matrices should not be changed unless the number of the steps for the simulations is changed. In that case just adjust each case for the number of simulations desired. All the For..if..else loops that come after are just to change the hard points to get all the simulations. All this loops can be taken out and changed for some other kind of code capable of generate different hard point's configurations to do the calculations. If the loops are to be kept it is possible to change the amplitude of the movement by changing the '10' for any other value.

Here the main part of the program where all the calculations are done starts. First of all the 'SDF' function calculates the SDFs for the configuration of hard points for an iteration. You can add more SDFs as output for this function if desired and add more points or geometrical information if it is necessary to calculate these new SDFs.

After the SDFs for the static case are calculated we proceed to apply lateral acceleration. The position of the body due to body roll is obtained with the function 'roll2travel'. This function gives the length parameter for both inner and outer wheels to use later in the kinematics and obtain the whole suspension position for a certain amount of lateral acceleration.

The next two sections calculate the position of the suspension for inner and outer wheel as described on chapter 3. Nothing must be changed here unless the user wants to change the type of suspension to study. After the suspension position is known we proceed to calculate the forces in the system. Lateral load transfer is calculated and the output values of vertical load for inner and outer wheel are used as inputs for the 'magicformula' function to calculate lateral force and self-aligning torque that the wheel is capable of generating for that load and a sweep of slip angles. The range of slip angles studied is specified in the 'magicformula' function. To change this value go into the function and change the alpha value set for default as linspace(0,15). In the 'magicformula' function the shifts Sh and Sv can be uncommented to add camber effect and other wheel effects. The camber should be declared as the second input variable for this function. With the forces and self-aligning torque in the tire patch now we calculate the forces into the suspension system as described on chapter 4. The function 'forceinrack' calculates the force in the rack with the previously calculated M_inner and suspension position. Same is done for the outer wheel.

With both calculated it is possible to calculate the overall force in the rack and plot it against lateral acceleration. Add or comment plots in the plots section and the same for entries to be done in the database

Appendix C

Matlab Model Code

C.1 Matlab main program

Contents

- This script takes the set of equations to solve for each scenario and
- calculate SDFs
- System solving for each step
- forces

This script takes the set of equations to solve for each scenario and

solves them to get the movement of the system

```
clear all
clc
tic

n=1;                %number of steps
g=9.8;

%vehicle info
mass=945;
heightCoG=0.5;
trackWidth=1.5;
wheelradiusloaded=289;
aymult=0.42819;

h3=[1721.542    -724.545    142.444]; %lower wishbone outer balljoint
h4=[1758.84     -572.697     798.379]; %strut top point
h8=[1728.1     -756.71     259.1]; %wheel center point
[h1, h2, h5, h6, h7, unsprungCoG,0,u1,u2,u3,0m,x0,Rw,Rs,q3,q5,q6,q8]=...
initcondition(h3,h4,h8);

% Preallocating matrix
movement=zeros(n,7);
hardPoint3Inner=zeros(n,3);
hardPoint5Inner=zeros(n,3);
hardPoint6Inner=zeros(n,3);
hardPoint8Inner=zeros(n,3);
hardPoint3Outer=zeros(n,3);
hardPoint5Outer=zeros(n,3);
hardPoint6Outer=zeros(n,3);
hardPoint8Outer=zeros(n,3);
HPInner=zeros(8,3,n);
```

```

HPOuter=zeros(8,3,n);
uWheel=zeros(n,3);
factor=zeros(256,9);
maxforce=zeros(256,1);
slip=zeros(256,1);
slope=zeros(256,1);
ForceInner=zeros(100,3);
M_Inner=zeros(100,3);
ForceOuter=zeros(100,3);
M_Outer=zeros(100,3);
slipVSay=zeros(21,1);
ForceVSay=zeros(21,1);
latacc=zeros(21,1);

```

```

for i=1:2
if i==1
h8(1)=h8(1)-10;
else
h8(1)=h8(1)+10;
end

```

```

for j=1:2
if j==1
h8(2)=h8(2)-10;
else
h8(2)=h8(2)+10;
end

```

```

for k=1:2
if k==1
h4(1)=h4(1)-10;
else
h4(1)=h4(1)+10;
end

```

```

for l=1:2
if l==1
h4(2)=h4(2)-10;
else
h4(2)=h4(2)+10;
end

```

```

for ii=1:2
if ii==1
h4(3)=h4(3)-10;
else
h4(3)=h4(3)+10;
end

```

```

for jj=1:2
if jj==1
h3(1)=h3(1)-10;
else

```

```
h3(1)=h3(1)+10;
end
```

```
for kk=1:2
if kk==1
h3(2)=h3(2)-10;
else
h3(2)=h3(2)+10;
end
```

```
for ll=1:2
if ll==1
h3(3)=h3(3)-10;
else
h3(3)=h3(3)+10;
end
```

calculate SDFs

```
[steeringAxisInclinationAngle,steeringAxisOffsetwc,castor,...
castorTrail,steeringAxisOffsetgnd,...
steeringAxisInclinationAngleSide,steeringAxisOffsetwcSide]=...
SDF(h3,h4,h8,n,uWheel,wheelradiusloaded);
for iiii=0:20

%initialize conditions
[ LstInner, LstOuter, h4Outer, h4Inner ] = roll2travel( aymult*iiii,h1,h3,h4,h5,0m );
h4Outer=[h4(1); h4Outer]'; h4Inner=[h4(1); h4Inner]';
```

System solving for each step

```
for iii=1:1
[phi1, phi2, phi3, phi4, phi5, phi6, phi7]=...
myfunsyms(LstInner,0,Rw,Rs,q3,q6,h1,h2,h4,h7);
```

```
F=vpa([phi1, phi2, phi3, phi4, phi5, phi6, phi7]);
movement(iii,:)=newtonraphson(F,x0,0.000001,20);
```

```
[HPInner(:, :, iii), uWheel(iii, :)] = ...
transformation(movement(iii, :), q3, q5, q6, q8, h1, h2, h4, h7, u3, u2, u1);
hardPoint3Inner(iii, :) = HPInner(3, :, iii);
hardPoint5Inner(iii, :) = HPInner(5, :, iii);
hardPoint6Inner(iii, :) = HPInner(6, :, iii);
hardPoint8Inner(iii, :) = HPInner(8, :, iii);
end
```

```
for iii=1:1
[phi1, phi2, phi3, phi4, phi5, phi6, phi7]=myfunsyms(LstOuter,0,Rw,Rs,q3,q6,h1,h2,h4,h7);
F=vpa([phi1, phi2, phi3, phi4, phi5, phi6, phi7]);
movement(iii,:)=newtonraphson(F,x0,0.000001,20);
```

```
[HPOuter(:, :, iii), uWheel(iii, :)] = ...
transformation(movement(iii, :), q3, q5, q6, q8, h1, h2, h4, h7, u3, u2, u1);
```

```
hardPoint30Outer(iii, :) = HPOuter(3, :, iii);
hardPoint50Outer(iii, :) = HPOuter(5, :, iii);
hardPoint60Outer(iii, :) = HPOuter(6, :, iii);
```

```

hardPoint8Outer(iii,:) = HPOuter(8,:,iii);
end

```

forces

```

LateralForce=mass*aymult*iiii;

```

```

[normalLoadLeft, normalLoadRight] =...
lateralLoadTransfer(mass,heightCoG,trackWidth,aymult*iiii);
[FxInner,FyInner,MzInner,~,~] = magicFormula(normalLoadLeft/1000,0,1);

```

```

uw=(h4Inner-hardPoint3Inner)/norm(h4Inner-hardPoint3Inner); %steering axis
A=[ 1 0 0 -uw(1)
    0 1 0 -uw(2)
    0 0 1 -uw(3)
    uw(1) uw(2) uw(3) 0];

```

```

b=[ hardPoint3Inner(1) hardPoint3Inner(2) hardPoint3Inner(3) ...
dot(uw,hardPoint8Inner-[0 0 wheelradiusloaded])]' ;

```

```

M1=A\b;
O_tp=(M1(1:3))';
r_steer_tirepatchInner= (O_tp-(hardPoint8Inner-[0 0 wheelradiusloaded]));
for q=1:100
ForceInner(q,:)= [0 FyInner(q) normalLoadLeft];
momentInner=(cross(ForceInner(q,:),r_steer_tirepatchInner)*uw')*uw;
selfAligningInner=([0 0 -MzInner(q)*1000]*uw')*uw;
% moment_coordinatesInner=dot(momentInner,uw);
M_Inner(q,:)= selfAligningInner+momentInner;
end

```

```

f_rackInner=...
forceinrack(M_Inner,ForceInner,hardPoint3Inner,h4Inner,hardPoint5Inner,...
hardPoint6Inner,h7,hardPoint8Inner);

```

```

[FxOuter,FyOuter,MzOuter,~,alphaRange] = magicFormula(normalLoadRight/1000,0,1);
uw0=(h4Outer-hardPoint30Outer)/norm(h4Outer-hardPoint30Outer); %steering axis
uw0(2)=-uw0(2);
A2=[ 1 0 0 -uw0(1)
    0 1 0 -uw0(2)
    0 0 1 -uw0(3)
    uw0(1) uw0(2) uw0(3) 0];

```

```

b2=[ hardPoint30Outer(1) -hardPoint30Outer(2) hardPoint30Outer(3)...
dot(uw0,[hardPoint80Outer(1) -hardPoint80Outer(2) hardPoint80Outer(3)]-[0 0 wheelradiusloaded])]' ;
M2=A2\b2;
O_tp_Outer=(M2(1:3))';

```

```

r_steer_tirepatchOuter= (O_tp_Outer-([hardPoint80Outer(1) -hardPoint80Outer(2) hardPoint80Outer(3)]-...
[0 0 wheelradiusloaded]));

```

```

for q=1:100
ForceOuter(q,:)= [0 FyOuter(q) normalLoadRight];
momentOuter=(cross(ForceOuter(q,:),r_steer_tirepatchOuter)*uw0')*uw0;
selfAligningOuter=([0 0 -MzOuter(q)*1000]*uw0')*uw0;
% moment_coordinatesOuter=dot(momentOuter,uw0);

```

```

M_Outer(q,:)=selfAligningOuter+momentOuter;
end

f_rackOuter=...
forceinrack(M_Outer,ForceOuter,hardPoint3Outer,h4Outer,...
hardPoint5Outer,hardPoint6Outer,h7,hardPoint8Outer);

f_rack= f_rackInner-f_rackOuter;
LateralForceTire=FyOuter+FyInner;
x=find(LateralForceTire>=LateralForce,1);
slipVSay(iiii+1)=alphaRange(x);
ForceVSay(iiii+1)=f_rack(x);
latacc(iiii+1)=iiii*aymult;

end

ayFine = 0:0.005:aymult*20;
forceVSayFine = spline(latacc,ForceVSay,ayFine);
slipVSayFine = spline(latacc,slipVSay,ayFine);

figure (1)
plot(ayFine,forceVSayFine)
title('Force in Rack against lateral acceleration')
xlabel('lateral acceleration [m/s^2]')
ylabel('Rack force [N]')
grid on
hold on

figure (2)
plot(slipVSayFine,forceVSayFine)
title('Force in Rack against slip angle')
xlabel('slip angle [deg]')
ylabel('Rack force [N]')
grid on
hold on

figure (3)
plot(slipVSayFine,ayFine)
title('lateral acceleration against slip angle')
xlabel('slip angle [deg]')
ylabel('lateral acceleration [m/s^2]')
grid on
hold on

[F_max,pos]=max(forceVSayFine(:,:));
indexx=(i-1)*2^7+(j-1)*2^6+(k-1)*2^5+(l-1)*2^4+(ii-1)*2^3+(jj-1)*2^2+(kk-1)*2+(ll-1)*1;
indexx=[ 'id', num2str(indexx)];
DATA.(index).HardPointsInner=HPInner;
DATA.(index).HardPointsOuter=HPOuter;
DATA.(index).SDF=[steeringAxisInclinationAngle,steeringAxisOffsetwc,castor,...
castorTrail,steeringAxisOffsetgnd,...
steeringAxisInclinationAngleSide,steeringAxisOffsetwcSide];
DATA.(index).A=F_max;
DATA.(index).B=ayFine(pos);
DATA.(index).C=(forceVSayFine(1713)-forceVSayFine(1635))/(slipVSayFine(1713)-slipVSayFine(1635));

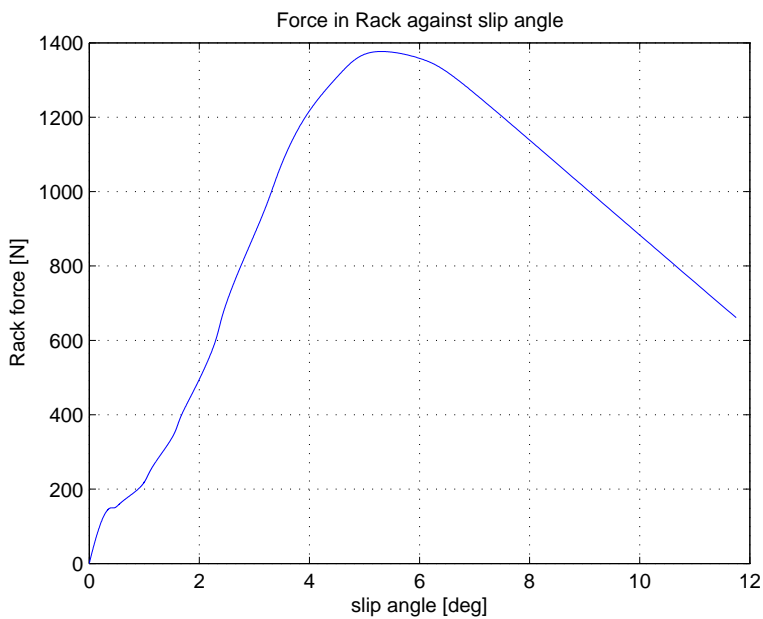
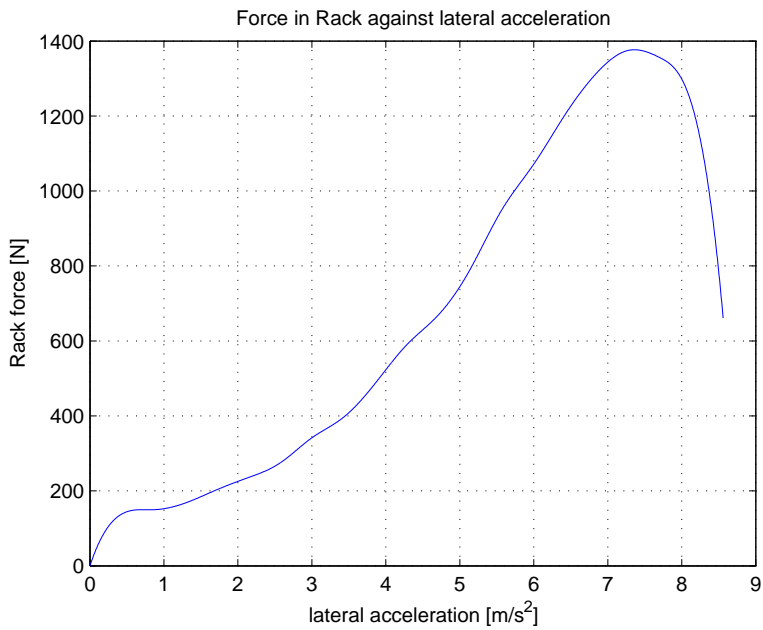
```

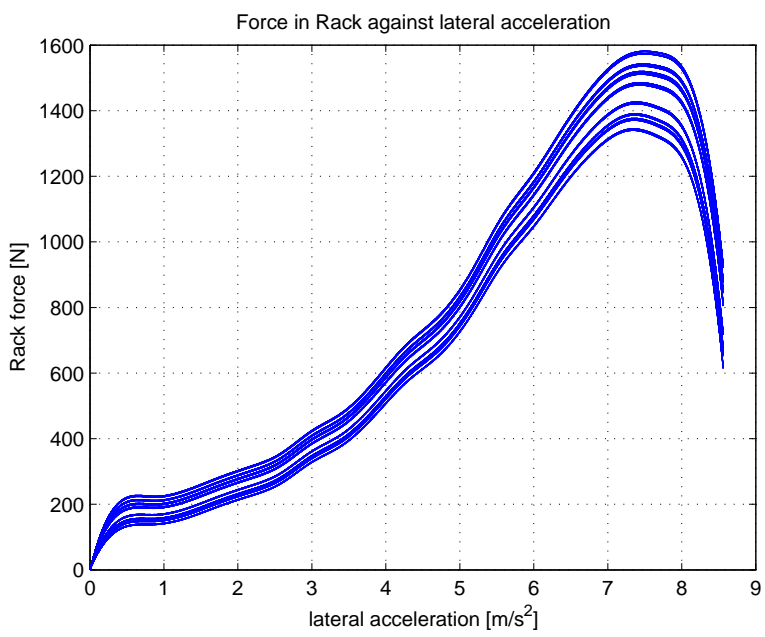
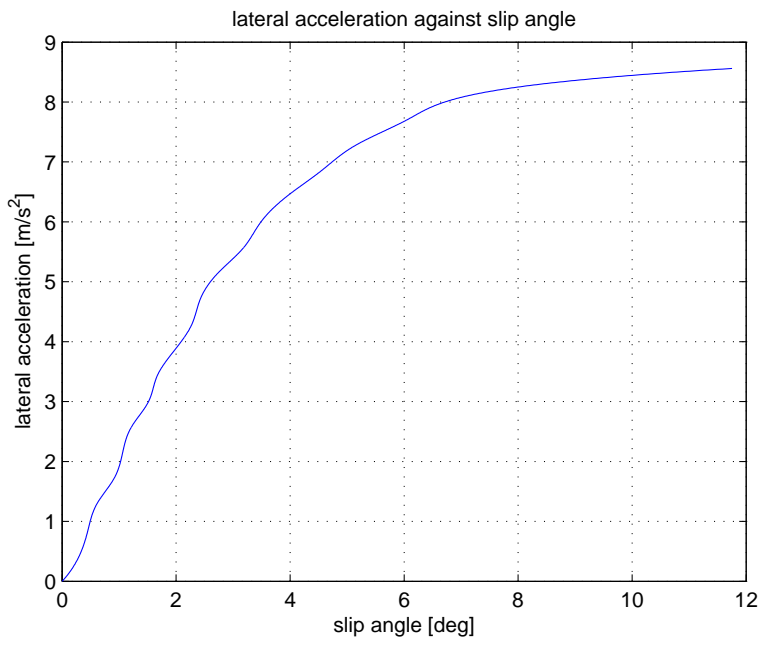
```

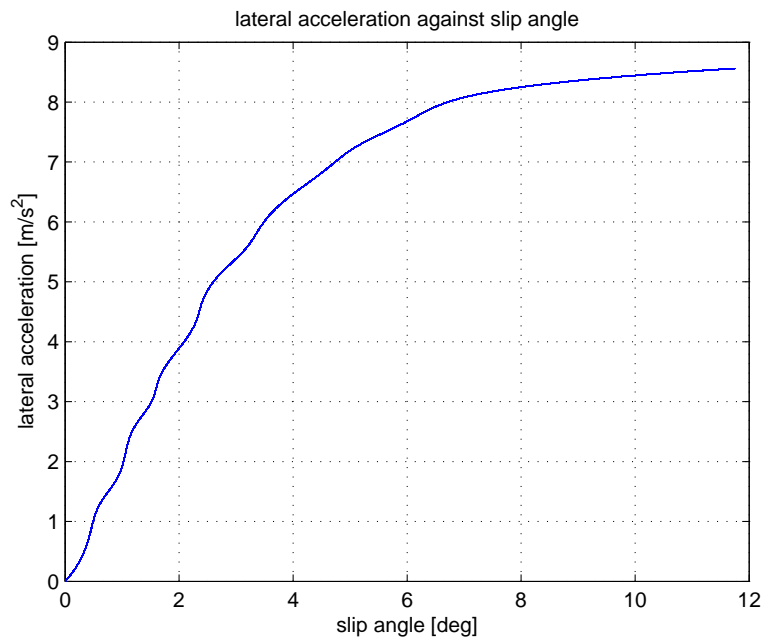
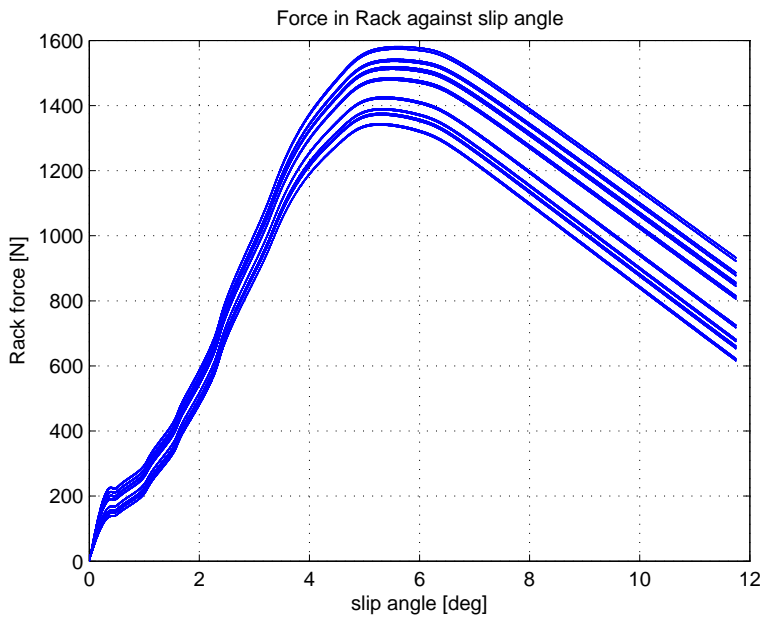
factor(indexx+1,1)=steeringAxisInclinationAngle;
factor(indexx+1,2)=steeringAxisInclinationAngleSide;
factor(indexx+1,3)=steeringAxisOffsetgnd;
factor(indexx+1,4)=steeringAxisOffsetwc;
factor(indexx+1,5)=castorTrail;
factor(indexx+1,6)=steeringAxisOffsetwcSide;
factor(indexx+1,7)=F_max;
factor(indexx+1,8)=(forceVSayFine(1713)-forceVSayFine(1635))/(slipVSayFine(1713)-slipVSayFine(1635));
factor(indexx+1,9)=(forceVSayFine(80)-forceVSayFine(1))/(slipVSayFine(80)-slipVSayFine(1));
factor(indexx+1,10)=slipVSayFine(pos);
factor(indexx+1,11)=(forceVSayFine(1713)-forceVSayFine(1635))/(ayFine(1713)-ayFine(1635));
factor(indexx+1,12)=(forceVSayFine(80)-forceVSayFine(1))/(ayFine(80)-ayFine(1));
factor(indexx+1,13)=ayFine(pos);

```

indexx







```

end
end
end
end
end
end
end
end
end

```

```
t=toc
```

```

% plot(F_max,ForceVSAy)
% figure (2)
% plot(latacc,slipVSAy)

```

```

% title('Force in Rack against slip angle at design height')
% xlabel('slip angle [deg]')
% ylabel('Rack force [N]')
% grid on
% hold on

```

C.2 Initial condition

Contents

- point O
- point Om
- fixed lengths
- Movable hardpoints coordinates in Local system

```
function [h1, h2, h5, h6, h7, unsprungCoG,0,u1,u2,u3,0m,x0,Rw,Rs,q3,q5,q6,q8]=initcondition(h3,h4,h8)
```

```

h1=[1660.748   -393.961   151.0192]; %lower wishbone front pivot
h2=[1959.    -378.     160.5]; %lower wishbone rear pivot
h5=[1735.09   -600.87   377.53]; %strut slider upper axis point
h6=[1862.58   -693.74   239.33]; %outer track rod ball joint
h7=[1898.0    -317.5    245.0]; %inner track rod ball joint 317.5
unsprungCoG=[1728.1-1   -756.71+5    259.1]; %wheel center point

```

point O

```

uw=(h1-h2)/norm(h1-h2); %Rotation axis of the wishbone
% wpn=cross(h1-h3,h2-h3)/norm(cross(h1-h3,h2-h3)); %normal vetor of wishbone plane
% nplane=cross(uw,wpn); %vector normal to the wishbone axis and contained in the plane
A=[ 1 0 0 -uw(1)
    0 1 0 -uw(2)
    0 0 1 -uw(3)
    uw(1) uw(2) uw(3) 0
    ];
b=[ h2(1) h2(2) h2(3) dot(uw,h3)]';
M=A\b;
O=(M(1:3))';
% Point calculated as an intersection of axis 1-2 and a plane perpendicular and containing h3

```

point Om

```

u1=(h4-h5)/norm(h4-h5);
uaux=(h7-h6)/norm(h7-h6);
u3=cross(uaux,u1);
u2=cross(u1,u3);
A2=[ 1 0 0 -u1(1)
     0 1 0 -u1(2)
     0 0 1 -u1(3)
     u1(1) u1(2) u1(3) 0
     ];
b2=[h4(1) h4(2) h4(3) dot(u1,h6)]';
M2=A2\b2;
Om=(M2(1:3))';
% Point calculated as an intersection of axis 4-5 and a plane perpendicular and containing h6

```

```
x0=[1726.391 -611.190 223.473 1 0 0 0]; %initial conditions for the solver
```

fixed lengths

```
Rw=norm(h3-0); % wishbone characteristic length
Rs=norm(h6-h7); % steering rod length
```

Movable hardpoints coordinates in Local system

```
q3=[u3' u2' u1']*(h3-0m); %Base change matrix * vector in global coordinates
q5=[u3' u2' u1']*(h5-0m);
q6=[u3' u2' u1']*(h6-0m);
q8=[u3' u2' u1']*(h8-0m);
```

C.3 SDF

```
function [steeringAxisInclinationAngle,steeringAxisOffsetwc,castor,...
castorTrail,steeringAxisOffsetgnd,...
steeringAxisInclinationAngleSide,steeringAxisOffsetwcSide]=...
SDF(hardPoint3,h4,hardPoint8,~,~,wheelradiusloaded)

% camber=-atand((hardPoint8(:,2)-hardPoint3(:,2))./(hardPoint8(:,3)-hardPoint3(:,3)));
% toe=asind(uWheel(:,1)./sqrt((uWheel(:,1)).^2+(uWheel(:,2)).^2));
steeringAxisInclinationAngle=atand((h4(2)-hardPoint3(:,2))./(h4(3)-hardPoint3(:,3)));
steeringAxisInclinationAngleSide=atand((h4(1)-hardPoint3(:,1))./(h4(3)-hardPoint3(:,3)));
% steeringAxisOffsetwc=sind(steeringAxisInclinationAngle(:)).*(hardPoint8(:,3)...
% -hardPoint3(:,3)+((hardPoint8(:,2)-hardPoint3(:,2))./tand(steeringAxisInclinationAngle(:))));

uw=(h4-hardPoint3)/norm(h4-hardPoint3); %steering axis
A=[ 1 0 0 -uw(1)
    0 1 0 -uw(2)
    0 0 1 -uw(3)
    uw(1) uw(2) uw(3) 0
    ];
b=[ hardPoint3(1) hardPoint3(2) hardPoint3(3) dot(uw,hardPoint8)]';
M1=A\b;
O_wc=(M1(1:3))';
r_steer_wc= (O_wc-hardPoint8);

steeringAxisOffsetwc=sqrt((r_steer_wc(3))^2+(r_steer_wc(2))^2);
steeringAxisOffsetwcSide=sqrt((r_steer_wc(3))^2+(r_steer_wc(1))^2);

% steeringAxisOffsetwcSide=sind(steeringAxisInclinationAngleSide(:)).*(hardPoint8(:,3)...
% -hardPoint3(:,3)+((hardPoint8(:,1)-hardPoint3(:,1))./tand(steeringAxisInclinationAngleSide(:))));
castor=-atand((hardPoint3(:,1)-h4(1))./(h4(3)-hardPoint3(:,3)));

castorTrail=tand(castor(:)).*(wheelradiusloaded+(((hardPoint3(:,1)-hardPoint8(:,1))./...
tand(castor(:)))+hardPoint8(:,3)-hardPoint3(:,3)));

steeringAxisOffsetgnd=tand(-steeringAxisInclinationAngle(:)).*(wheelradiusloaded-...
((hardPoint8(:,3)-hardPoint3(:,3))+((+hardPoint3(:,2)-hardPoint8(:,2))./...
tand(steeringAxisInclinationAngle)))));
```

C.4 Roll to travel

```

function [ LstInner, LstOuter, h4_outer, h4_inner ] = roll2travel( ay,h1,h3,h4,h5,Om )
%UNTITLED Summary of this function goes here
% Detailed explanation goes here
g=9.81;
K=4; %roll gradient [deg/g]
ay_g=ay/g;
alpha=K*ay_g;

h1=[h1(2) h1(3)];
h3=[h3(2) h3(3)];
h4=[h4(2) h4(3)];
h5=[h5(2) h5(3)];
ground=[-756.71      259.1-289];
Om=[Om(2) Om(3)];

a_1=(h5(2)-h4(2))/(h5(1)-h4(1)); %previous calculations for Roll center height
a=-1/a_1; %previous calculations for Roll center height
b= ((h3(2)-h1(2))/(h3(1)-h1(1))); %previous calculations for Roll center height
A1=zeros(2,2); %previous calculations for Roll center height
A1(1,1)=1; %previous calculations for Roll center height
A1(1,2)=-a; %previous calculations for Roll center height
A1(2,1)=1; %previous calculations for Roll center height
A1(2,2)=-b; %previous calculations for Roll center height
B=[((-a*h4(1))+h4(2)),((-b*h3(1)+h3(2)))]';
X=linsolve(A1,B'); %intersection point wishbone-perpendicular to strut
rch=[0 (X(1)-((ground(2)-X(1))/((ground(1)-X(2))))*X(2))-ground(2)];
%Roll centre height above ground [mm]

R_outer=[cosd(alpha) -sind(alpha)
         sind(alpha) cosd(alpha)
         ];
h4_outer=R_outer*h4'+rch';
LstOuter=norm(h4_outer-Om');

R_inner=[cosd(-alpha) -sind(-alpha)
         sind(-alpha) cosd(-alpha)
         ];
h4_inner=R_inner*h4'+rch';
LstInner=norm(h4_inner-Om');

end

```

C.5 myfunsyms

Contents

- Unknowns: Euler rodriques rotation matrix and origin of local reference system
- wishbone restrictions
- Steering rod equation
- Strut equations
- Euler constraint

```
function [phi1, phi2, phi3, phi4, phi5, phi6, phi7]=myfunsyms(Lst,0,Rw,Rs,q3,q6,h1,h2,h4,h7)
```

```
digits(50) %set number of decimals when using sym
% coder.extrinsic('syms'); %in case the script is used in simulink
```

```
X = sym('X','real');
Y = sym('Y','real');
Z = sym('Z','real');
e0 = sym('e0','real');
e1 = sym('e1','real');
e2 = sym('e2','real');
e3 = sym('e3','real');
```

Unknowns: Euler rodriques rotation matrix and origin of local reference system

```
B=2*[ e0^2+e1^2-0.5      e1*e2-e0*e3      e1*e3+e0*e2
      e1*e2+e0*e3      e0^2+e2^2-0.5      e2*e3-e0*e1
      e1*e3-e0*e2      e2*e3+e0*e1      e0^2+e3^2-0.5
      ];
```

```
r0m=[X Y Z];
```

wishbone restrictions

```
a=(h1-h2)/norm(h1-h2); %wishbone rotation axis
phi1=(norm(r0m+(B*q3)')-0))-Rw; %length constraint
phi2=dot(a,(r0m+(B*q3)')-0)); %plane of movement perpendicular to axis constraint
```

Steering rod equation

```
phi3= (norm(r0m+(B*q6)')-h7))-Rs; %Length constraint
```

Strut equations

```
phi4=B(:,1)'*((h4-r0m))'; %normal to x'' and y'' (Local reference axis)
phi5=B(:,2)'*((h4-r0m))';
phi6=(norm(h4-r0m))^2-Lst^2; %length constraint
```

Euler constraint

```
phi7=e0^2+e1^2+e2^2+e3^2-1;
```

```
end
```

C.6 Newton-Raphson

solution by the Newton-Raphson iteration method

f is the functions vector x0 is the initial conditions vector tol is the tolerance of the algorithm c is maximum number of iterations until reaching a solution

```
function sol=newtonraphson(f,x0,tol,c)
digits(50)
i=0;
jac=jacobian(f);
vars=findsym(f);
deltax=x0;
while norm(deltax)>norm(x0)*tol && i<c
```

```

    fx0=vpa(subs(f,vars,x0));
    dfx0=vpa(subs(jac,vars,x0));
    deltax=dfx0\(-fx0)';
    x0=x0+deltax';
    i=i+1;
end
if i<c
    sol=x0;
else
    sol= 'no convergence';
end

```

C.7 Transformation

Contents

- new set of hardpoints

```
function [HP,uWheel] =transformation(movement,q3,q5,q6,q8,h1,h2,h4,h7,u3,u2,u1)
```

```

B=2*[ movement(4)^2+movement(5)^2-0.5, ...
movement(5)*movement(6)-movement(4)*movement(7), ...
movement(5)*movement(7)+movement(4)*movement(6);
movement(5)*movement(6)+movement(4)*movement(7), ...
movement(4)^2+movement(6)^2-0.5, ...
movement(6)*movement(7)-movement(4)*movement(5);
movement(5)*movement(7)-movement(4)*movement(6), ...
movement(6)*movement(7)+movement(4)*movement(5), ...
movement(4)^2+movement(7)^2-0.5];

```

new set of hardpoints

```

h3=movement(1:3)+(B*q3)';
h5=movement(1:3)+(B*q5)';
h6=movement(1:3)+(B*q6)';
h8=movement(1:3)+(B*q8)';

```

```

HP = [h1
      h2
      h3
      h4
      h5
      h6
      h7
      h8
      ];

```

```

b=[0 -1 0]';
uWheelM=[u3' u2' u1']*b;
uWheel=B'*uWheelM/norm(B'*uWheelM);
end

```

C.8 Lateral load transfer

```
function [normalLoadLeft, normalLoadRight] = lateralLoadTransfer(mass,heightCoG,trackWidth,ay)
```

```

g=9.81;

normalLoadLeft = mass*((g/2)-ay*(hightCoG/trackWidth));
percentageLeft = normalLoadLeft/(mass*g);

normalLoadRight = mass*((g/2)+ay*(hightCoG/trackWidth));
percentageRight = normalLoadRight/(mass*g);

end

```

C.9 Magic formula

Contents

- Longitudinal force (there is not variation between left and right wheels)
- Lateral force
- Aligning moment

```

function [Fx,Fy,Mz,x,alpha] = magicFormula(Fz,camber,~)

% w      angular velocity of the wheel
% rd     reference radius
% vAx    longitudinal velocity of the wheel centre
% vAy    transversal velocity of the wheel centre
% Fz     vertical force, normal to the ground (kN)
% r      distance from the centre to the ground
% gamma  camber angle
% Pacejka parameters

% Pacejka parameters
pacejka.BCD=[];
pacejka.fz = [2,4,6,8]';
% Longitudinal force
pacejka.a_Fx = [-21.3, 1144, 49.6, 226, 0.069, -0.006, 0.056, 0.486];
pacejka.BCD_Fx= [0.178*1.55*2193
                0.171*1.69*4236
                0.210*1.67*6090
                0.214*1.78*7711];
pacejka.Sv_Fx = [25, 70.6, 80.1, 104]';
pacejka.Sh_Fx = [0, 0, 0, 0]';
% Lateral force
pacejka.a_Fy = [-22.1, 1011, 1078, 1.82, 0.208, 0.000, -0.354, 0.707,...
                0.028, 0.000, 14.8, 0.022, 0.000];
pacejka.Sv_Fy = [-118, -156, -181, -240]';
pacejka.Sh_Fy = [-0.280, -0.049, -0.126, -0.125]';
% Aligning moment
pacejka.a_Mz = [-2.72, -2.28, -1.86, -2.73, 0.110, -0.070, 0.643, -4.04,...
                0.015,-0.066, 0.945, 0.030, 0.070];
pacejka.Sv_Mz = [-12.5, -11.7, -6.0, -4.22]';
pacejka.Sh_Mz = [-0.464, -0.082, -0.125, 0.009]';

X=linspace(-100,100);
alpha=linspace(0,15);

```

Longitudinal force (there is not variation between left and right wheels)

```
D = pacejka.a_Fx(1)*Fz^2+pacejka.a_Fx(2)*Fz;
C = 1.65;
% The BCD values for Fx are obtained by means of interpolation
BCD = (pacejka.a_Fx(3)*Fz^2+pacejka.a_Fx(4)*Fz)/(exp(pacejka.a_Fx(5)*Fz));
B = BCD/(C*D);
E = pacejka.a_Fx(6)*Fz^2+pacejka.a_Fx(7)*Fz+pacejka.a_Fx(8);
Sv = interpo2(pacejka.fz,pacejka.Sv_Fx,Fz);
Sh = interpo2(pacejka.fz,pacejka.Sh_Fy,Fz);
x=X+Sh;
Fx = D*sin(C*atan(B*x-E*(B*x-atan(B*x))))+Sv;
```

Lateral force

```
D = pacejka.a_Fy(1)*Fz^2+pacejka.a_Fy(2)*Fz;
C = 1.30;
BCD = pacejka.a_Fy(3)*sin(pacejka.a_Fy(4)*atan(pacejka.a_Fy(5)*Fz));
B = BCD/(C*D);
E = (pacejka.a_Fy(6)*Fz^2+pacejka.a_Fy(7)*Fz+pacejka.a_Fy(8))/(1-pacejka.a_Fy(13)*abs(camber));
% Sh = interpo2(pacejka.fz,pacejka.Sh_Fy,Fz)+pacejka.a_Fy(9)*camber;
% Sv = interpo2(pacejka.fz,pacejka.Sv_Fy,Fz)+(pacejka.a_Fy(10)*Fz^2+pacejka.a_Fy(11)*Fz)*camber;
xd = alpha; %Sh+alpha;
Fy = D*sin(C*atan(B*xd-E*(B*xd-atan(B*xd)))));
Fy = Fy; %+ Sv;
```

Aligning moment

```
D = (pacejka.a_Mz(1)*Fz.^2+pacejka.a_Mz(2)*Fz);
C = 2.40;
BCD = (pacejka.a_Mz(3)*Fz^2+pacejka.a_Mz(4)*Fz)/(exp(pacejka.a_Mz(5)*Fz));
B = BCD/(C*D);
E = (pacejka.a_Mz(6)*Fz^2+pacejka.a_Mz(7)*Fz+pacejka.a_Mz(8))/(1-pacejka.a_Mz(13)*abs(camber));
% Sh = interpo2(pacejka.fz,pacejka.Sh_Mz,Fz)+pacejka.a_Mz(9)*camber;
% Sv = interpo2(pacejka.fz,pacejka.Sv_Mz,Fz)+(pacejka.a_Mz(10)*Fz^2+pacejka.a_Mz(11)*Fz)*camber;
xd = alpha; %Sh+alpha;
Mz = D*sin(C*atan(B*xd-E*(B*xd-atan(B*xd)))));
Mz = Mz; %+ Sv;
```

C.10 Force in the rack

```
function f_rack=forceinrack(M,Force,h3,h4,h5,h6,h7,h8)
```

```
uw=(h4-h3)/norm(h4-h3); %steering axis
A=[ 1 0 0 -uw(1)
    0 1 0 -uw(2)
    0 0 1 -uw(3)
    uw(1) uw(2) uw(3) 0
    ];
b=[ h3(1) h3(2) h3(3) dot(uw,h6)]';
M1=A\b;
O_st=(M1(1:3))';
% Point calculated as an intersection of axis 3-4 and a plane perpendicular and containing h6
r_steer_str= (O_st-h6);
u_steer=(h6-h7)/norm(h6-h7);
```

```

% chi1=zeros(100,3);
R_steel=zeros(100,3);
f_rack=zeros(1,100);

for i=1:100
%   chi1(i,:)=-dot(M(i,:),uw)*uw-cross(Force(i,:),r_tireforce);

%   R_steel(i,:)=-u_steel*norm(chi1(i,:))/(norm(r_steel_str)*norm(cross(u_steel,r_steel_str))/...
% (norm(u_steel)*norm(r_steel_str)));

%   f_rack(i)=R_steel(i,2);
%   dir=cross(u_steel,r_steel_str);
%   R_steel(i,:)=[M(i,1)/dir(1) M(i,2)/dir(2) M(i,3)/dir(3)];
%   f_rack(i)=R_steel(i,2);
R_steel=norm(M(i,:))/(sin(acos(dot(r_steel_str,u_steel)/norm(r_steel_str)))*norm(r_steel_str));
f_rack(i)=R_steel*u_steel(2);
end

```

C.11 interpo

```

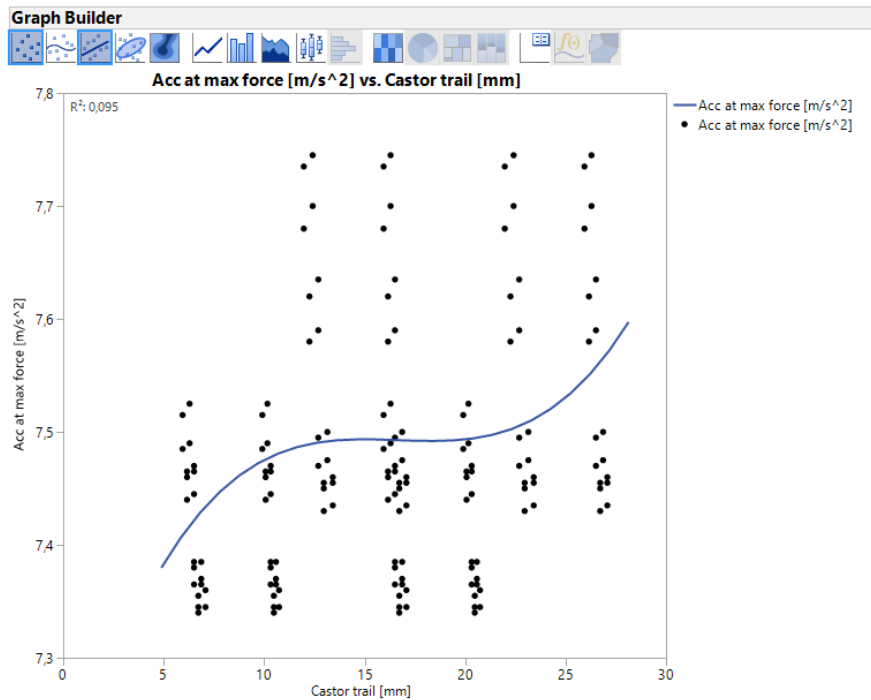
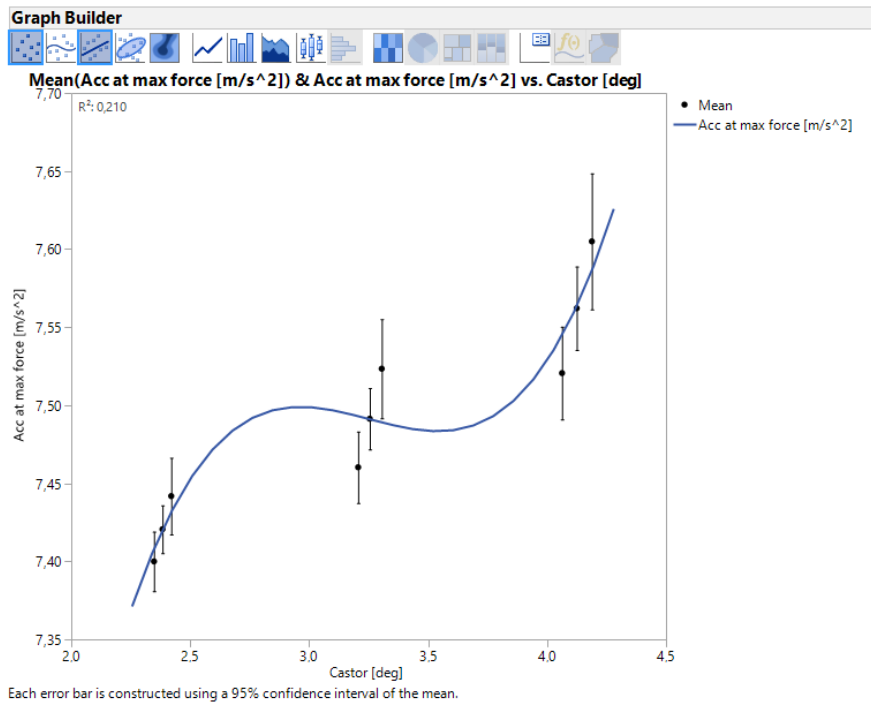
function y = interpo2(X,Y,x)
n=length(X);
b=Y;
for j=2:n
    for i=n:-1:j
        b(i)=(b(i)-b(i-1))/(X(i)-X(i-j+1));
    end
end
y=b(1)+b(2)*(x-X(1))+b(3)*(x-X(1))*(x-X(2))+b(4)*(x-X(1))*(x-X(2))*(x-X(3));

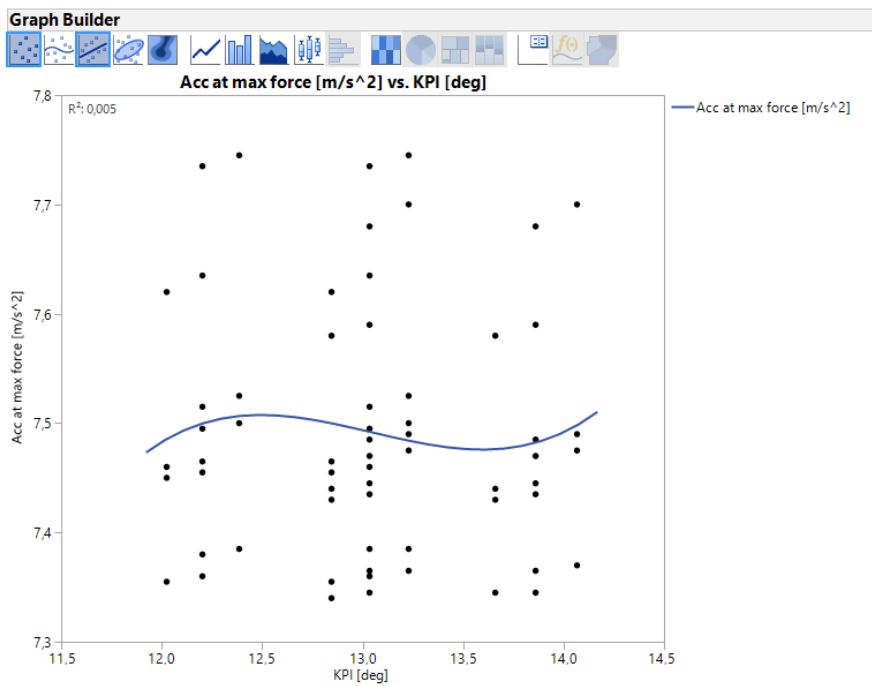
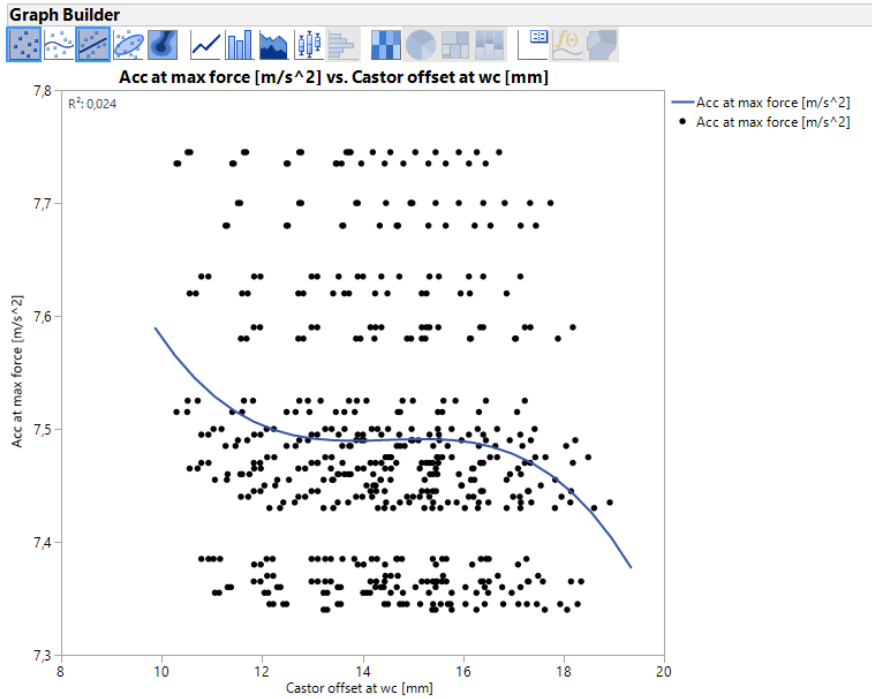
```

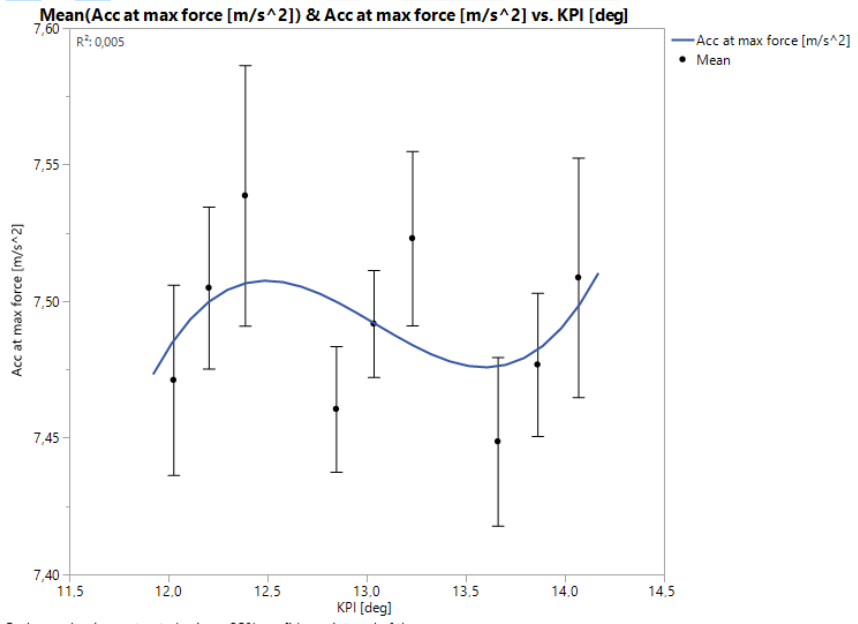
Appendix D

Statistical Data

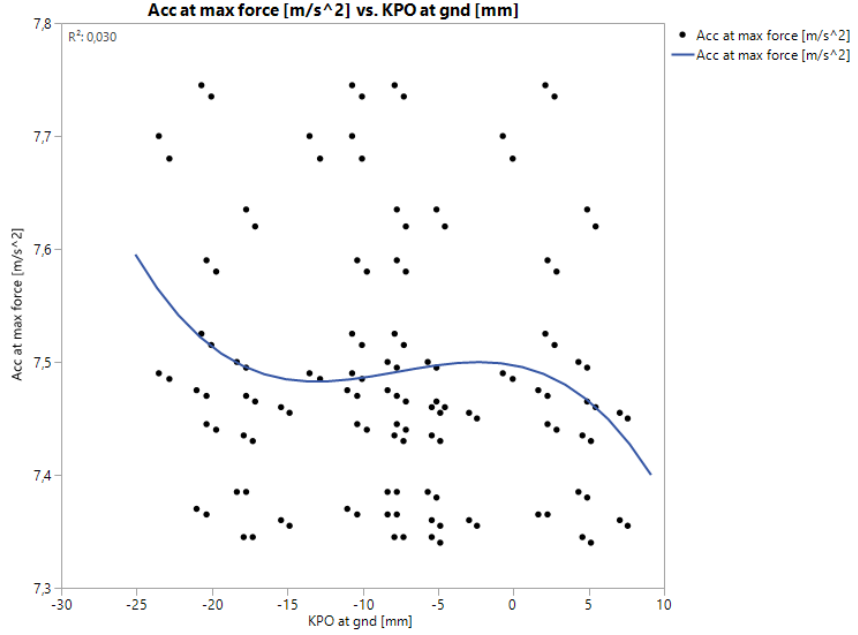
D.1 Lateral acceleration at maximum force



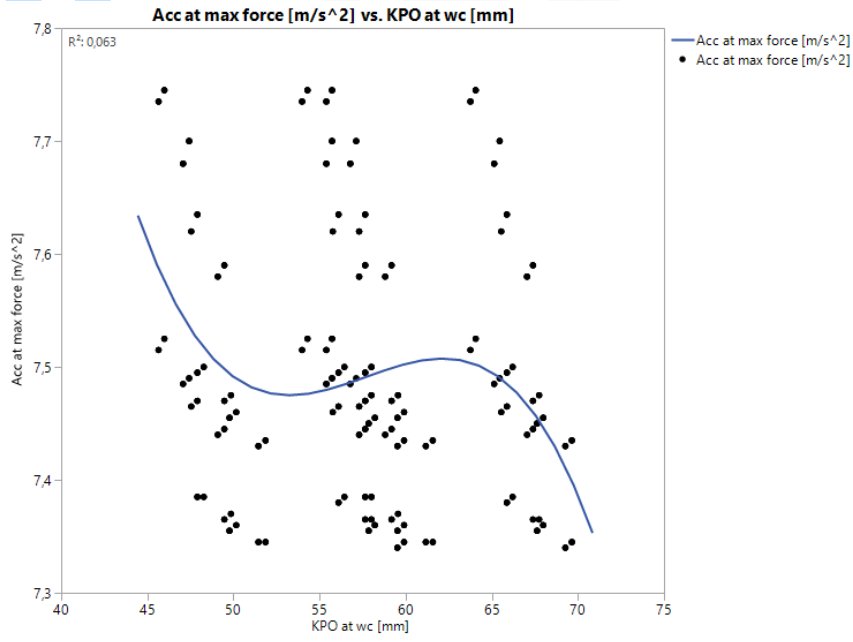




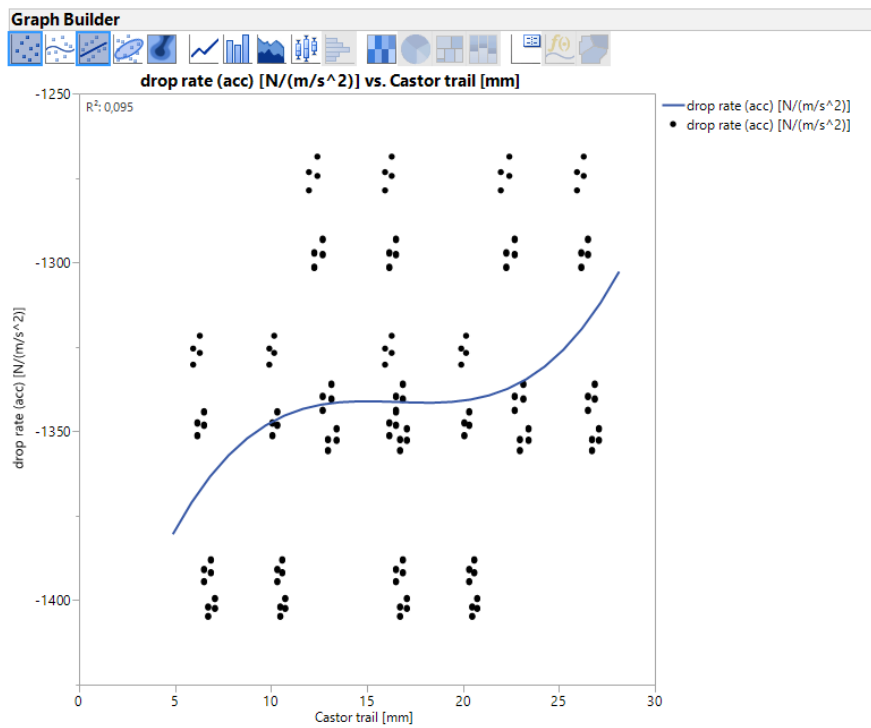
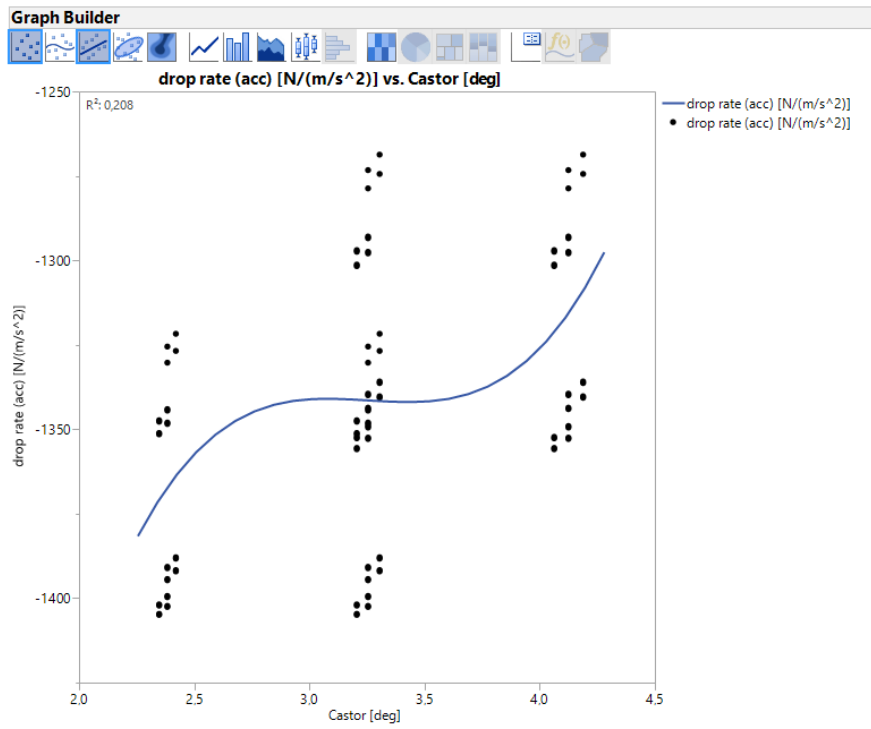
Each error bar is constructed using a 95% confidence interval of the mean.

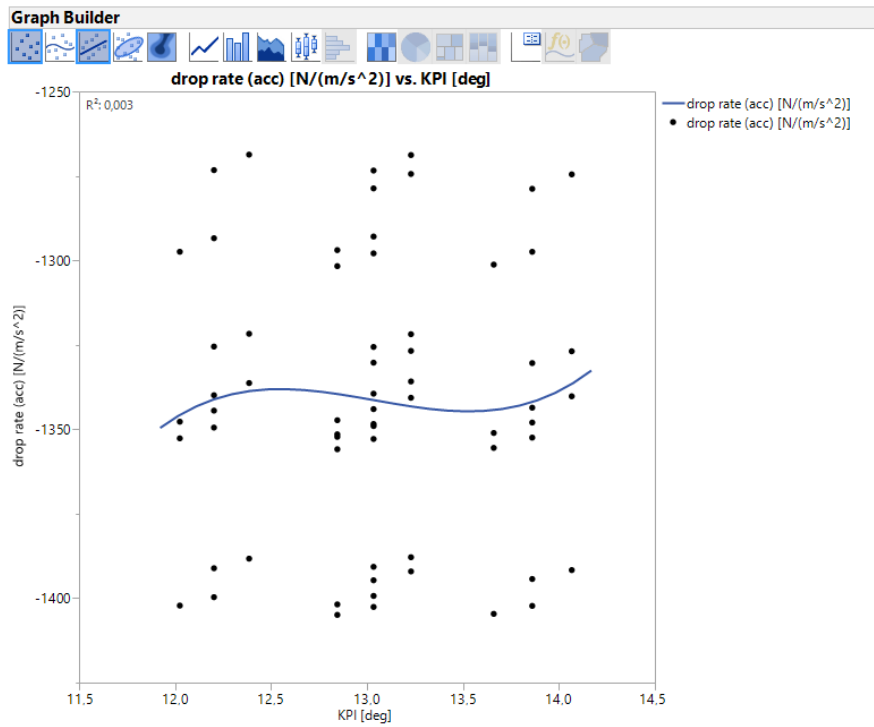
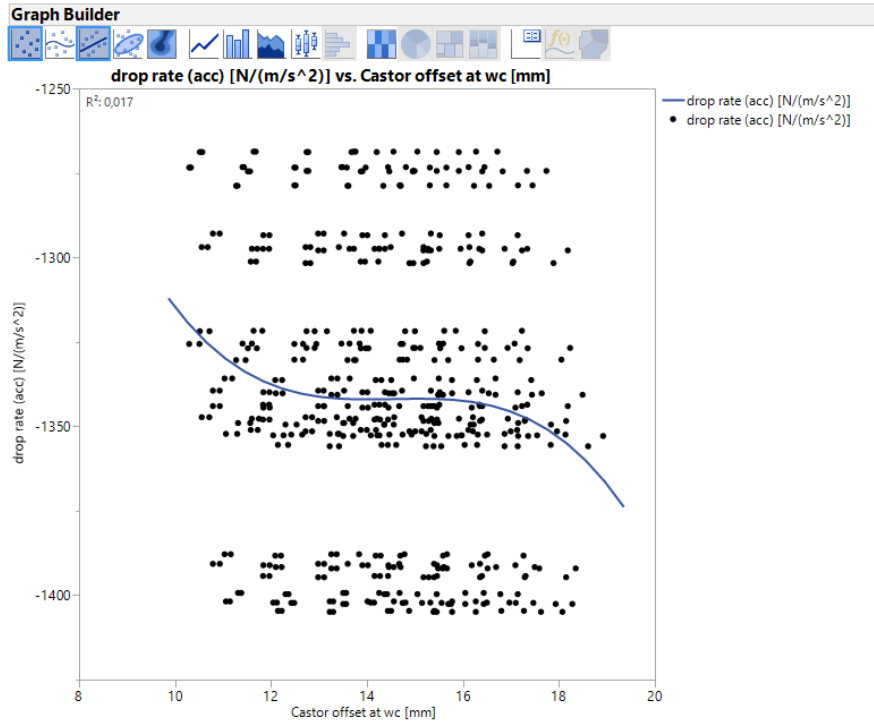


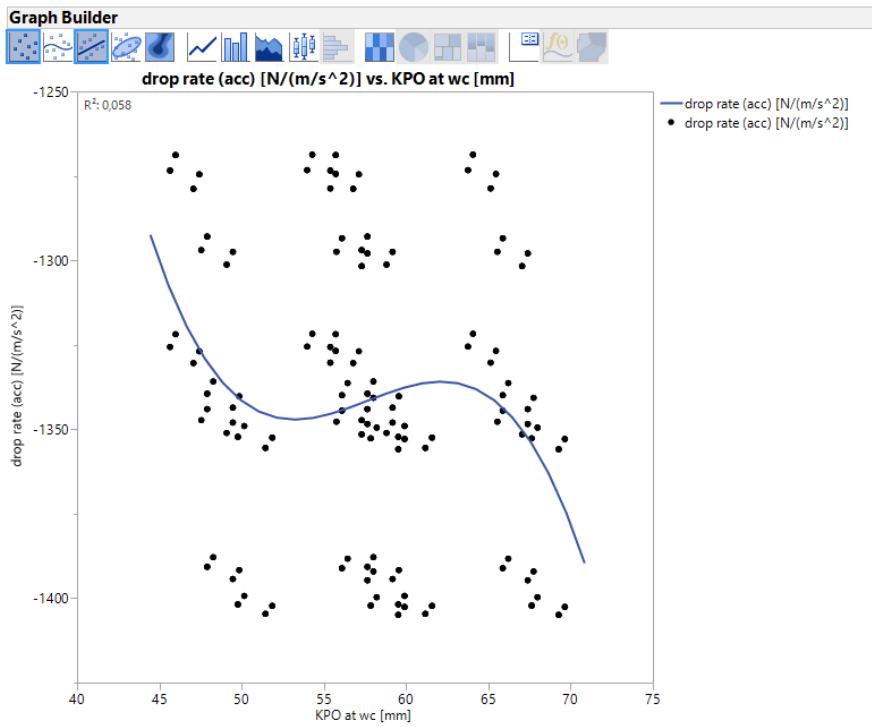
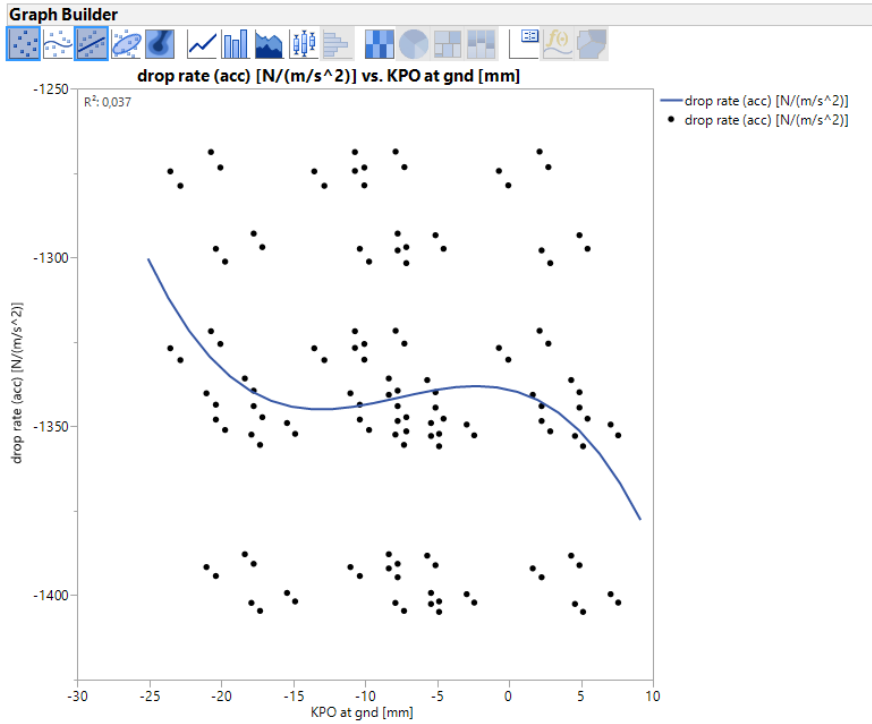
Graph Builder

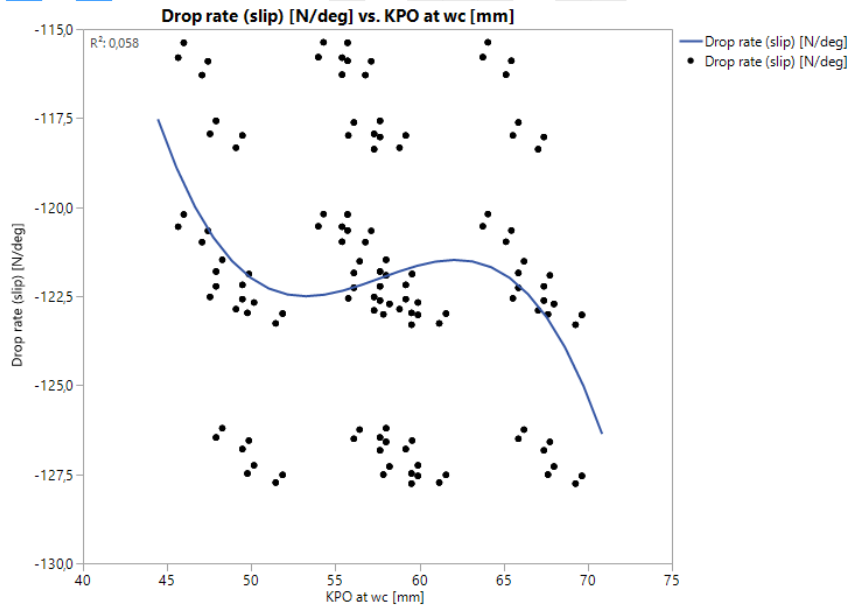
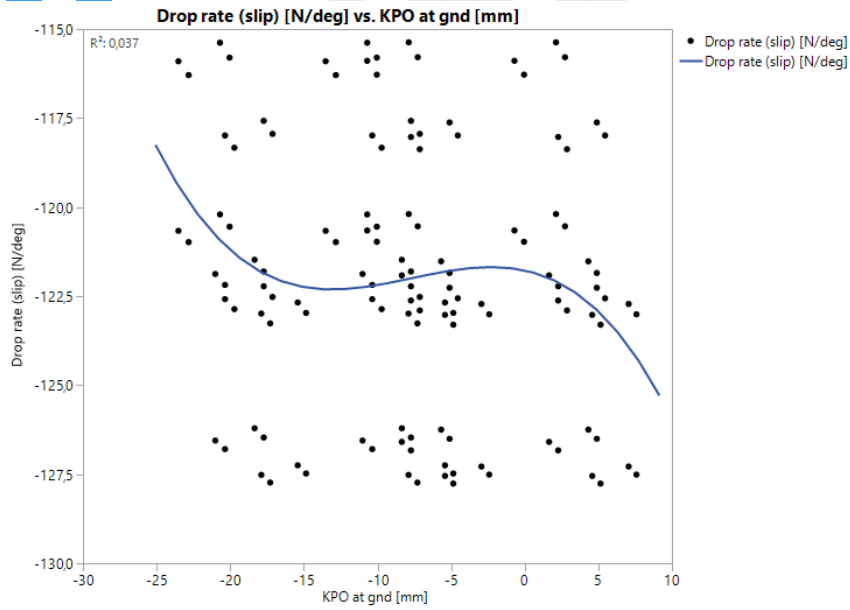


D.2 Drop rate (acceleration)

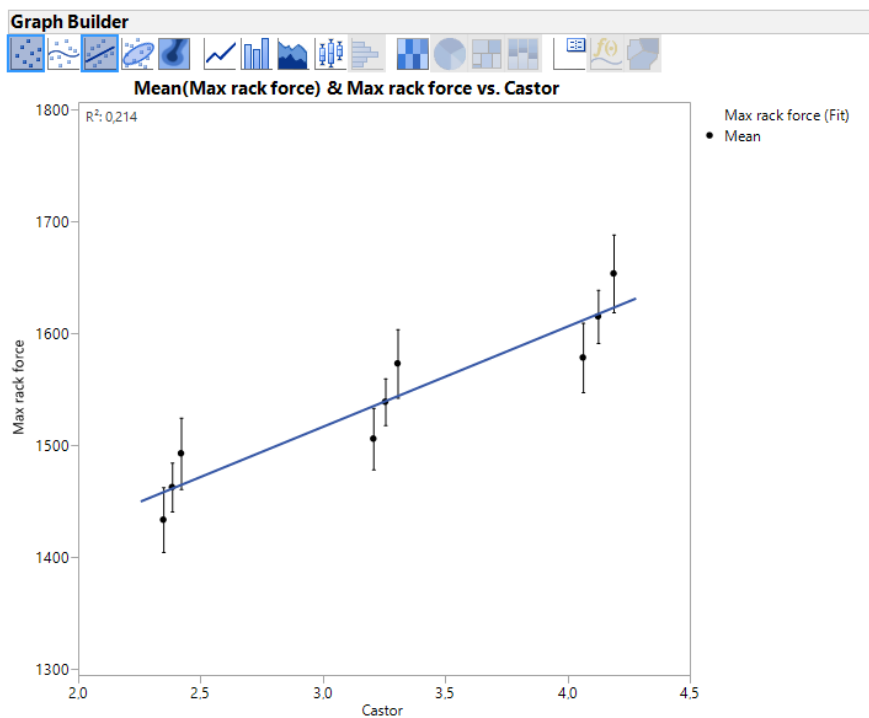
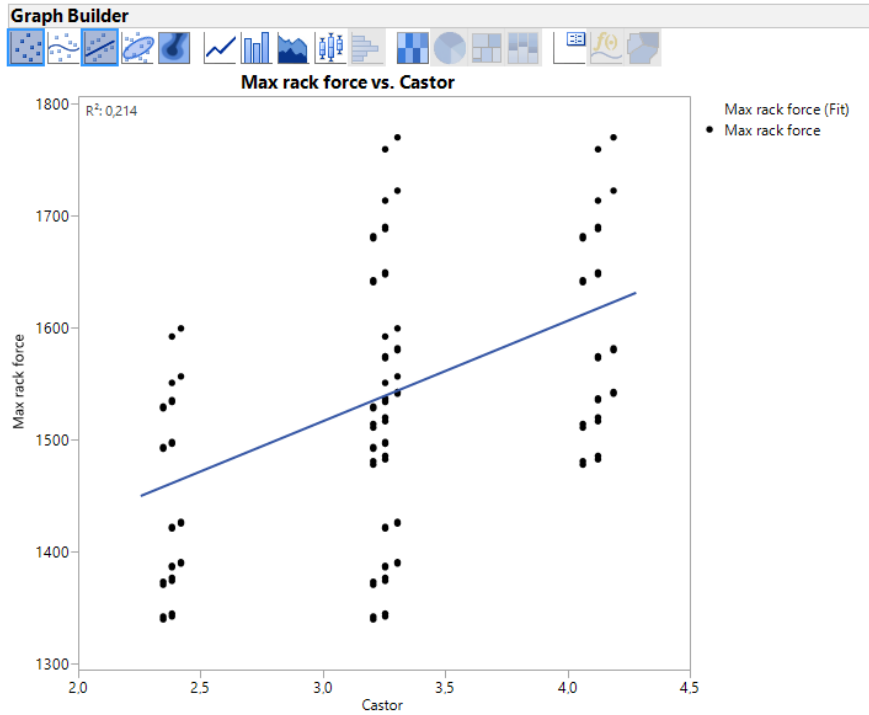






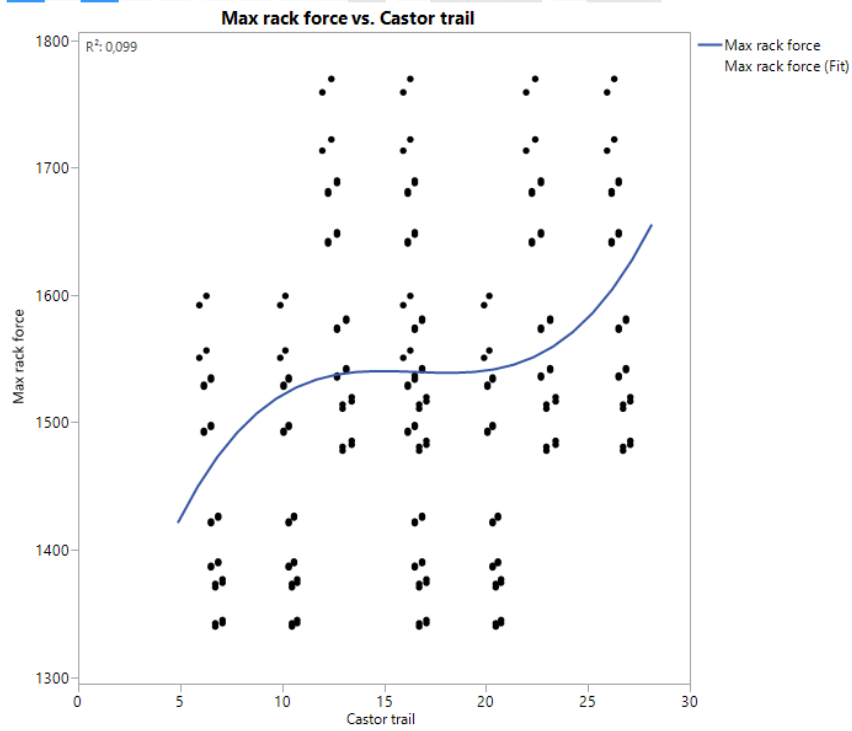


D.4 Maximum force in the steering rack

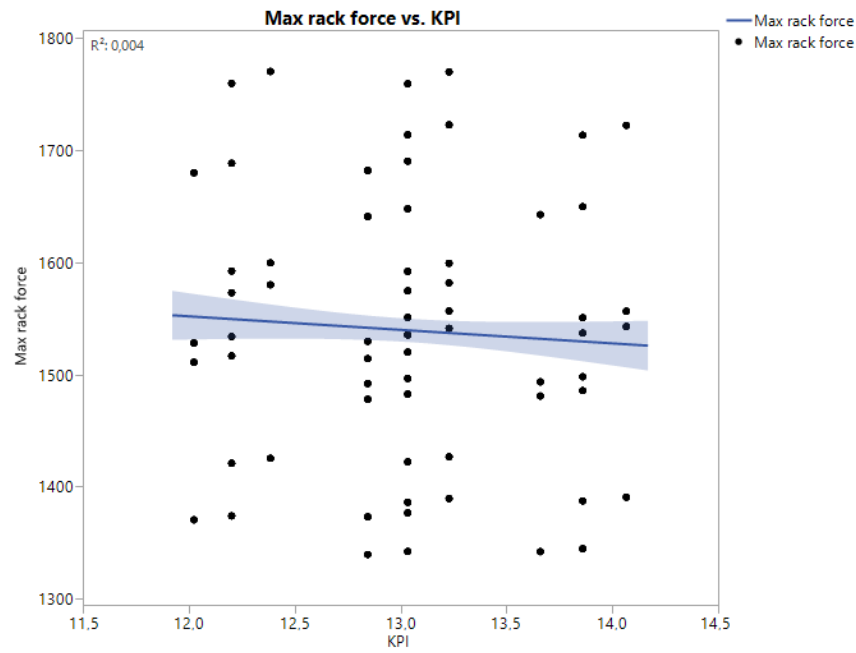


Each error bar is constructed using a 95% confidence interval of the mean.

Graph Builder



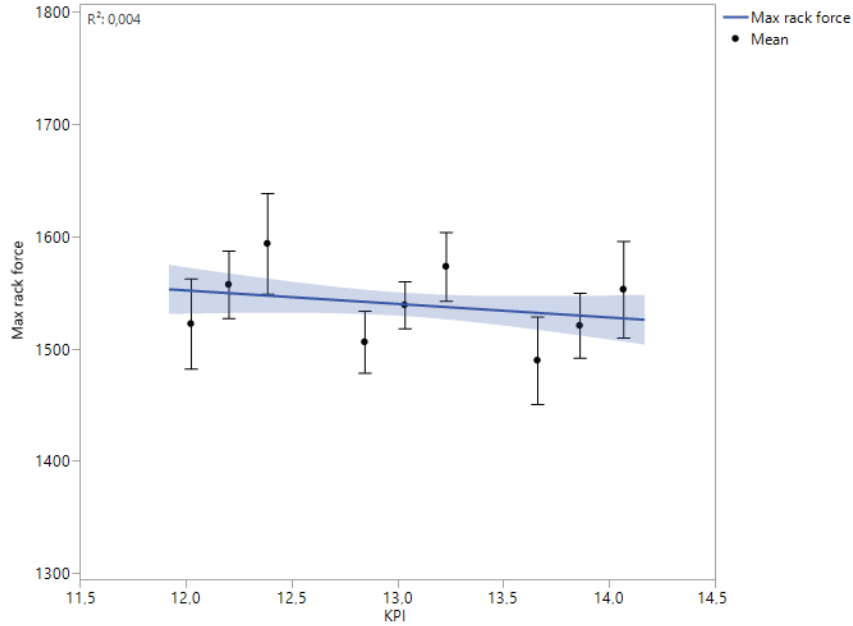
Graph Builder



Graph Builder



Mean(Max rack force) & Max rack force vs. KPI

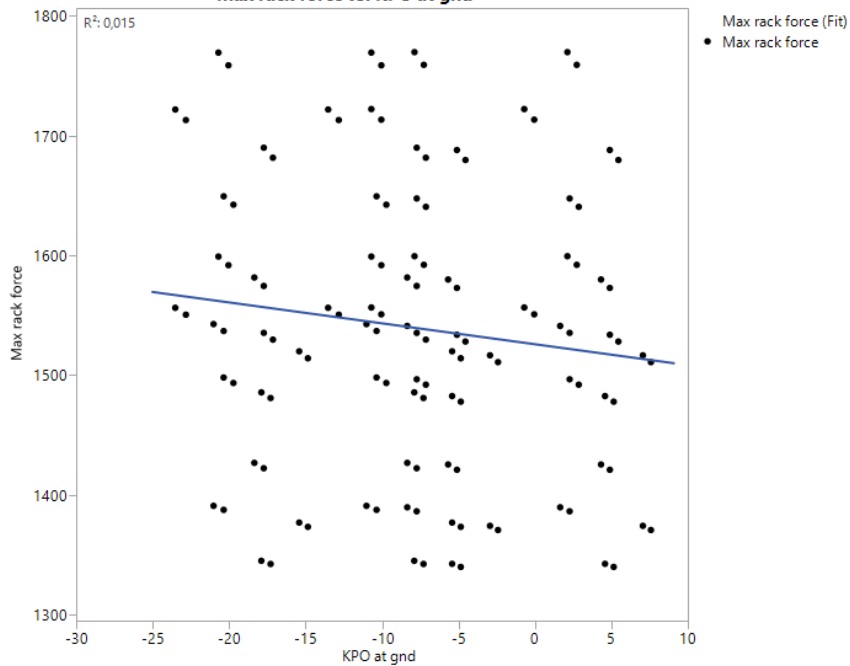


Each error bar is constructed using a 95% confidence interval of the mean.

Graph Builder



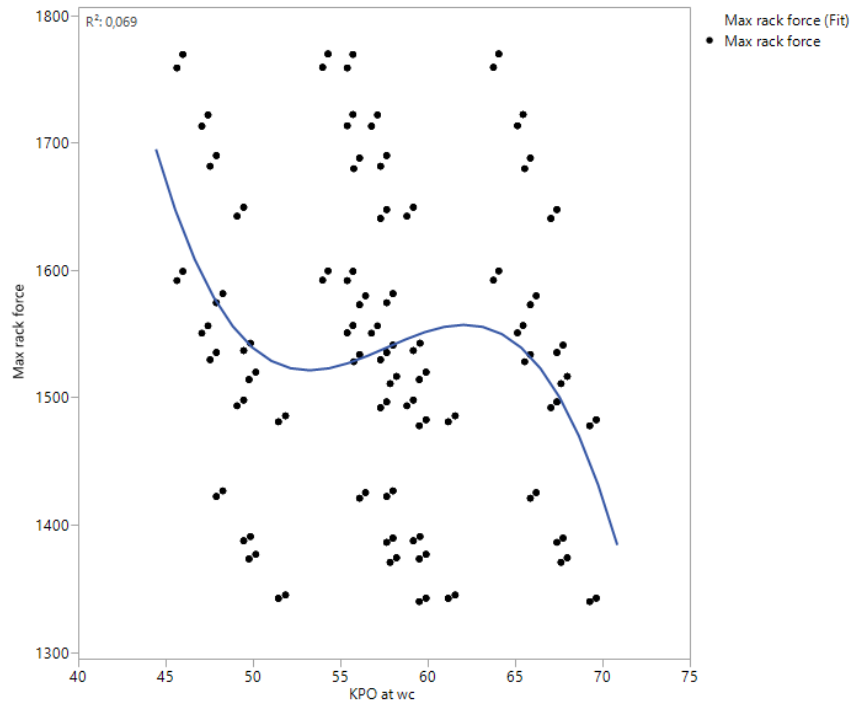
Max rack force vs. KPO at gnd



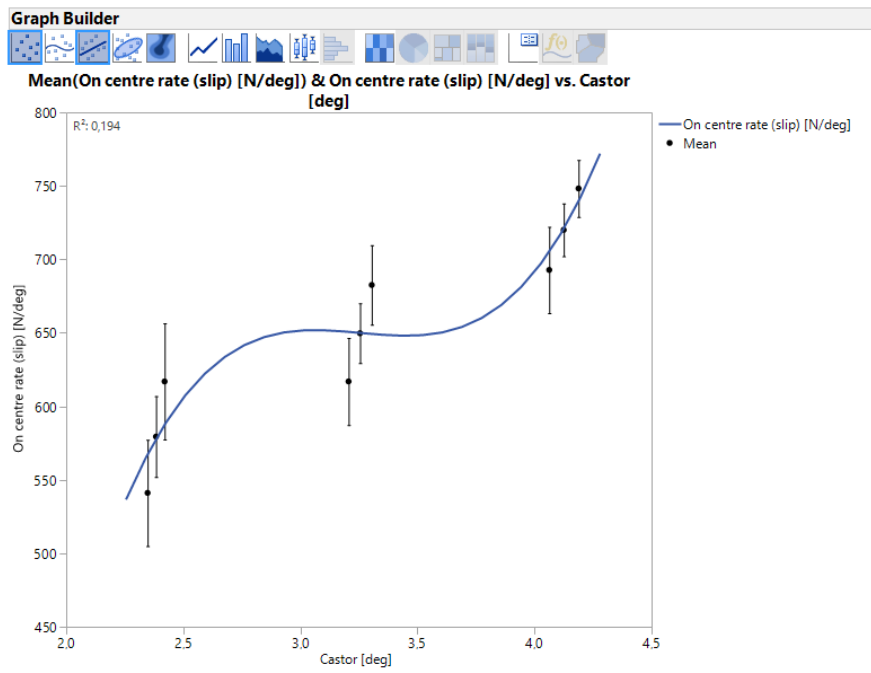
Graph Builder



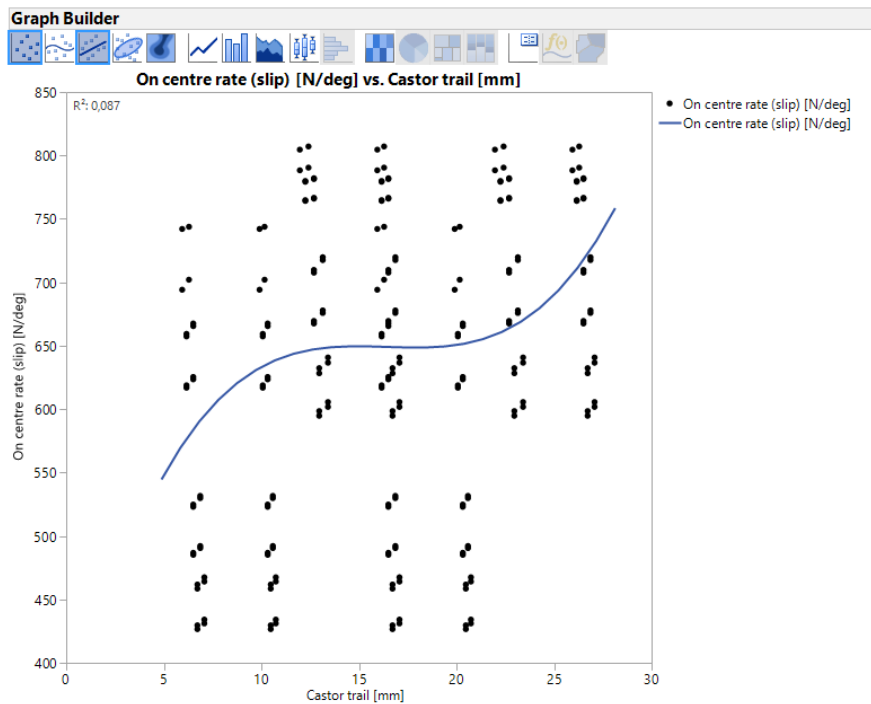
Max rack force vs. KPO at wc



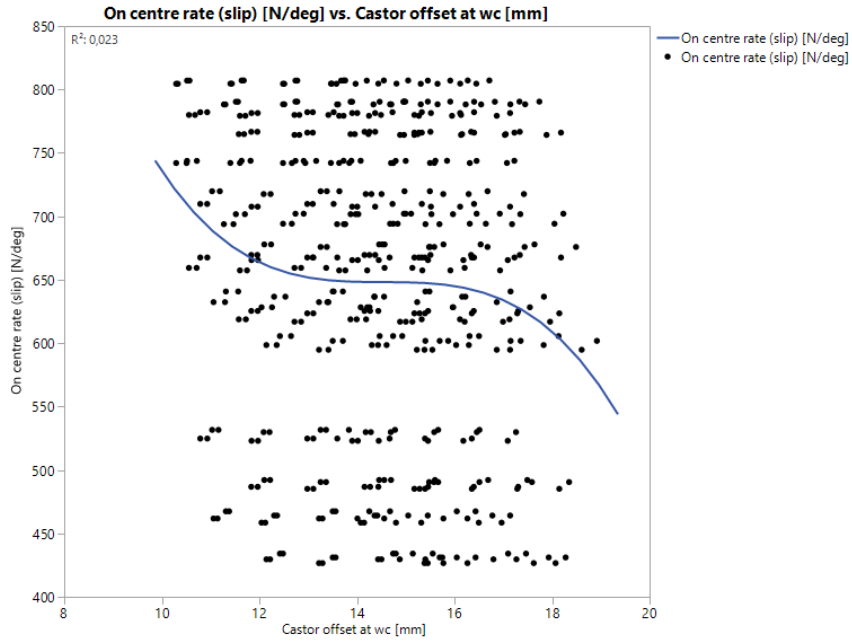
D.5 On-centre slip angle



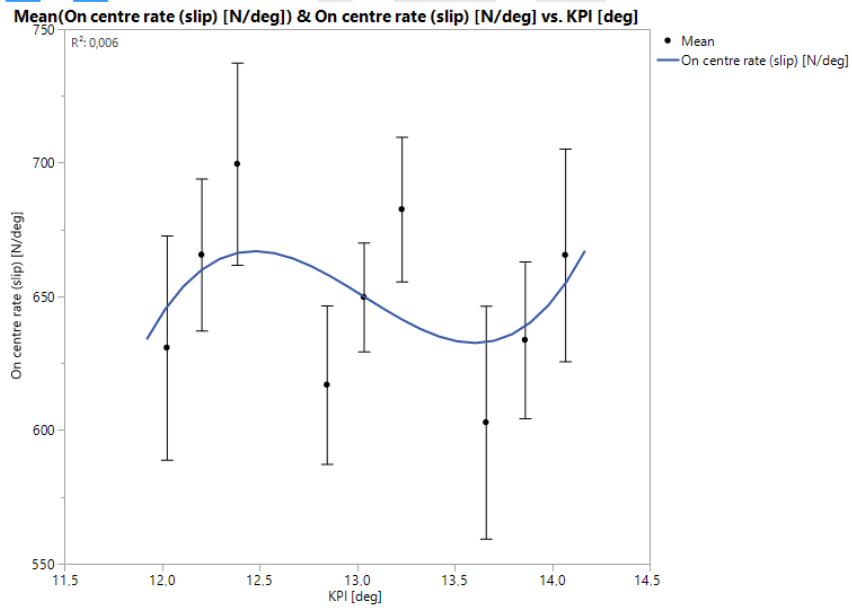
Each error bar is constructed using a 95% confidence interval of the mean.



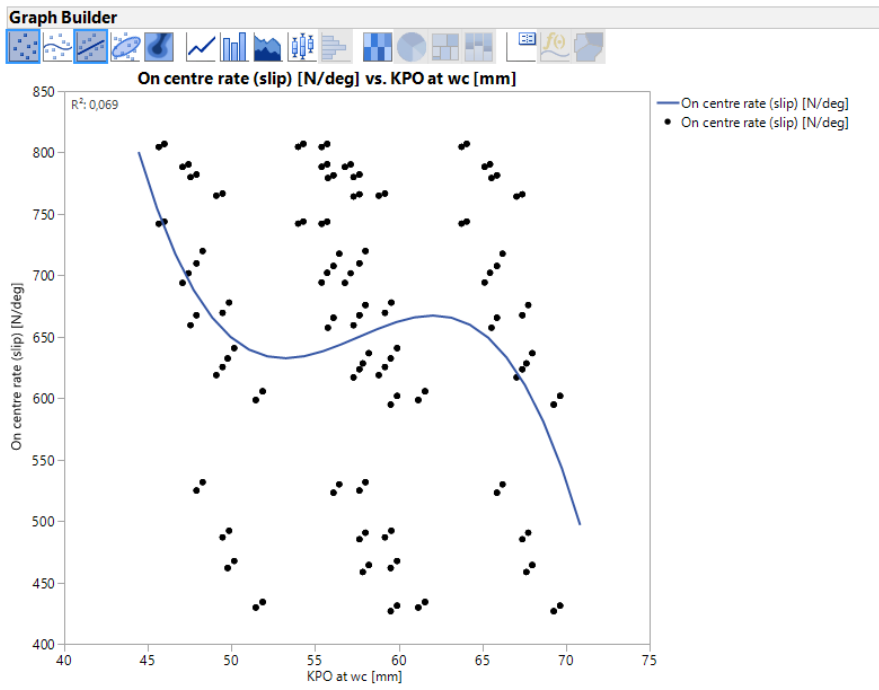
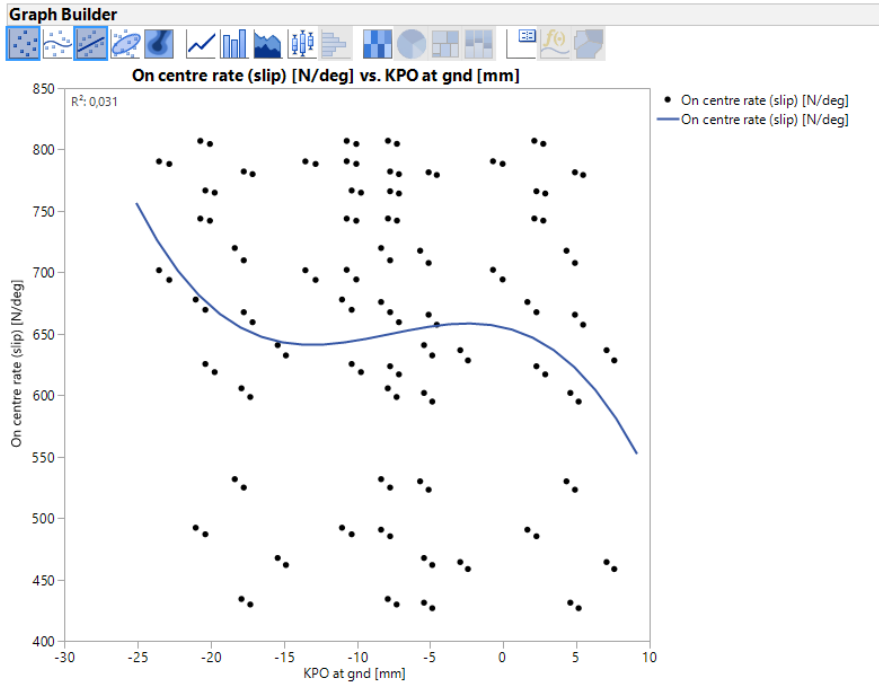
Graph Builder



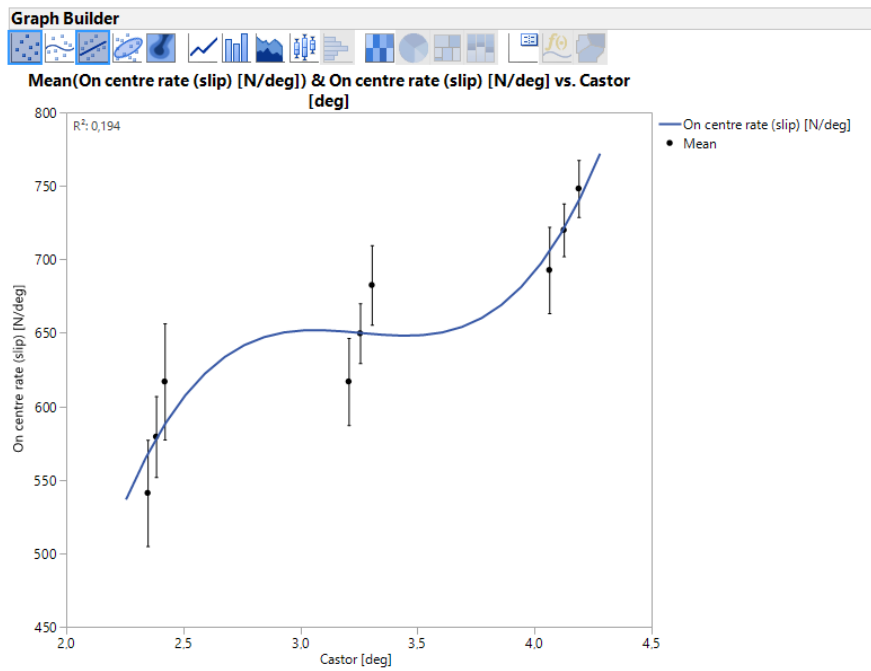
Graph Builder



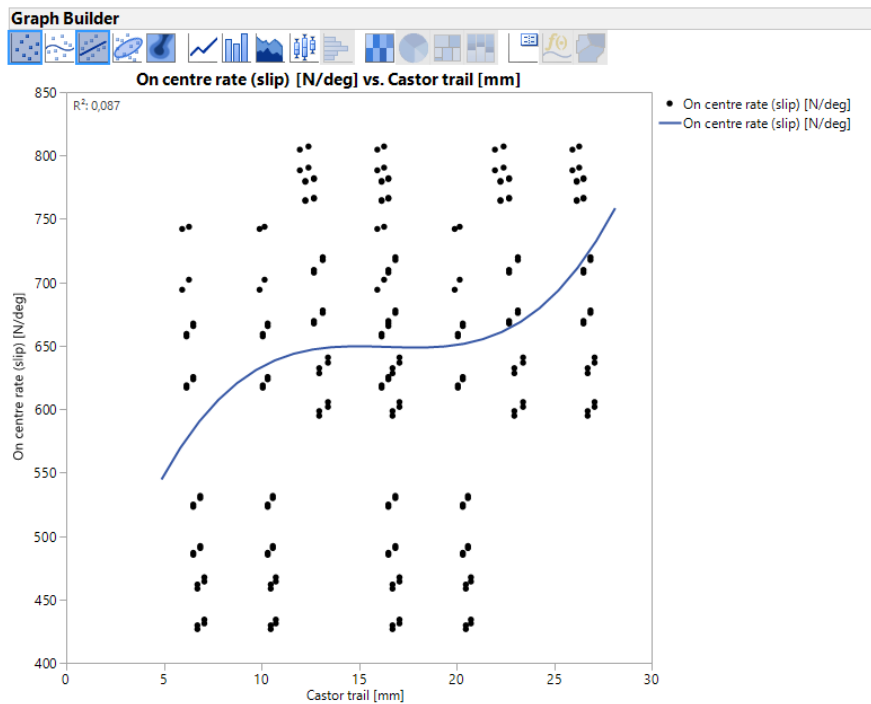
Each error bar is constructed using a 95% confidence interval of the mean.

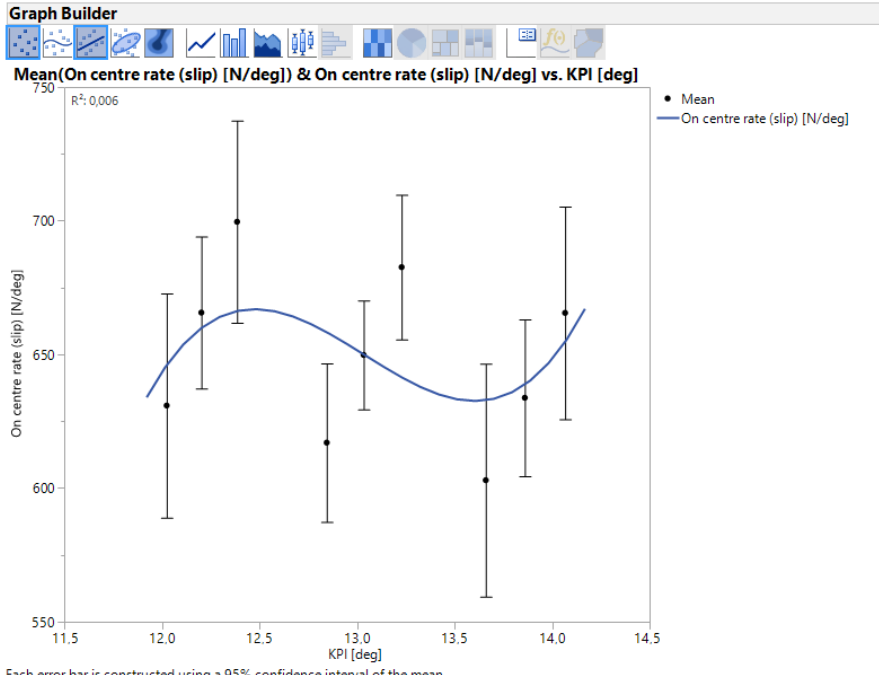
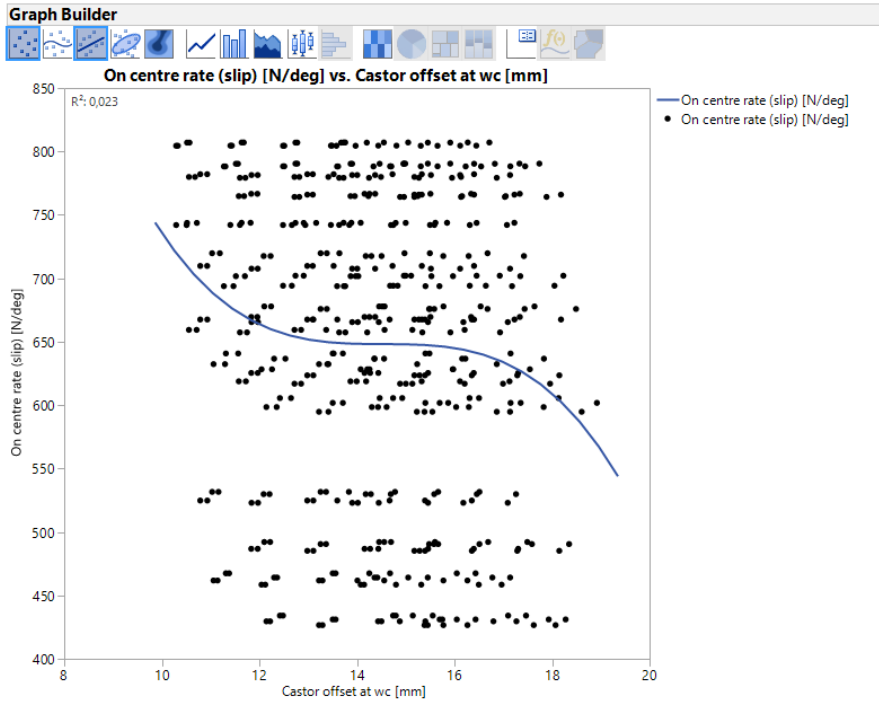


D.6 On-centre rate (acceleration)

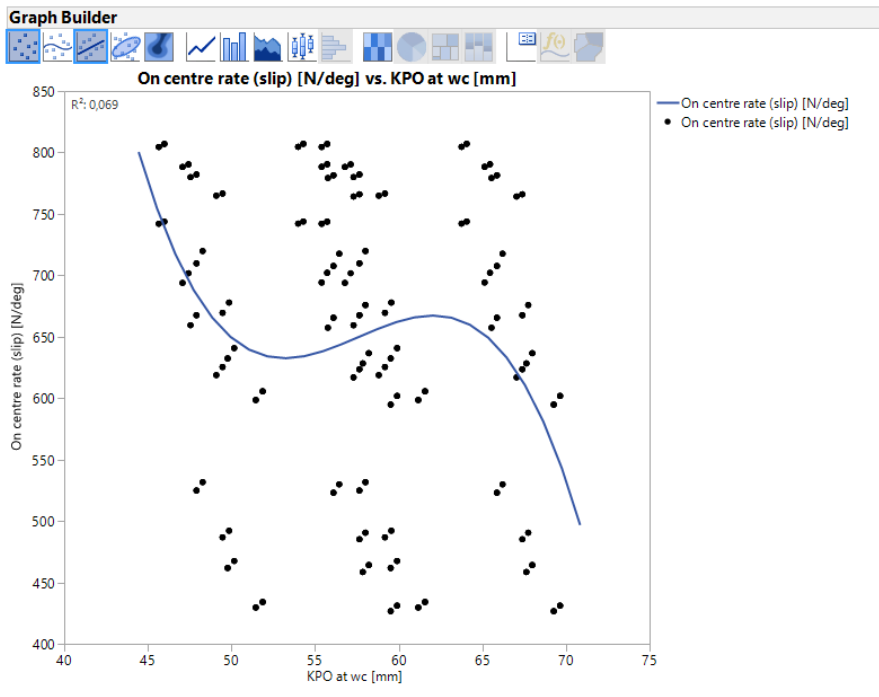
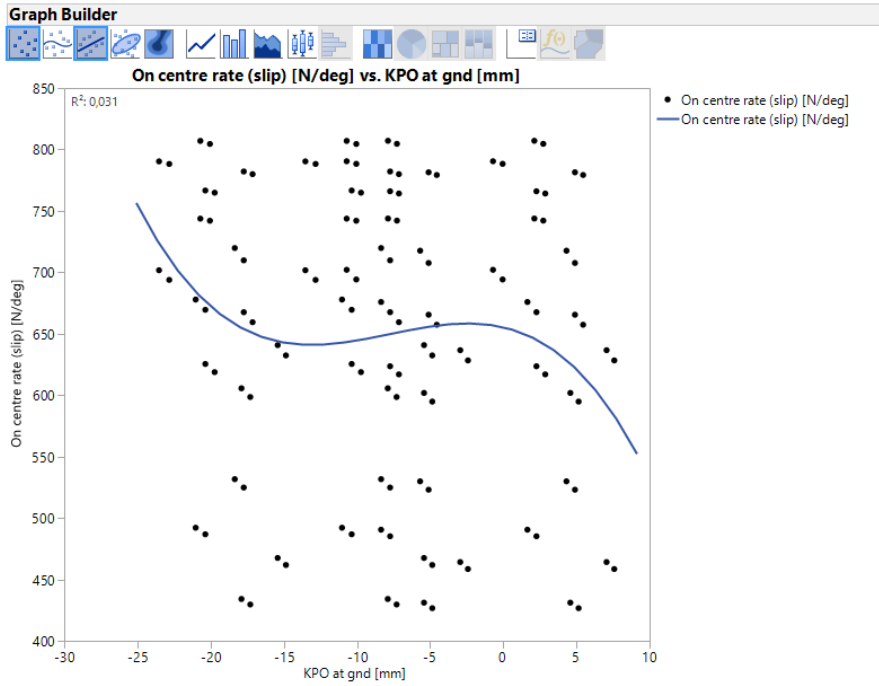


Each error bar is constructed using a 95% confidence interval of the mean.

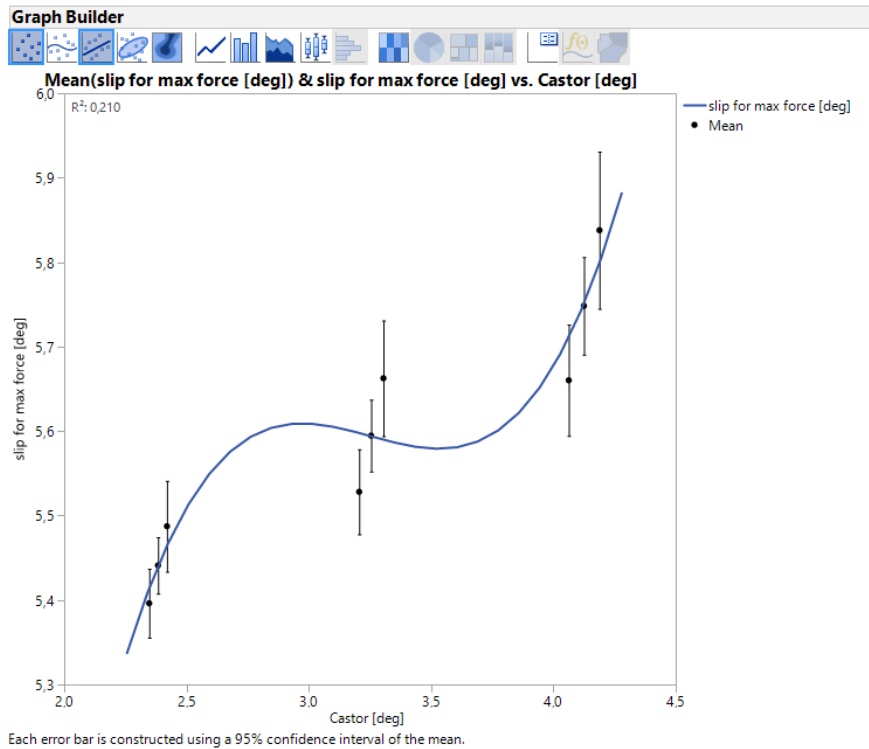




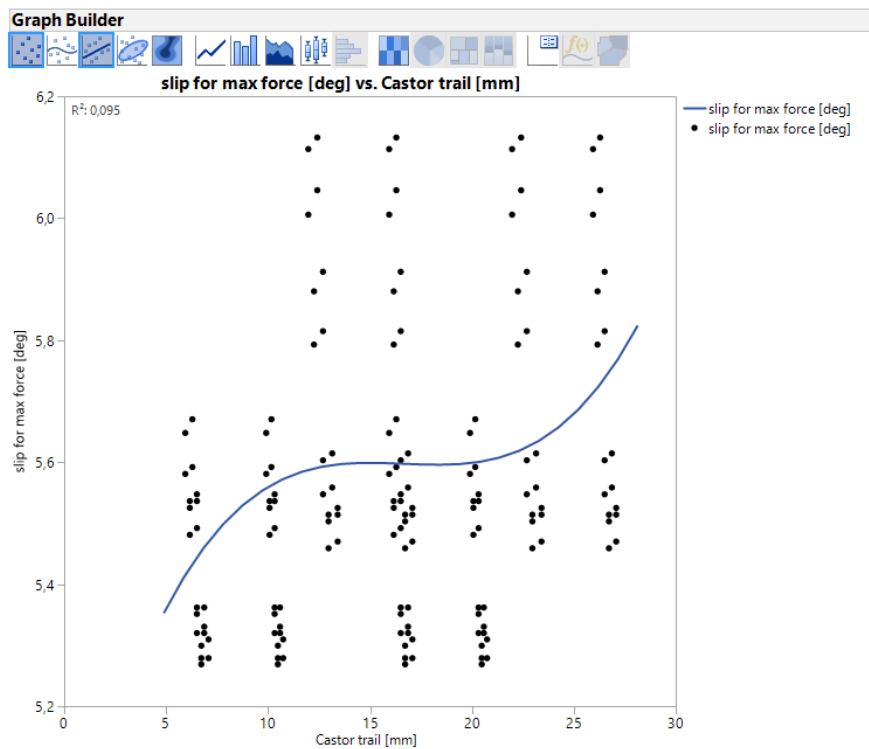
Each error bar is constructed using a 95% confidence interval of the mean.



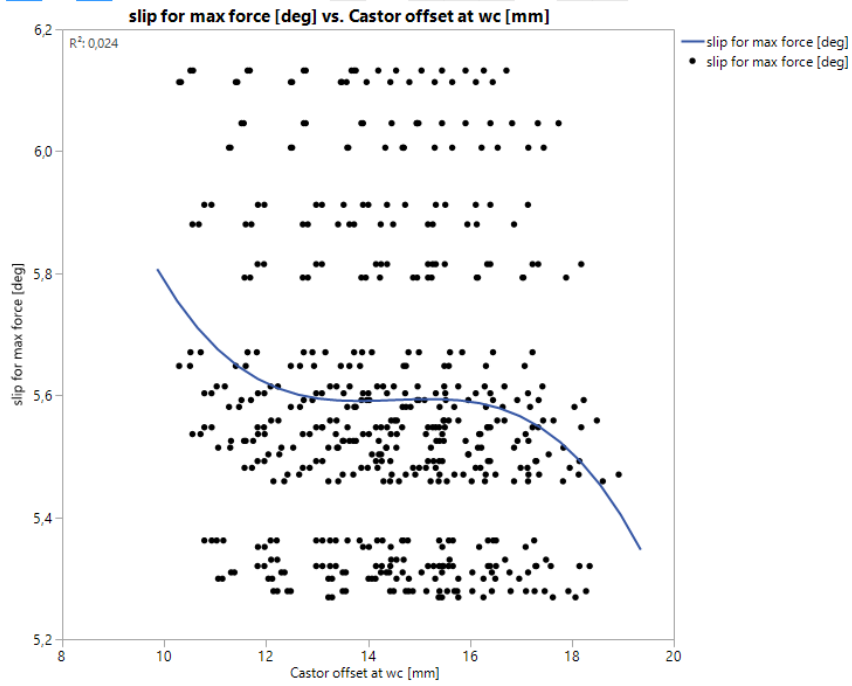
D.7 Slip angle for maximum force



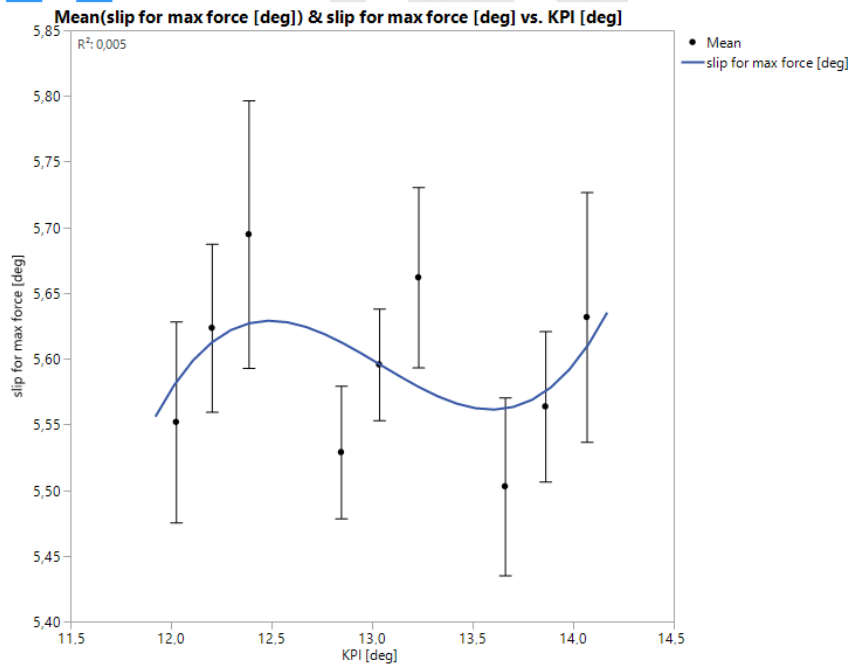
Each error bar is constructed using a 95% confidence interval of the mean.



Graph Builder



Graph Builder



Each error bar is constructed using a 95% confidence interval of the mean.

